

UC Berkeley

UC Berkeley Electronic Theses and Dissertations

Title

Development of Cysteine Protease Inhibitors and Their Application Towards Huntington's Disease and Malaria Therapeutic Models

Permalink

<https://escholarship.org/uc/item/9vv042zr>

Author

Leyva, Melissa Jessica

Publication Date

2010

Peer reviewed|Thesis/dissertation

Development of Cysteine Protease Inhibitors and Their Application Towards
Huntington's Disease and Malaria Therapeutic Models

by

Melissa Jessica Leyva

A dissertation submitted in partial satisfaction of the

requirements for the degree of

Doctor of Philosophy

in

Chemistry

in the

Graduate Division

of the

University of California, Berkeley

Committee in charge:

Professor Carolyn R. Bertozzi, Chair

Professor Matthew B. Francis

Professor Sharon E. Fleming

Fall 2010

Abstract

Development of Cysteine Protease Inhibitors and Their Application Towards Huntington's Disease and Malaria Therapeutic Models

by

Melissa Jessica Leyva

Doctor of Philosophy in Chemistry

University of California, Berkeley

Professor Carolyn R. Bertozzi, Chair

Proteases are enzymes that catalyze the hydrolysis of amide bonds in peptides and proteins. Due to the vital role of proteases in various diseases, protease inhibitors have been aggressively pursued as therapeutic targets but most are peptidic structures. Although peptidic protease inhibitors are identified by traditional methods, drug candidacy is compromised with peptides because of poor metabolic stability and poor cell penetration. Therefore, a more viable approach to obtain drug-like structures is to identify and develop nonpeptidic protease inhibitors with improved pharmacokinetic properties. In this dissertation, approaches to nonpeptidic inhibitor development and studies of protease involvement in relevant diseases are described.

Chapter 1. A brief introduction on proteases and traditional methods used to obtain protease inhibitors is discussed.

Chapter 2. The identification of nonpeptidic pan-caspase inhibitors using the Substrate Activity Screening (SAS) method is described. Application of the SAS method against caspase-3 and caspase-6 resulted in the identification of three novel, pan-caspase inhibitors that block proteolysis of Htt at caspase-3 and -6 cleavage sites. In a Huntington's disease (HD) model, all three inhibitors rescued cell death in striatal and cortical neurons at nanomolar concentrations. Overall, these inhibitors have validated the correlation between blocking caspase Htt cleavage and rescue of HD-mediated neurodegeneration.

Chapter 3. The development of dipeptidyl aminopeptidase (DPAP) inhibitors and application of a novel fragmenting hybrid approach is described. Homology

modeling and computational docking were utilized to design and synthesize nonpeptidic DPAP1 inhibitors that kill *Plasmodium falciparum* at low nanomolar concentrations. A fragmenting hybrid was developed as an alternative to artemisinin combination therapy, which incorporated a trioxolane agent conjugated to our most potent nonpeptidic inhibitor of DPAP1. This strategy showed the slow release of our lead inhibitor and sustained DPAP1 inhibition in *Plasmodium falciparum* parasites. Overall, we validated DPAP1 as a valuable anti-malarial target and demonstrated that our fragmenting hybrid can be successfully used to deliver secondary anti-malarial agents into parasite-infected erythrocytes.

Chapter 4. A summary of the projects described in Chapters 2-3 and a brief discussion of future directions is included.

In summary, the projects described in this dissertation contribute to the traditional approaches to protease inhibitor development and enhance the tools available to study proteases in pertinent diseases.

Development of Cysteine Protease Inhibitors and Their Application towards
Huntington's Disease and Malaria Therapeutic Models

Table of Contents

Chapter 1: Introduction	1
Proteases	2
Methods for Acquiring Protease Inhibitors	2
References	5
Chapter 2: Identification and Evaluation of Novel Small Molecule Pan-Caspase Inhibitors in Huntington's Disease Models	7
Introduction	8
Substrate Library Synthesis and Screening	9
Substrate-Activity Relationship of AMCA Substrates against Caspase-3	9
Substrate Screening and Optimization against Caspase-6	13
Inhibitor Synthesis and Screening	16
Evaluating Inhibitors in Huntington's Disease Models	18
Conclusions	24
Experimental	24
References	50
Chapter 3: Design of <i>Plasmodium falciparum</i> Dipeptidyl Aminopeptidase I Inhibitors and Development of Fragmenting Hybrid Approach for Anti-malarial Delivery	54
Introduction	55

Computational Design, Synthesis, and Evaluation of Nonpeptidic Inhibitors	56
Design and Synthesis of a Fragmenting Hybrid Approach	66
Evaluation of Fragmenting Hybrids <i>In Vitro</i> and <i>In Vivo</i>	68
Conclusions	70
Experimental	70
References	103
Chapter 4: Future Directions	107
Identification and Evaluation of Novel Small Molecule Pan-Caspase Inhibitors in Huntington's Disease Models	108
Design of <i>Plasmodium falciparum</i> Dipeptidyl Aminopeptidase I Inhibitors and Development of Fragmenting Hybrid Approach for Anti-malarial Delivery	108
Conclusions	109
References	110

Acknowledgments

I would first like to thank Professor Jonathan Ellman for being a great advisor. His enthusiasm and extensive scientific knowledge never failed to amaze and inspire me. His guidance during my summer undergraduate research experience provided me with the confidence to apply to the UC Berkeley graduate program. I am exceedingly grateful for the advice and mentorship he has provided over the last five years as a graduate student.

I had the pleasure of working with many talented people in the Ellman group over the past five years. Specifically, I am grateful for the research mentorship I received from Andy Patterson while I interned as a summer undergraduate student and through most of my graduate career. My days in 908 were more enjoyable having someone to talk to about non-chemistry topics such as music and sports. He and his lovely wife, Sara, became amazing friends and accompanied me to concerts and baseball games! I would also like to thank Yazmin Rosa for guiding me through the lab and for being a great life-long friend. She has always been there for me through the good and bad times and I am eternally grateful. I'm also honored to be an "aunt" to her beautiful daughter, Danicey. Monica Trincado and I became good friends while sitting next to each other during her post-doc. She is kind, supportive, and makes the best paella. Denise Colby and I got close when Andy left 908. She introduced me to music that reminded me of Nintendo video games and I'll never forget taking turns waiting in line for the Radiohead concert. Melissa "Beenen" Herbage kept the lab stocked with delicious baked goods and we had a blast singing along to classic Journey songs at karaoke. Katherine Rawls and I shared a lot of fun experiences as 1st years such as attending Andy's bachelor party, crazy parties after Phys-Org exams, and staying for the epically long Green Day set while missing the last BART train out of SF. I enjoyed her company during our much needed coffee breaks when we became bitter 5th years. Sirilata "Van" Yotphan is a hilarious person and replaced Beenen as the loudest person in the group. I'm thankful for her friendship and enjoyed our shopping trips together. Andy Tsai is one of the most enthusiastic individuals I've ever encountered and I have no doubt he's being a great Ellman group leader at Yale. Pete Marsden is the only male I know who doesn't watch football or baseball, but at least we shared an interest in beach volleyball. He made me laugh and I applaud him for enduring Van's torture. Tyler Baguley became my new sports friend in 908 and was the Oregon Ducks green version of me (I wore UT Longhorns burnt orange). I wish him the best of luck as the sole member of team SAS at Yale.

I'm also grateful for the friends outside of the Ellman group who kept me sane during my graduate studies. Thanks to Nancy Martinez and Israel Garcia-Martinez for making the trip for my GRS and being amazing friends! Semarhy "Grizz" Quinonez (Yazmin's former roommate) and I met and bonded at a 30 Seconds to Mars concert after being arm's length away from Jared Leto's serenade and sharing our disappointment in leaving the show after three songs. She quickly became a great friend and concert buddy. I'll never forget our times in the pit, backstage encounters with rock stars, learning guitar/bass, and making up for the last 30STM concert by invading Jared Leto's personal

space. Sandra Villa and Mitch Garcia were great friends and I wish them a long and happy marriage. Elena Arceo is a lively and fun person and I am grateful for our friendship (no hard feelings on stealing the spotlight at my karaoke birthday party after first meeting).

Last but not least, I would especially like to thank my family for their love and constant support. My parents may not understand what I've done in grad school but they have always provided me with encouragement and emotional support. They continue to be my biggest fans and I am blessed to have them as parents! I enjoyed their visits and had a blast with my sisters and brother, including the concerts in northern California, exploring SF tourist sites, swimming in the freezing Santa Cruz water, and cheering on the SF Giants (it's too bad we didn't know we were rooting for the team that would beat our beloved Texas Rangers in the World Series).

Chapter 1. Introduction.

Proteases are enzymes that catalyze the hydrolysis of amide bonds in peptide and protein substrates. Proteases are important therapeutic targets because they play a role in various biological processes. This chapter will introduce protease nomenclature and briefly discuss some of the methods used to obtain protease inhibitors.

Proteases

Proteases are enzymes that catalyze the hydrolysis of amide bonds in peptides and proteins. The human genome encodes over 500 proteases, which are divided into 5 major classes based on the catalytic mechanism.¹ In this chapter, cysteine proteases will be emphasized. Cysteine proteases use a cysteine residue in the enzyme active site to nucleophilically attack the scissile amide bond of the peptide or protein substrate undergoing hydrolytic cleavage.² Interactions between the enzyme active site and the side-chain amino acid residues of the peptide or protein substrate are a basis for protease selectivity (Figure 1.1). Side-chain amino acids of a peptide or protein substrate are designated as P₃, P₂, P₁, P₁' , P₂' , P₃' . Binding sites in the protease active site are designated as S₃, S₂, S₁, S₁' , S₂' , S₃' .³

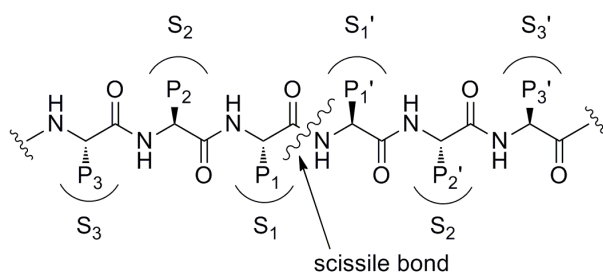


Figure 1.1. Protease substrate binding nomenclature.

Proteolytic cleavage of peptides or proteins plays a role in various biological processes such as protein synthesis, turnover, and function. These enzymes are important therapeutic targets because unregulated proteolysis can affect physiological processes such as digestion, blood coagulation, immune response, cell signaling, and apoptosis.⁴ Proteases are also promising viral, bacterial, and parasitic drug targets due to their involvement in the life cycle of pathogenic viruses, bacteria, and parasites. Inhibitors of proteases are approved drugs, including inhibitors of HIV-1 protease for the treatment of AIDS and inhibitors of angiotensin converting enzyme for the treatment of hypertension. Many other protease inhibitors also show therapeutic utility, targeting cathepsin K in osteoporosis, thrombin in coronary infarction, and β -secretase in Alzheimer's disease.⁵

Methods for Acquiring Protease Inhibitors

The current challenges of developing therapeutically relevant protease inhibitors include achieving selectivity and good pharmacokinetic properties.² Protease inhibitors have been traditionally designed based on the selective recognition of polypeptides in the active-site of the target protease. Although peptide inhibitors are identified by traditional methods, drug candidacy is compromised with peptides because of poor metabolic stability and poor cell penetration. Ideal protease inhibitor drugs are low-molecular weight compounds with few or no peptide bonds and with high specificity.⁶ A more

viable route for inhibitor design is the use of a fragment-based approach where nonpeptidic, low-molecular weight compound fragments are identified and optimized for potency, selectivity, and pharmacokinetic properties.

Among numerous fragment-based screening methods currently employed in drug discovery for the identification of weak-binding, nonpeptidic fragments, the current standard is the use of functional inhibition assays to screen compound libraries for weak-binding inhibitors.⁷ This method is easy to automate but results in a high occurrence of false positives due to protein aggregation and non-specific binding.^{8,9}

More precise methods, such as Structure Activity Relationships (SAR) by NMR and X-ray crystallography, eliminate the possibility of false positives by the detection of direct binding.^{10,11,12} Although these methods provide structural information that can be utilized in fragment optimization, they possess disadvantages. For instance, large quantities of protein are required to attain binding information and these methods require more intricate procedures involving the dedicated use of expensive instrumentation.^{7,13}

Another fragment-based identification method is tethering, in which mass spectrometry is employed to detect binding that results from disulfide interchange of a thiol-derivatized ligand and a cysteine thiol located proximal to the protein binding site.¹² Although the frequency of false positives is minimized and small amounts of protein are required, the limitations of this method include the generation of a disulfide library and the requirement of a cysteine residue in or near the enzyme active site.⁵

The Ellman group has recently reported the first substrate-based fragment identification method, Substrate Activity Screening (SAS).¹⁴ The SAS method can be outlined in three steps. The first step involves generating a library of *N*-acyl aminocoumarin analogs by using support-bound 7-amino-4-methyl-3-carboxymethylcoumarin (AMCA) and screening the library against a protease target using a fluorescence-based assay (Figure 1.2). The second step involves the optimization of the *N*-acyl fragments through solid-phase synthesis and subsequent screening of focused substrate libraries. In the third step, the aminocoumarin is replaced with a mechanism-based pharmacophore to provide protease inhibitors directly.

Numerous characteristics make the SAS method advantageous over other approaches for developing nonpeptidic protease inhibitors. The screening step is high throughput and eliminates the incidence of false positives due to aggregation, protein precipitation, and non-specific binding because substrate cleavage with release of the fluorogenic reporter group only occurs upon active enzyme catalyzed hydrolysis. Since the assay screens for catalytic substrate turnover, in contrast to traditional inhibitor assays, signal amplification is also observed. This attribute allows for the identification of very low affinity fragments at low substrate concentrations. The rapid conversion of weak-binding nonpeptidic substrates into inhibitors gives rise to another important attribute of the SAS method. Substrate cleavage is only observed when the amide carbonyl of *N*-acyl aminocoumarin is properly positioned in the enzyme active site, thus allowing for the aminocoumarin group to be replaced by a mechanism-based pharmacophore to produce reversible or irreversible inhibitors. The SAS method has been previously applied to proteases of the papain family by our group.¹⁴⁻¹⁷

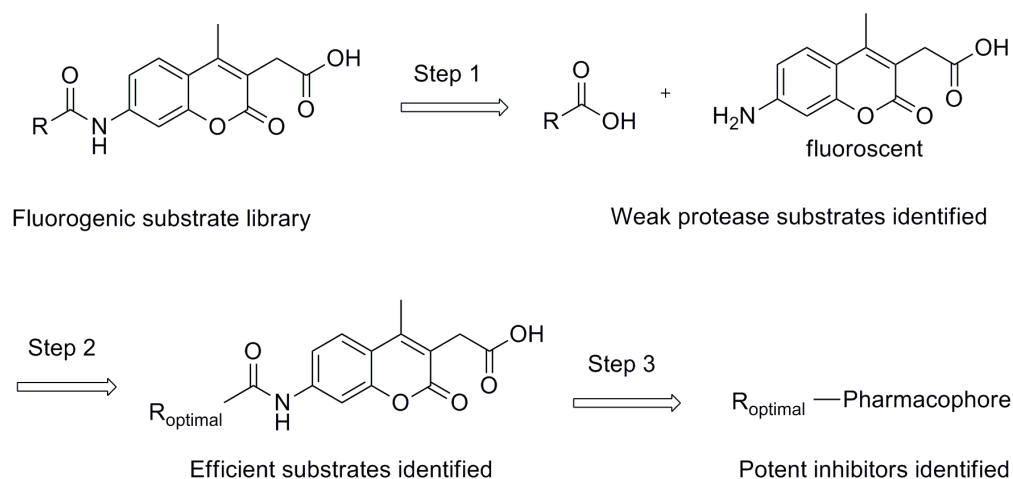


Figure 1.2. Outline of Substrate Activity Screening (SAS) method.

In chapter 2, the utilization of the SAS method on caspase-3 and -6, is described.¹⁸ Caspases-3 and -6 are two of fourteen identified caspases and belong to the subfamily of apoptosis activation.¹⁹⁻²¹ Dysregulation of apoptosis, or programmed cell death, is implicated in several diseases including liver disease, myocardial infarction, and neurodegenerative diseases such as Huntington's disease and Alzheimer's disease.¹⁷ Various caspase-3 inhibitors have been developed but are mostly peptidomimetic in nature.^{22,23} Developing nonpeptidic caspase inhibitors has proven to be a challenge due to the highly specific requirement of an aspartic acid residue at the C-terminal site of substrate cleavage, making them some of the most specific proteases known.²⁴ Therefore, the advancement of nonpeptidic caspase inhibitors could prospectively lead to efficient drugs for numerous diseases. Employing this method provided potent, nonpeptidic inhibitors, which were used to validate caspases as viable targets in Huntington's disease.

In silico docking is a computational approach to identify protease inhibitors and is widely used in drug discovery. Docking involves the prediction of ligand or small molecule conformation and orientation within a targeted protein binding site.²⁵⁻²⁷ The main objectives of docking studies include accurate structural modeling and correct prediction of activity. However, the identification of molecular features that are responsible for specific biological recognition, or the prediction of compound modifications that affect potency, are complex and difficult to computationally simulate. In addition to identifying inhibitor structures, lead hits can be structurally optimized using docking analysis to guide the design of more potent inhibitors. In silico screening, design, and optimization have been used to identify various inhibitors of proteases involved in relevant diseases.²⁸⁻³¹

In chapter 3, the use of in silico methods to build a homology model of dipeptidyl aminopeptidase I (DPAP1) and inhibitor design, is described. To guide the synthesis of

new compounds, we built a homology model of DPAP1 based on the crystal structure of cysteine protease, human cathepsin C.³² Moreover, homology modeling and computational docking methods resulted in the improvement of specificity of our initial inhibitor hit. This suggests that in silico methods can be successfully applied to design potent DPAP nonpeptidic inhibitors. Overall, our results validate the identified DPAP1 as a viable anti-malarial target.

References

- (1) Puente, X. S.; Sanchez, L. M.; Overall, C. M.; Lopez-Otin, C. *Nature reviews. Genetics* **2003**, *4*, 544.
- (2) Leung, D.; Abbenante, G.; Fairlie, D. P. *Journal of Medicinal Chemistry* **2000**, *43*, 305.
- (3) Schechter, I.; Berger, A. *Biochemical and Biophysical Research Communications* **1967**, *27*, 157.
- (4) Powers, J. C.; Asgian, J. L.; Ekici, O. D.; James, K. E. *Chemical Reviews* **2002**, *102*, 4639.
- (5) Abbenante, G.; Fairlie, D. P. *Medicinal Chemistry* **2005**, *1*, 71.
- (6) Whittaker, M. *Current Opinion in Chemical Biology* **1998**, *2*, 386.
- (7) Erlanson, D. A.; McDowell, R. S.; O'Brien, T. *Journal of Medicinal Chemistry* **2004**, *47*, 3463.
- (8) McGovern, S. L.; Caselli, E.; Grigorieff, N.; Shoichet, B. K. *Journal of Medicinal Chemistry* **2002**, *45*, 1712.
- (9) McGovern, S. L.; Shoichet, B. K. *Journal of Medicinal Chemistry* **2003**, *46*, 1478.
- (10) Hartshorn, M. J.; Murray, C. W.; Cleasby, A.; Frederickson, M.; Tickle, I. J.; Jhoti, H. *Journal of Medicinal Chemistry* **2004**, *48*, 403.
- (11) Hajduk, P. J.; Boyd, S.; Nettlesheim, D.; Nienaber, V.; Severin, J.; Smith, R.; Davidson, D.; Rockway, T.; Fesik, S. W. *Journal of Medicinal Chemistry* **2000**, *43*, 3862.
- (12) Hajduk, P. J.; Shuker, S. B.; Nettlesheim, D. G.; Craig, R.; Augeri, D. J.; Betebenner, D.; Albert, D. H.; Guo, Y.; Meadows, R. P.; Xu, L.; Michaelides, M.; Davidsen, S. K.; Fesik, S. W. *Journal of Medicinal Chemistry* **2002**, *45*, 5628.
- (13) Erlanson, D. A.; Braisted, A. C.; Raphael, D. R.; Randal, M.; Stroud, R. M.; Gordon, E. M.; Wells, J. A. *Proceedings of the National Academy of Sciences of the United States of America* **2000**, *97*, 9367.
- (14) Wood, W. J. L.; Patterson, A. W.; Tsuruoka, H.; Jain, R. K.; Ellman, J. A. *Journal of the American Chemical Society* **2005**, *127*, 15521.
- (15) Brak, K.; Doyle Patricia, S.; McKerrow James, H.; Ellman Jonathan, A. *Journal of the American Chemical Society* **2008**, *130*, 6404.
- (16) Inagaki, H.; Tsuruoka, H.; Hornsby, M.; Lesley Scott, A.; Spraggon, G.; Ellman Jonathan, A. *Journal of Medicinal Chemistry* **2007**, *50*, 2693.
- (17) Patterson, A. W.; Wood, W. J. L.; Hornsby, M.; Lesley, S.; Spraggon, G.; Ellman, J. A. *Journal of Medicinal Chemistry* **2006**, *49*, 6298.

- (18) Leyva, M. J.; DeGiacomo, F.; Kaltenbach, L. S.; Holcomb, J.; Zhang, N.; Gafni, J.; Park, H.; Lo, D. C.; Salvesen, G. S.; Ellerby, L. M.; Ellman, J. A. *Chemistry & Biology* **2010**, *17*, 1189.
- (19) Fan, T.-J.; Han, L.-H.; Cong, R.-S.; Liang, J. *Acta Biochimica et Biophysica Sinica* **2005**, *37*, 719.
- (20) Fadeel, B.; Orrenius, S. *Journal of Internal Medicine* **2005**, *258*, 479.
- (21) Talanian, R. V.; Brady, K. D.; Cryns, V. L. *Journal of Medicinal Chemistry* **2000**, *43*, 3351.
- (22) Becker, J. W.; Rotonda, J.; Soisson, S. M.; Aspiotis, R.; Bayly, C.; Francoeur, S.; Gallant, M.; Garcia-Calvo, M.; Giroux, A.; Grimm, E.; Han, Y.; McKay, D.; Nicholson, D. W.; Peterson, E.; Renaud, J.; Roy, S.; Thornberry, N.; Zamboni, R. *Journal of Medicinal Chemistry* **2004**, *47*, 2466.
- (23) Goode, D. R.; Sharma, A. K.; Hergenrother, P. J. *Organic Letters* **2005**, *7*, 3529.
- (24) Talanian, R. V.; Quinlan, C.; Trautz, S.; Hackett, M. C.; Mankovich, J. A.; Banach, D.; Ghayur, T.; Brady, K. D.; Wong, W. W. *Journal of Biological Chemistry* **1997**, *272*, 9677.
- (25) Kitchen, D. B.; Decornez, H.; Furr, J. R.; Bajorath, J. *Nature reviews. Drug discovery* **2004**, *3*, 935.
- (26) Bajorath, J. *Nature reviews. Drug discovery* **2002**, *1*, 882.
- (27) Langer, T.; Hoffmann, R. D. *Current Pharmaceutical Design* **2001**, *7*, 509.
- (28) Kumar, M.; Verma, S.; Sharma, S.; Srinivasan, A.; Singh, T. P.; Kaur, P. *Chemical Biology & Drug Design* **2010**, *76*, 277.
- (29) Murray, C. W.; Blundell, T. L. *Current Opinion in Structural Biology* **2010**, *20*, 497.
- (30) Simmons, K. J.; Chopra, I.; Fishwick, C. W. G. *Nat Rev Micro* **2010**, *8*, 501.
- (31) Talele, T. T.; Khedkar, S. A.; Rigby, A. C. *Current Topics in Medicinal Chemistry* **2010**, *10*, 127.
- (32) Deu, E.; Leyva, M. J.; Albrow, V. E.; Rice, M. J.; Ellman, J. A.; Bogoy, M. *Chemistry & Biology* **2010**, *17*, 808.

Chapter 2. Identification and Evaluation of Novel Small Molecule Pan-Caspase Inhibitors in Huntington's Disease Models.

*Huntington's Disease (HD) is characterized by a mutation in the huntingtin gene encoding an expansion of glutamine repeats on the N-terminus of the huntingtin (Htt) protein. Numerous studies have identified Htt proteolysis as a critical pathological event in post mortem human tissue and mouse HD models, and proteases known as caspases have emerged as attractive HD targets. We report the use of the substrate activity screening method against caspases-3 and -6 to identify three novel, pan-caspase inhibitors that block proteolysis of Htt at caspase-3 and -6 cleavage sites. In HD models, these irreversible inhibitors suppressed Hdh^{111Q/111Q}-mediated toxicity and rescued rat striatal and cortical neurons from cell death. In this study the identified nonpeptidic caspase inhibitors were used to confirm the role of caspase-mediated Htt proteolysis in HD. These results further implicate caspases as promising targets for HD therapeutic development. The majority of this work has been published (Leyva, M. J.; DeGiacomo, F.; Kaltenbach, L. S.; Holcomb, J.; Zhang, N.; Gafni, J.; Park, H.; Lo, D. C.; Salvesen, G. S.; Ellerby, L. M.; Ellman, J. A. *Chemistry & Biology* **2010**, 17, 1189.)*

Authorship

I synthesized all substrates and optimized their structures to improve caspase activity. Furthermore, I chose the specific pharmacophore to convert lead caspase substrates into potent, irreversible inhibitors. I performed the substrate and inhibitor assays against caspases and related cysteine proteases (legumain and cathepsins B, S, and V). Inhibitor studies with Htt23Q and Htt148Q and *Hdh*^{7Q/7Q} and *Hdh*^{111Q/111Q} cells were conducted by Francesco DeGiacomo, Jennifer Holcomb, Ningzhe Zhang, Juliette Gafni, and Dr. Ellerby at the Buck Institute for Age Research. Dr. Kaltenbach conducted the HttN90Q73-induced degeneration studies at Duke University Medical Center.

Introduction

Huntington's disease (HD) is a dominantly inherited neurodegenerative disorder characterized by progressive deterioration of neurons in the striatum and cortex. Symptoms can occur at any age but usually arise with an adult-onset and patients exhibit progressive loss of cognitive and motor function. HD is an incurable disease caused by a mutation in the Htt gene with a trinucleotide (CAG) expansion encoding glutamine repeats in the N-terminus of huntingtin (Htt), a scaffold protein with many interacting proteins that has been shown to be involved in vesicular trafficking.¹ Major research efforts have focused on the relationship of HD pathogenesis and polyglutamine repeats, but the molecular mechanisms leading to neuronal death are not fully understood. Proposed mechanisms leading to neuronal dysfunction and death include formation of polyglutamine aggregates and inclusions,^{2,3} altered conformation of mutant huntingtin leading to transcriptional dysregulation,⁴⁻⁶ excitotoxic neuron damage by excessive stimulation of glutamine receptors,⁷⁻⁹ and induction of apoptosis and proteolysis. A neuropathological hallmark of HD in human and mouse models is the accumulation of N-terminal Htt fragments leading to cytotoxicity, suggesting that Htt proteolysis is a critical event in pathogenesis.¹⁰⁻¹⁶

A great amount of work has focused on the proteolytic cleavage of Htt by multiple proteases, including aspartyl proteases, calpains, and caspases.^{13,15-18} Caspases are cysteine proteases characterized by their high specificity for substrates with an aspartic acid at the site of cleavage in the P1 position and play a prominent role in apoptosis.¹⁹ Dysregulation of apoptosis has been implicated in stroke, neuronal degeneration, liver disease, cancer, and autoimmune disorders.²⁰ Due to the dramatic neuronal cell death in HD, it is not surprising that Htt was the first neuronal protein identified as a caspase substrate.¹³ A number of studies have defined the cleavage sites of Htt for caspase-3 at amino acids 513 and 552, for caspase-2 at amino acid 552, and for caspase-6 at amino acid 586.^{18,21} Recently, caspase-6 cleavage of mutant Htt and activation of caspase-6 has been shown to play a significant role in HD pathogenesis in HD mouse models and is also activated in HD postmortem tissue.^{22,23}

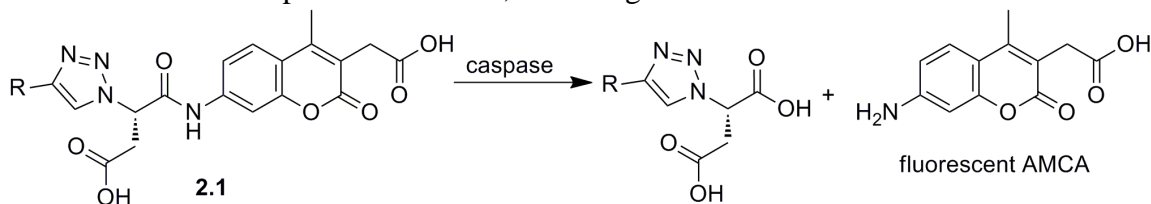
Although the aforementioned studies clearly implicate caspase-mediated cleavage of Htt in HD, few studies have evaluated the effects of caspase inhibition on cell death. The non-specific irreversible, peptidic fluoromethyl ketone inhibitor, zVAD-fmk,

protected striatal neurons against malonate-induced excitotoxicity,²⁴ and the reversible caspase-3 specific inhibitor, M826, significantly displayed neuroprotection against malonate-induced striatal injury in a rat model of HD.²⁵ Additionally, through indirect means minocycline, a tetracycline derivative with the ability to cross the blood-brain barrier, inhibits caspase-1 and caspase-3 transcriptional upregulation and delays cell death in HD transgenic mouse models.²⁶ The development of small molecule, nonpeptidic inhibitors of both caspase-3 and -6 and their evaluation in HD biology would provide useful tool compounds to the field. Unfortunately, while numerous caspase inhibitors have been developed,^{27,28} most are peptidic in nature and efficacy in cells and animals is compromised due to poor cell penetration and ADME (Absorption, Distribution, Metabolism, and Excretion) properties, respectively.²⁹ We therefore applied a substrate-based fragment approach called substrate activity screening (SAS) to the development of nonpeptidic inhibitors of caspases-3 and -6. In the SAS method, which has previously been applied to proteases of the papain family,³⁰⁻³³ weak binding nonpeptidic substrate fragments are identified, optimized, and then converted to potent inhibitors. Herein, we report the identification of three novel, nonpeptidic pan-caspase irreversible inhibitors that blocked proteolysis of Htt at caspase-3 and caspase-6 sites, suppressed *Hdh*^{111Q/111Q}-mediated toxicity, and rescued HttN90Q73-induced degeneration of rat striatal and cortical neurons.

Substrate Library Synthesis and Screening

To target caspase-3, we initially set out to create a library that incorporated the P1 aspartic acid required for caspase recognition and amide bond hydrolysis. To satisfy the goal of identifying nonpeptidic fragments, we synthesized an initial library of 1,4-disubstituted-1,2,3-triazole substrates **2.1** (Scheme 2.1) because triazoles have been demonstrated as efficient amide bond replacements in the development of protease inhibitors,^{33,34} and diverse functionality could readily be introduced into the substrates using solid-phase methods (see Experimental Section). Substrates were screened in a high-throughput fluorometric assay to detect caspase-3-catalyzed amide bond proteolysis and liberation of the fluorophore, 7-amino-4-methylcoumarin-3-acetic acid (AMCA) (Scheme 2.1).

Scheme 2.1. First step in SAS method, screening diverse AMCA substrates **2.1**



Structure-Activity Relationship (SAR) of AMCA Substrates Against Caspase-3

Table 2.1 exhibits the relative cleavage efficiencies of a subset of initial substrates that were evaluated. Substrate **2.2** with a phenylethyl group at the R position had the

lowest cleavage efficiency of all of the substrates for which turnover was detected and was assigned a relative cleavage efficiency value of 1. Substrates for which no turnover was detected were given a relative cleavage efficiency value of 0. Substrates **2.8** and **2.9** with α -branching at the R position as provided by the cyclohexyl moiety along with hydroxyl and amide groups, respectively, that are both capable of H-bonding, showed the highest activity. Substrate **2.9** was particularly appealing because the amine functionality provides the opportunity to introduce a variety of additional functionality through amine acylation and reductive amination chemistry.

Table 2.1. Relative cleavage efficiencies of initial substrate library incorporating alkyl and polar R groups against caspase-3

Substrate	R	Rel. k_{cat}/K_m	Substrate	R	Rel. k_{cat}/K_m
2.2		1.0	2.6		2.0
2.3		2.0	2.7		0.0
2.4		2.0	2.8		7.8
2.5		2.0	2.9		7.9

The relative k_{cat}/K_m of the least efficiently cleaved substrate for which turnover could be detected was assigned a value of 1.0. For caspase-3, substrate **2.2** was assigned a value of 1.0.

To further explore the effect of α -branched substituents within the amide framework present in substrate **2.9**, an additional collection of substrates was prepared and evaluated (Table 2.2). When the cyclohexyl group that introduces α,α -dibranching in substrate **2.9** was replaced by the α -monobranched structures in substrates **2.10-2.14**, no substrate turnover was observed, which suggests the importance of maintaining dibranching functionality at this position. Similarly, dibranching substituents with the smaller methyl, ethyl, and isopropyl groups all displayed reduced cleavage efficiency (substrates **2.15-2.17**). In contrast, substrate **2.18**, which incorporated methyl and cyclohexyl substituents with an (*S*)-configuration, showed a greater than five-fold increase in cleavage efficiency relative to the initial cyclohexyl amide substrate **2.9**. It is noteworthy that caspase-3 showed very strong chiral recognition with no turnover for

substrate **2.19**, which is the (*R*)-epimer of substrate **2.18**. The strong preference for the (*S*)-epimer suggests the importance of this configuration for proper orientation and enhanced binding in the S2 pocket of caspase-3.

Table 2.2. Cleavage efficiencies of α -substituted amide R structures against caspase-3

Substrate	R	Rel. k_{cat}/K_m	Substrate	R	Rel. k_{cat}/K_m
2.9		7.9	2.15		0.0
2.10		0.0	2.16		3.4
2.11		0.0	2.17		4.2
2.12		0.0	2.18		39.3
2.13		0.0	2.19		0.0
2.14		0.0			

With substrate **2.18** incorporating cyclohexyl and methyl substituents with (*S*)-configuration providing the highest cleavage efficiency, we next chose to evaluate the replacement of the acetamide group with a variety of different amides and amines to identify key binding interactions for this region of the substrate (representative structures shown in Table 2.3). Replacing the acetamide in substrate **2.18** with the *N,N*-diethyl moiety in substrate **2.20** almost completely eliminated substrate turnover suggesting the importance of the H-bond donor or accepting capability of the amide functionality. In contrast, replacing the acetamide in substrate **2.18** with the benzamide in substrate **2.21** resulted in only a modest reduction in cleavage efficiency demonstrating that groups

considerably larger than acetamide can be accommodated in the enzyme active site. The isosteric secondary amine in substrate **2.22** resulted in a >10-fold reduction in cleavage efficiency of the substrate again confirming the importance of the amide functionality either for orientation or for hydrogen bonding interactions. The phenylacetamide present in substrate **2.23** resulted in a modest increase in cleavage efficiency while the isosteric phenylmethanesulfonamide present in **2.24**, which maintains hydrogen-bond donor and accepting capability, provided a considerable boost in cleavage efficiency. Finally, introduction of a second carboxylic acid in substrates **2.25-2.26** resulted in a considerable increase in cleavage efficiency with substrate **2.25** providing the highest cleavage efficiency out of all the substrates tested. This result is consistent with the known peptide substrate specificities for many of the caspases, which prefer a second aspartic acid residue at the P4 position, i.e., four amino acids away from the cleavage site.²⁹

Table 2.3. Cleavage efficiencies of *N*-substituted amide substrates with (*S*)-configured methyl and cyclohexyl substituents against caspase-3

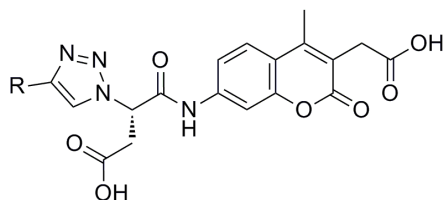
Substrate	R	Rel. k_{cat}/K_m	Substrate	R	Rel. k_{cat}/K_m
2.18		39.3	2.23		47
2.20		0.7	2.24		133
2.21		36.7	2.25		194
2.22		3.0	2.26		88

Substrate Screening and Optimization against Caspase-6

For peptide substrates, caspases-3 and -6 both require an aspartic acid residue at the site of cleavage but differ in preferred amino acid side chains two (P2) and four (P4) amino acids from the cleavage site.³⁵ In P2, caspase-3 shows a strong preference for small hydrophobic residues, while caspase-6 tolerates larger residues. In P4, caspase-3 demonstrates an almost absolute requirement for an aspartic acid residue, while larger aliphatic residues are tolerated by caspase-6. Therefore, all of the previously synthesized caspase-3 substrates were assayed against caspase-6 with key substrate activity relationships represented by the substrates shown in Table 2.4. No substrate turnover was observed for α -monobranched substrates as exemplified by substrates **2.10** and **2.13** therefore they were given the relative cleavage efficiencies of 0. Out of all the α,α -dibranched substrates, only substrates **2.18** and **2.19** with methyl and cyclohexyl substituents resulted in cleavage. Substrate **2.19** gave the lowest cleavage efficiency out of all the substrates for which turnover was detected for caspase-6 and was assigned a relative cleavage efficiency of 1. The (*S*)-epimer of substrate **2.18** provided a five-fold increase in cleavage efficiency relative to substrate **2.19** consistent with the stereochemical preference observed for caspase-3. Substrate **2.25** incorporating the carboxylic acid functionality resulted in a greater than two-fold increase in cleavage efficiency, while no substrate turnover was detected for substrate **2.26**, which also contains the carboxylic functionality but with a shorter chain length. The importance of the H-bond accepting capability of the amide carbonyl is apparent by comparing the cleavage rate of amide substrate **2.21** and amine substrate **2.22**. The phenylacetamide substrate **2.23** provided a considerable increase in cleavage efficiency with the corresponding isosteric phenylmethylsulfonamide substrate **2.24** also serving as a good substrate but with ~3-fold lower efficiency than **2.23**.

Table 2.4 displays notable differences in structure-activity relationships between caspase-3 and caspase-6 substrates. The chiral preference for (*S*)-epimer **2.18** was stronger for caspase-3 over caspase-6. This can be explained by the difference in size of the S2 pocket between caspase-3 and caspase-6. Various substitutions are tolerated in P2 for both caspases but caspase-6 is able to accommodate larger aliphatic and aromatic residues in contrast to caspase-3. A significant difference in relative cleavage efficiencies between benzamide **2.21** and phenylacetamide **2.23** was observed for caspase-3 and caspase-6. Substrate **2.23** showed only a modest increase in cleavage efficiency compared to substrate **2.21** for caspase-3, while **2.23** displayed a >18-fold increase compared to **2.21** for caspase-6. Consistent with the known peptidic substrate specificity data for caspases-3 and -6 (vide infra), substrate **2.25** with an acidic side chain capable of binding in the S4 pocket was the most efficiently cleaved by caspase-3; while substrate **2.23** displaying hydrophobic functionality was the most efficiently cleaved by caspase-6.

Table 2.4. Relative cleavage efficiencies of a select number of previously synthesized AMCA substrates against caspase-3 and -6



Substrate	R	Rel. k_{cat}/K_m		Substrate	R	Rel. k_{cat}/K_m		Substrate	R	Rel. k_{cat}/K_m	
		Casp3	Casp6			Casp3	Casp6			Casp3	Casp6
2.10		0.0	0.0	2.18		39.3	5.0	2.21		36.7	7.8
2.13		0.0	0.0	2.19		0.0	1.0	2.22		3.0	0.0
2.9		7.9	0.0	2.25		194	12.6	2.23		47	146
2.14		0.0	0.0	2.26		88	0.0	2.24		133	44
2.17		4.2	0.0								

The relative k_{cat}/K_m of the least efficiently cleaved substrate for which turnover could be detected was assigned a value of 1.0. For caspase-3, substrate **2.2** was assigned a value of 1.0 (Table 2.1). For caspase-6, substrate **2.19** was assigned a value of 1.0.

Because substrate **2.23** incorporating the phenylacetamide showed by far the greatest cleavage efficiency by caspase-6, analogues with substitution on the phenyl ring were prepared and evaluated (Table 2.5). Methyl and phenyl electron donating substituents at the *meta* position in substrates **2.27** and **2.28** decreased cleavage efficiency. The considerably lower cleavage efficiency of substrate **2.28** can be attributed

to unfavorable steric interactions with the large phenyl substituent. Modest reductions in cleavage efficiency were also observed for substrates with meta-substitution with the more strongly electron donating phenoxy and methoxy substituents, **2.29** and **2.30**, respectively, as well as with the electron-withdrawing trifluoromethyl substituent (substrate **2.31**). The electron-donating methoxy substituent at the *para* position provided an ~eight-fold drop in cleavage efficiency (substrate **2.32**). A slight decrease in cleavage efficiency was also observed for the electron-withdrawing chloro substituent at both the *para* and *ortho* positions, present in substrates **2.33** and **2.34**, respectively.

Table 2.5. Cleavage efficiencies of newly synthesized substituted phenylacetamide substrates against caspase-6

Substrate	R	Rel. k_{cat}/K_m	Substrate	R	Rel. k_{cat}/K_m
2.23		146	2.31		47
2.27		47	2.32		17
2.28		2.4	2.33		105
2.29		93	2.34		88
2.30		48			

Inhibitor Synthesis and Screening

The final step in the SAS method is conversion of the most active substrates to inhibitors.³³ Substrate cleavage is only observed when the amide carbonyl of the *N*-acyl aminocoumarin is properly positioned in the enzyme active site, thus allowing for the aminocoumarin group to be replaced by a mechanism-based pharmacophore to produce reversible or irreversible inhibitors. Pharmacophore selection was based upon a class of peptidic pan-caspase inhibitors containing the 2,3,5,6-tetrafluorophenoxy ketone irreversible inhibitor pharmacophore developed by Idun Pharmaceuticals because members of this inhibitor series have advanced the farthest in clinical development.^{36,37} Indeed, inhibitor **IDN-6556** (Figure 2.1) was determined to be nontoxic in mouse models and has entered Phase II clinical trials for the treatment of human liver preservation injury.³⁸ The 2,3,5,6-tetrafluorophenoxyketone pharmacophore was incorporated into three distinct substrates, **2.23-2.25**, that showed good cleavage efficiency by both caspase-3 and -6 to provide inhibitors **2.35-2.37** (see Experimental Section for inhibitor synthesis and characterization). The inhibitory activity of these compounds was then characterized against a full panel of caspases-1, -2, -3, -6, -7, -8, and -9 (Table 2.6). All three inhibitors provided potent inhibition of caspases-3 and -6 with k_{inact}/K_i values of $>20,000 \text{ M}^{-1}\text{s}^{-1}$ for each enzyme. Each of the inhibitors also provided potent inhibition of caspases-1, -7, -8 and -9 as would be expected by the similar substrate specificities across these enzymes. In contrast to the other caspases, caspase-2 has an extended binding pocket, and a P5 residue has shown to be critical for increased cleavage efficiency.^{29,39} Due to this extended binding requirement, it is not surprising that for inhibitors **2.35-2.37** poor inhibition of caspase-2 was observed with k_{inact}/K_i values of $< 33 \text{ M}^{-1}\text{s}^{-1}$.

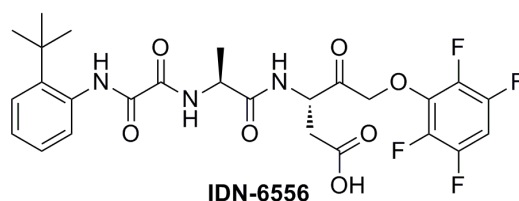


Figure 2.1. Pan caspase inhibitor incorporating a 2,3,5,6-tetrafluorophenoxy methyl ketone pharmacophore developed by Idun Pharmaceuticals.

Table 2.6. Inactivation rates of irreversible 2,3,5,6-tetrafluorophenoxymethyl inhibitors against caspases -1, -2, -3, -5, -6, -7, -8, and -9, cathepsins B, S, and V, and legumain

R =

2.35

2.36

2.37

	2.35	2.36	2.37
caspase 1	55,200 ± 2,600	243,250 ± 350	55,200 ± 200
caspase 2 ^b	33.0 ± 0.5	2.0 ± 0.1	6.90 ± 0.3
caspase 3	47,000 ± 1,400	81,700 ± 6,900	29,850 ± 850
caspase 6	23,100 ± 1,900	32,950 ± 1,650	45,750 ± 450
caspase 7	27,700 ± 2,000	57,250 ± 1,550	34,200 ± 3,800
caspase 8	82, 850 ± 1,150	30, 650 ± 1,950	60,000 ± 2,800
caspase 9	18,250 ± 4,050	7,550 ± 1,650	28,100 ± 2,500
cathepsin B ^c	no inhibition	no inhibition	no inhibition
cathepsin S	1,138 ± 526	331 ± 44	535 ± 44
cathepsin V ^c	no inhibition	no inhibition	no inhibition
legumain	not detected ^d	not detected ^d	no inhibition ^c

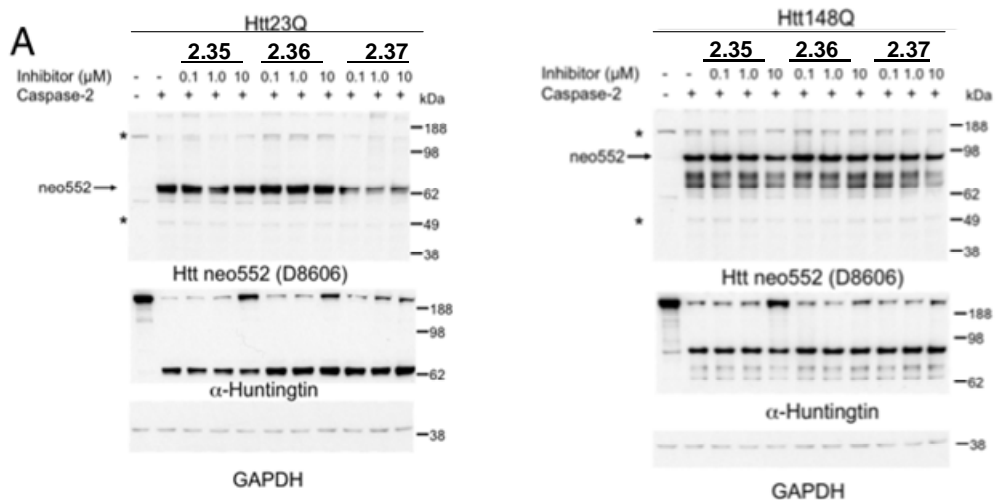
^a Assays determining k_{inact}/K_i ($M^{-1}s^{-1}$) were performed in duplicate with SD values included. ^b Assays determining k_{ass} ($M^{-1}s^{-1}$) were performed in duplicate with SD values included. ^c No inhibition after 15 min of preincubation with various concentrations of inhibitor of up to 400 μM . ^d Very weak inhibitory activity prevented determination of k_{inact}/K_i values, but IC_{50} values of 200-350 μM were obtained after 15 min of preincubation.

Recent studies have demonstrated that incorporation of P1 aspartyl side chain functionality in caspase inhibitors does not necessarily afford selective caspase inhibition. Aspartyl peptidyl fluoromethyl and chloromethyl ketones have been reported to efficiently inhibit other cysteine proteases such as cathepsin B, S and V as well as legumain.⁴⁰ More recently, aspartyl peptidic acyloxymethyl ketones have been utilized

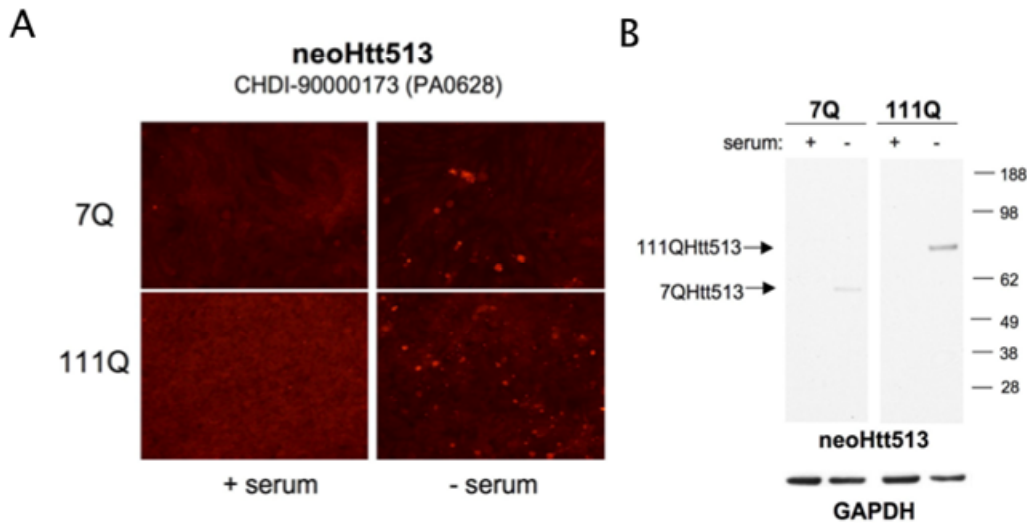
as efficient cell-permeable activity-based probes for legumain.⁴¹ Due to the aforementioned studies, all three inhibitors were screened against multiple cathepsins and legumain to evaluate cross-reactivity. Inhibitors **2.35**, **2.36**, and **2.37** displayed no inhibition of cathepsins B and V. Weak inhibition was observed for cathepsin S with k_{inact}/K_i values of $< 1,138 \text{ M}^{-1}\text{s}^{-1}$. Inhibition of legumain by **2.35** and **2.36** was so poor ($\text{IC}_{50} = 200\text{-}350 \text{ }\mu\text{M}$ at 15 min preincubation) that k_{inact}/K_i values could not be calculated, and for inhibitor **2.37** absolutely no inhibition of this enzyme could be detected. Overall, the caspase-designed aryloxymethyl ketone irreversible inhibitors showed little to no inhibition against legumain, cathepsin B, S, and V.

Evaluating Inhibitors in Huntington's Disease Models

In vitro, huntingtin is preferentially cleaved at amino acid 552 by caspase-2, 513 by caspase-3, and 586 by caspase-6.^{21,23} Inhibitors **2.35**, **2.36**, and **2.37** were each evaluated for Htt proteolysis by caspases-2, -3 and -6 with neopeptide antibodies that recognize the specific Htt cleavage products using an *in vitro* assay. Figure 2.2A shows western blot analysis of cellular lysates expressing full-length Htt23Q and Htt148Q treated with caspase-2, -3, and -6 and the three inhibitors at various concentrations using the neo-specific Htt antibodies. While minimal protection against cleavage of Htt by caspase-2 was observed as expected (Figure 2.2A), inhibitors **2.35**, **2.36**, and **2.37** each effectively blocked proteolysis by caspase-3 at amino acid 513 at all of the tested concentrations (0.1, 1.0 and 10 μM , Figure 2.2B). For full-length Htt treated with caspase-6, all three inhibitors, **2.35**, **2.36**, and **2.37** also showed complete protection from cleavage at amino acid 586 at concentrations of 1.0 and 10 μM (Figure 2.2C).



cells and evaluated Htt proteolysis 24 h after serum withdrawal. We found neoHtt513 antibody detected proteolysis of Htt in cells and lysates (Figure 2.3A,B). The levels of Htt proteolysis are higher in the *Hdh*^{111Q/111Q} when compared to *Hdh*^{7Q/7Q} lines (Figure 2.3A). Caspases are known to cleave the huntingtin protein containing the polyglutamine expansion and evidence suggests that these N-terminal cleavage products lead to cellular toxicity and apoptosis.¹⁸ All three irreversible inhibitors, **2.35**, **2.36**, and **2.37** at concentrations of 1-100 μ M were evaluated in *Hdh*^{7Q/7Q} and *Hdh*^{111Q/111Q} cells and were found to significantly block caspase activity in both the normal and expanded huntingtin cell model 24 h after serum deprivation (Figure 2.3C). Further, all three irreversible inhibitors, **2.35**, **2.36**, and **2.37** at concentrations of 10-100 μ M blocked the proteolysis of Htt as detected by neoHtt513 (Figure 2.3D). To determine the IC₅₀ values for inhibitors **2.35-2.37**, DEVDase activity was measured as a function of concentration for each inhibitor (Figure 2.4). The IC₅₀ values for inhibitor **2.35** and **2.36** were approximately 73-74 nM suggesting that these two inhibitors were most effective in blocking caspase activation in *Hdh*^{111Q/111Q} cells. Of note, the concentration needed to block caspase activity was lower in the HD cells compared to WT. Perhaps doses of caspase inhibitors can be utilized in therapeutics that do not impact normal cellular function. We do not know the exact mechanism for the lower dose required to inhibit the caspases in the *Hdh*^{111Q/111Q} cells but two possible explanations are: (1) the *Hdh*^{7Q/7Q} caspase-3 activity is from the proform of the enzyme which has a distinct kcat and Km when compared to active caspase-3 (*Hdh*^{111Q/111Q} could have more) or (2) alternatively the endogenous inhibitors of caspases are lower in the disease HD cells due to activation of degradative pathways such as proteasome or autophagy.



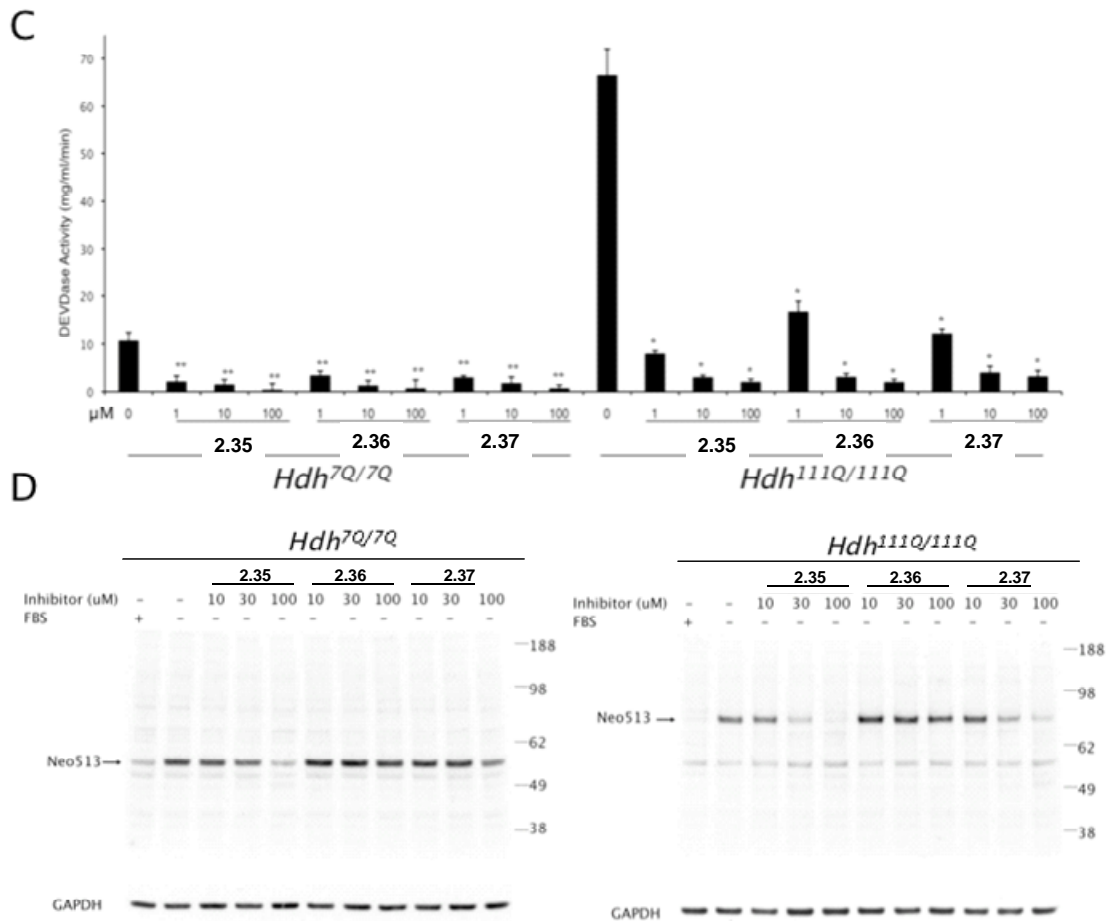


Figure 2.3. Inhibitors **2.35**, **2.36** and **2.37** Block Caspase Activation in Mouse Striatal *Hdh*^{7Q/7Q} and *Hdh*^{111Q/111Q} Cells. (A) Striatal *Hdh*^{7Q/7Q} and *Hdh*^{111Q/111Q} cells were cultured for 48 h and then subjected to analysis 24 h after serum withdrawal. Immunocytochemistry of *Hdh*^{7Q/7Q} and *Hdh*^{111Q/111Q} cells with neoHtt513 demonstrates cleavage of Htt. More Htt cleavage is found in the *Hdh*^{111Q/111Q} cells. (B) Western blot analysis using neoHtt513 antibody demonstrates proteolysis of Htt at the caspase-3 cleavage site located at amino acid 513 after serum withdrawal. (C) Striatal *Hdh*^{7Q/7Q} and *Hdh*^{111Q/111Q} cells were cultured for 48 h and then caspase activity was measured 24 h after serum withdrawal. *Hdh*^{111Q/111Q} cells have a 7-fold increase in caspase activation compared to control *Hdh*^{7Q/7Q}. Inhibitors **2.35**, **2.36**, **2.37** blocked caspase activity at the doses indicated. (D) Striatal *Hdh*^{7Q/7Q} and *Hdh*^{111Q/111Q} cells were cultured for 48 h and 24 h after serum withdrawal cells lysates were prepared. Inhibitors **2.35**, **2.36**, **2.37** blocked the proteolysis of Htt at the caspase-3 cleavage site located at amino acid 513 at the indicated doses.

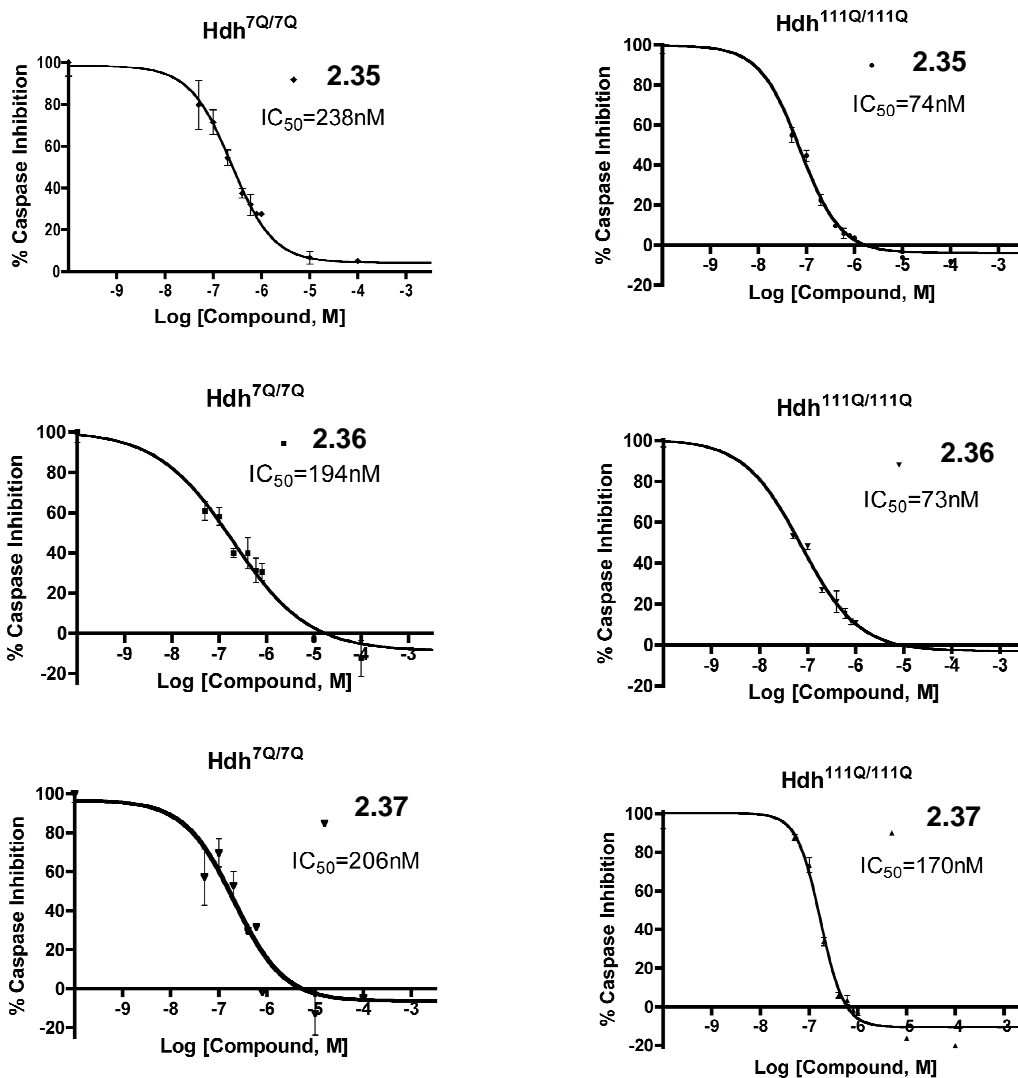


Figure 2.4. Inhibitors **2.35**, **2.36** and **2.37** Block Caspase Activation in Mouse Striatal *Hdh*^{7Q/7Q} and *Hdh*^{111Q/111Q} Cells with IC₅₀ in the nanomolar range.

Next, we evaluated these inhibitors *ex vivo*, using primary co-cultures of striatal and cortical neurons expressing normal and expanded Htt N-terminal fragments-Htt N90Q73, which induces degeneration of rat striatal and cortical neurons in primary co-cultures. We use co-cultures because in HD it is known that non-cell autonomous interactions and deficits in cortico-striatal circuitry occur. We use a fragment HD model because we have found these toxic Htt fragments cause the activation of the same proteases involved in cleaving full-length Htt and producing neurotoxicity. The percentage of healthy striatal and cortical neurons after treatment with varied concentrations of the irreversible inhibitors is shown in Figure 2.5. All three inhibitors

rescued striatal neurons from cell death, and treatment with inhibitor **2.35** resulted in the most significant increase of healthy striatal neurons at 0.4, 1.2, and 3.7 nM. The same trend is observed for the treatment of cortical neurons, with **2.35** resulting in a substantial increase (25-175%) in healthy neurons. The control is transfection of the fluorescent protein-encoding plasmid and empty plasmid in place of Htt plasmid. For the striatal, the control is 237% +/- 25. For the cortical, control is 311% +/- 60. This suggests that some doses of the inhibitors completely rescued the cell death mediated by mutant Htt. The efficacy of the inhibitors at even single digit nanomolar concentrations is likely due to the greater sensitivity of primary cultures to cell death when compared to the immortalized cells. Primary cultures are terminally differentiated and the culture conditions are distinct when compared to the immortalized mouse striatal *Hdh*^{7Q/7Q} and *Hdh*^{111Q/111Q} cell system.

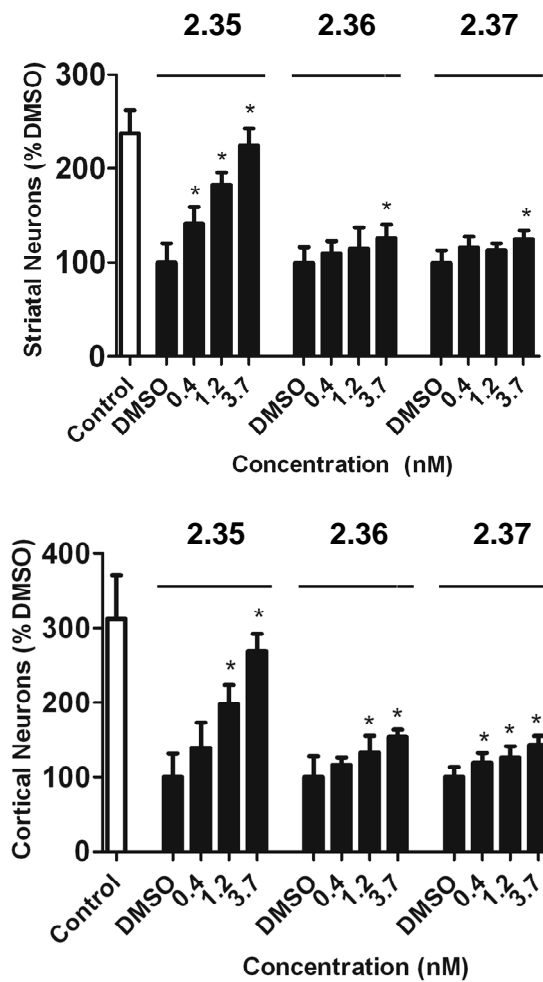


Figure 2.5. Protective Effects of Caspase Inhibitors in HttN90Q73-Induced Degeneration of Rat Striatal and Cortical Neurons in Primary Co-Culture.

Conclusions

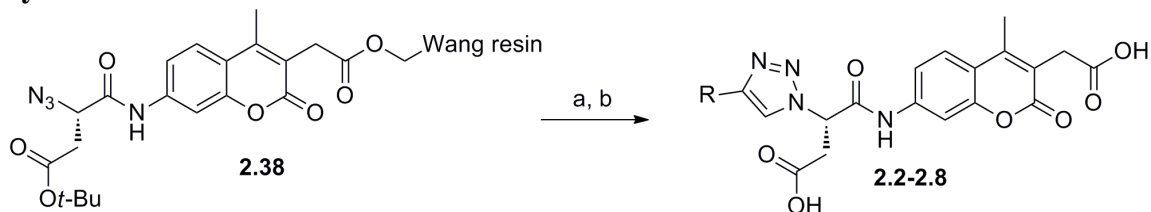
The substrate activity screening method was applied to caspases-3 and -6 leading to the identification of 1,2,3-triazole-based nonpeptidic substrates with high cleavage efficiencies. Subsequent replacement of the aminocoumarin reporter group with the 2,3,5,6-tetrafluorophenoxymethyl ketone pharmacophore in the most efficient substrates led to three novel nonpeptidic irreversible inhibitors showing strong potency against caspases and weak to no inhibition of other cysteine proteases previously reported to have cross reactivity with published caspase inhibitors. *In vitro*, all three inhibitors (**2.35**, **2.36** and **2.37**) blocked proteolysis of Htt at the caspase-3 and -6 cleavage sites, amino acids 513 and 586, respectively. Moreover, in a Huntington's disease model, all three inhibitors rescued cell death in striatal and cortical neurons at nanomolar concentrations. Overall, the identified inhibitors have validated the correlation between blocking caspase Htt cleavage and rescue of HD-mediated neurodegeneration.

Experimental

General Methods. Unless otherwise noted, all chemicals were obtained from commercial suppliers and used without further purification. Wang resin was purchased from Novabiochem (San Diego). *O*-(7-Azabenzotriazol-1-yl)-1,1,3,3-tetramethyluronium hexafluorophosphate (HATU) was purchased from PerSeptive Biosystems (Foster City, CA). (*S*)-*tert*-Butanesulfinamide was provided by AllyChem Co. Ltd (Dalian, China). *N*-(9-Fluorenylmethoxycarbonyl)-7-amino-4-methyl-3-carboxymethylcoumarin (Fmoc-AMCA) and N₃-AMCA-Wang resin **2.38** were prepared by a previously described procedure.³³ The hydrochloride salt of (*S*)-2-amino-2-cyclohexyl-3-butyne **2.40** was prepared from (*S*)-*tert*-butanesulfinamide by a previously described procedure.⁴³ Low amine content *N,N*-dimethylformamide (DMF) was purchased from EM Science (Cincinnati, OH), and anhydrous DMF was purchased from Acros (Morris Plains, NJ). Anhydrous THF, CH₂Cl₂, were obtained from Seca Solvent Systems by GlassContour and were dried over alumina under a nitrogen atmosphere. Solid-phase reactions were conducted in 12- or 35-mL polypropylene cartridges equipped with 70 mm PE frits attached to Teflon stopcocks. Cartridges and stopcocks were purchased from Applied Separations (Allentown, PA). Syringe barrels from 10-mL disposable syringes were used as stoppers for the 12-mL cartridges and polyethylene stoppers were used for the 35-mL cartridges. Solid phase reactions were rocked on an orbital shaker to agitate the resin. Solvents were expelled from the cartridges using pressurized air after removing the cartridge stopper and opening the stopcock. Resin was washed for a duration of 2-5 min. Solvents were removed using a Buchi rotary evaporator under reduced pressure. Reaction progress was monitored using thin-layer chromatography on Merck 60 F₂₅₄ 0.25 μm silica plates. Fmoc quantitation was performed according to literature procedure (Wood et al., 2005). High-performance liquid chromatography (HPLC) analysis was performed with a C18 reverse phase column (4.6 x 100 mm) with UV detection at 220, 254, and 280 nm. Reaction progress was monitored using thin-layer chromatography on Merck 60 F₂₅₄ 0.25 μm silica plates.

Liquid chromatography-mass spectrometry (LC/MS) data were obtained using a Hewlett Packard 1100 series liquid chromatography instrument and mass selective detector. ^1H and ^{13}C NMR spectra were measured with Bruker AVB-400, AVQ-400, and AV-300 spectrometers. NMR chemical shifts are reported in ppm downfield relative to the internal solvent peak, and coupling constants are reported in Hz. High-resolution mass spectra (HRMS) were performed by the University of California at Berkeley Mass Spectrometry Facility.

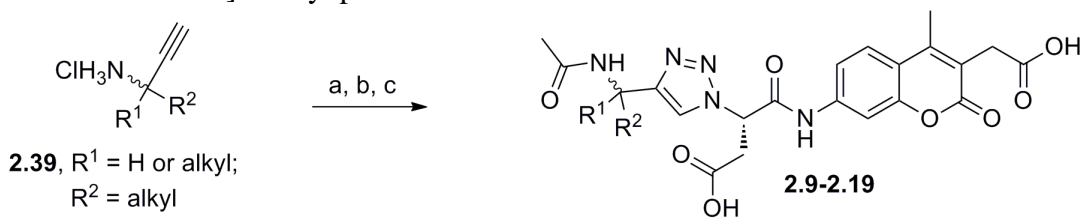
Synthesis of AMCA Substrates



Conditions: (a) alkyne, CuI, *i*-Pr₂EtN, THF rt; (b) CF₃CO₂H, CH₂Cl₂, rt

General Synthesis of 1,2,3-triazole-AMCA Substrates 2.2-2.8 (Table 2.1). To N₃-AMCA-Wang **38** resin (0.150 mmol) were added alkyne (0.02 M final concentration, 0.30 mmol, 2 equiv), *i*-Pr₂EtN (1.0 M final concentration, 15 mmol, 1.90 g, 100 equiv), and CuI (0.45 mmol, 0.09 g, 3 equiv) in THF, and the mixture was shaken for 48 h. After filtration, the resin was washed with three 10-mL portions each of THF, CH₃OH, THF, and CH₂Cl₂. The support-bound triazole product was cleaved from support and purified according to the general conditions described below. Alternatively, the support-bound triazole product was submitted to additional transformations before cleavage from support.

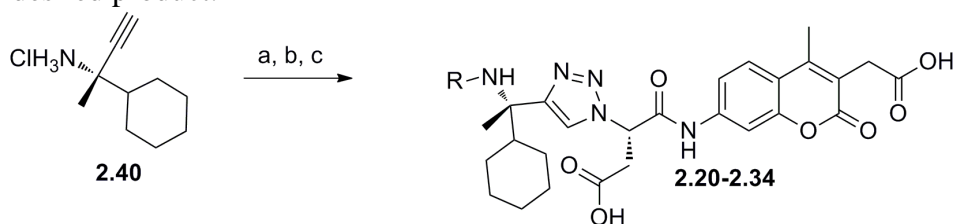
Cleavage and Purification conditions. The resin was swollen in CH₂Cl₂ in a cartridge. To 0.05 – 0.2 g of derivatized resin was added a 5 mL solution of 95% CF₃CO₂H, 2.5% H₂O, and 2.5% triisopropylsilane. The mixture was shaken for 1 h. Upon filtration, the resin was washed with the cleavage solution and three 10-mL portions of CH₂Cl₂. The filtrate and combined washes were concentrated under reduced pressure to yield the crude cleavage product. The crude product mixture was purified by HPLC [preparatory reverse phase C18 column (24.1 x 250 mm), acetonitrile/H₂O-0.1% TFA; 5-95% over 50 min then maintained at 95% acetonitrile for 10 min; 10 mL/min; 254 nm detection] and lyophilized.



2.39, R¹ = H or alkyl;
R² = alkyl

Conditions: (a) **1.38**, CuI, *i*-Pr₂EtN, THF rt; (b) acetic anhydride, *i*-Pr₂EtN, THF; (c) CF₃CO₂H, CH₂Cl₂.

General Synthesis of Acetylated Substrates 2.9-2.19 (Table 2.2). The hydrochloride salts **2.39** of 1-cyclohexylprop-2-yn-1-amine, 1-cyclopentylprop-2-yn-1-amine, 5-methylhex-1-yn-3-amine were synthesized from cyclohexanecarbaldehyde, cyclopentanecarbaldehyde, 3-methylbutanal, respectively following a previously described procedure.⁴⁴ The hydrochloride salts **2.39** of 4-methylpent-1-yn-3-amine and (*S*)-3,4-dimethylpent-1-yn-3-amine were synthesized from (*R*)-*tert*-Butanesulfinamide and (*S*)-*tert*-Butanesulfinamide, respectively by a previously reported procedure (Patterson et al., 2006). 3-ethylpent-1-yn-3-amine, 2-methylbut-3-yn-2-amine, and 1-ethynylcyclohexylamine were obtained from commercial suppliers. To the resin obtained above using the above amines or hydrochloride salts (0.300 mmol, 0.06 g, 2.0 equiv) was added acetic anhydride (0.4 M final concentration, 0.08 g, 0.750 mmol, 5 equiv) and *i*-Pr₂EtN (1.0 M final concentration, 1.50 mmol, 0.19 g, 10 equiv) in DMF. The resulting mixture was shaken for 18 h. After filtration followed by washing with three 10-mL portions each of DMF, THF, CH₃OH, THF, and CH₂Cl₂, the substrate was cleaved from the solid support and purified using the general cleavage and purification procedures to give the desired product.



Conditions: (a) **2.38**, CuI, *i*-Pr₂EtN, THF; (b) anhydride, *i*-Pr₂EtN, THF or carboxylic acid, triphosgene, 2,4,6-collidine, *i*-Pr₂EtN or aldehyde, NaBH(OAc)₃, THF or BnSO₂Cl, DMAP, Et₃N, DMF; (c) CF₃CO₂H, CH₂Cl₂.

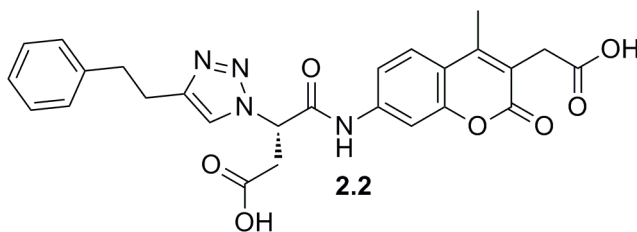
General Synthesis of Acylated Substrates 2.25 and 2.26 from Anhydrides (Table 2.3). To the resin obtained above using the hydrochloride salt of (*S*)-2-amino-2-cyclohexyl-3-butyne **2.40** (0.300 mmol, 0.06 g, 2.0 equiv) was added acetic, glutaric, or succinic anhydride (0.4 M final concentration, 0.750 mmol, 5 equiv) and *i*-Pr₂EtN (1.0 M final concentration, 1.50 mmol, 0.19 g, 10 equiv) in DMF. The resulting mixture was shaken for 18 h. After filtration followed by washing with three 10-mL portions each of DMF, THF, CH₃OH, THF, and CH₂Cl₂, the substrate was cleaved from the solid support and purified using the general cleavage and purification procedures to give the desired product.

General Synthesis of Acylated Substrates 2.21, 2.23, and 2.27-2.34 from Carboxylic Acids (Tables 2.3-2.4). To the resin obtained above using the hydrochloride salt of (*S*)-2-amino-2-cyclohexyl-3-butyne **2.40** (0.300 mmol, 0.06 g, 2.0 equiv) was added *i*-Pr₂EtN (1.20 mmol, 0.16 g, 8 equiv). To a THF solution of carboxylic acid (0.1 M final concentration, 0.525 mmol, 3.5 equiv) and triphosgene (0.03 M final concentration, 0.165 mmol, 0.05 g, 1.1 equiv) was added 2,4,6-collidine (0.3 M final

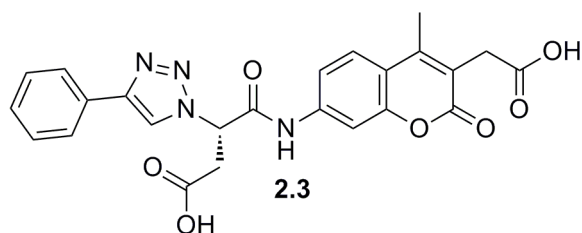
concentration, 1.50 mmol, 0.18 g, 10 equiv). The resulting slurry was stirred for 1 min and was added to the derivatized resin. The resulting mixture was shaken for 4-12 h. After filtration, the resin was washed with three-10 mL portions of THF and procedure was repeated two times. After filtration followed by washing with three 10-mL portions each of THF, CH₃OH, THF, and CH₂Cl₂, the substrate was cleaved from the solid support and purified using the general cleavage and purification procedures to give the desired product.

Synthesis of Sulfonamide Substrate 2.24 (Table 2.3). To the resin obtained above using the hydrochloride salt of (*S*)-2-amino-2-cyclohexyl-3-butyne **2.40** (0.300 mmol, 0.06 g, 2.0 equiv) was added phenylmethanesulfonyl chloride (0.33 mmol, 0.06 g, 1.10 equiv), DMAP (0.06 mmol, 0.007 g, 0.2 equiv), and NEt₃ (0.66 mmol, 0.07 g, 2.2 equiv) in CH₂Cl₂ (2.0 mL). The resulting mixture was shaken for 48 h. After filtration, the resin was washed with three-10 mL portions of THF and procedure was repeated two times. After filtration followed by washing with three 10-mL portions each of THF, CH₃OH, THF, and CH₂Cl₂, the substrate was cleaved from the solid support and purified using the general cleavage and purification procedures to give the desired product.

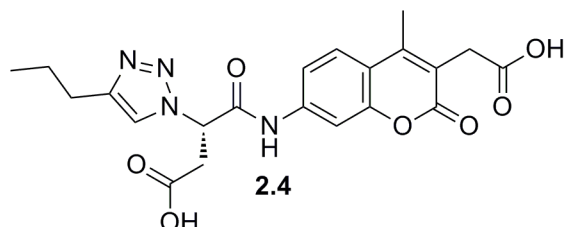
General Synthesis of Amine Substrates 2.20 and 2.22 (Table 2.3). To the resin obtained above using the hydrochloride salt of (*S*)-2-amino-2-cyclohexyl-3-butyne **2.40** (0.300 mmol, 0.06 g, 2.0 equiv) was added aldehyde (0.8 M final concentration, 1.50 mmol, 10 equiv), acetic acid (1.50 mmol, 0.09 g, 10 equiv), and NaHB(OAc)₃ (1.50 mmol, 0.32 g, 10 equiv) in THF. The resulting mixture was shaken for 36 h. After filtration followed by washing with three 10-mL portions each of THF, CH₃OH, THF, and CH₂Cl₂, the substrate was cleaved from the solid support and purified using the general cleavage and purification procedures to give the desired product.



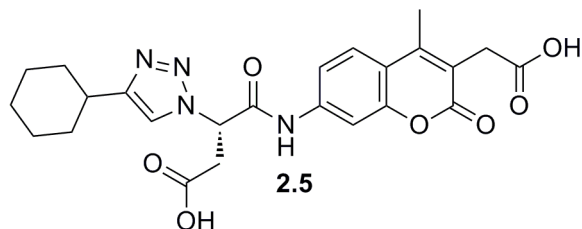
Substrate 2.2: ¹H NMR (400 MHz, DMSO *d*-6): δ 2.37 (s, 3), 2.92 (s, 4), 3.21-3.39 (m, 2), 3.59 (s, 2), 5.74-5.78 (t, 1, *J* = 7.4), 7.14-7.17 (m, 1), 7.20-7.26 (m, 4), 7.48-7.50 (d, 1, *J* = 8.8), 7.71 (s, 1), 7.79-7.81 (d, 1, *J* = 8.8), 8.02 (s, 1), 11.00 (s, 1). HRMS (FAB+) *m/z*: 505.1723 (MH⁺ C₂₆H₂₅N₄O₇ requires 505.1737).



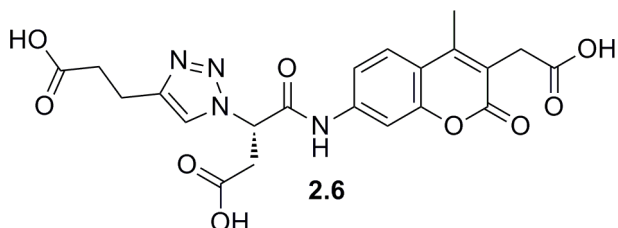
Substrate 2.3: ^1H NMR (400 MHz, DMSO *d*-6): δ 2.37 (s, 3), 3.38-3.43 (m, 2), 3.58 (s, 2), 5.86-5.89 (t, 1, $J = 7.2$), 7.32-7.36 (t, 1, $J = 7.6$), 7.44-7.48 (t, 2, $J = 7.6$), 7.51-7.53 (d, 1, $J = 7.6$), 7.73 (s, 1), 7.80-7.82 (d, 1, $J = 8.8$), 7.87-7.88 (d, 2, $J = 7.6$), 8.82 (s, 1), 11.01 (s, 1). HRMS (FAB+) m/z : 477.1410 (MH^+ $\text{C}_{24}\text{H}_{21}\text{N}_4\text{O}_7$ requires 477.1424).



Substrate 2.4: ^1H NMR (400 MHz, DMSO *d*-6): δ 0.88-0.92 (t, 3, $J = 7.4$), 1.58-1.62 (t, 2, $J = 7.2$), 2.36 (s, 3), 2.54-2.61 (m, 2), 3.23-3.38 (m, 2), 3.58 (s, 2), 5.76-5.74 (t, 1, $J = 6.8$), 7.48-7.50 (d, 1, $J = 8.4$), 7.71 (s, 1), 7.79-7.81 (d, 1, $J = 8.4$), 8.03 (s, 1), 10.99 (s, 1). HRMS (FAB+) m/z : 443.1567 (MH^+ $\text{C}_{21}\text{H}_{23}\text{N}_4\text{O}_7$ requires 443.1555).

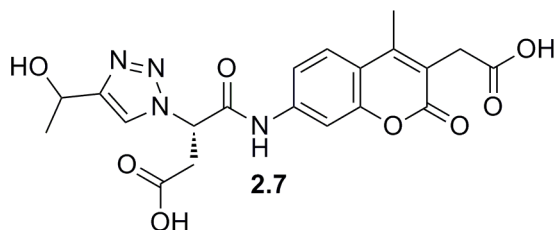


Substrate 2.5: ^1H NMR (400 MHz, DMSO *d*-6): δ 1.17-1.22 (m, 1), 1.29-1.41 (m, 4), 1.64-1.67 (m, 1), 1.69-1.73 (m, 2), 1.93-2.07 (m, 2), 2.36 (s, 3), 2.65-2.7 (m, 1), 3.22-3.39 (m, 2), 3.58 (s, 2), 5.72-5.76 (t, 1, $J = 7.4$), 7.49-7.51 (d, 1, $J = 8.8$), 7.72 (s, 1), 7.79-7.80 (d, 1, $J = 8.8$), 8.01 (s, 1), 11.01 (s, 1). HRMS (FAB+) m/z : 483.1879 (MH^+ $\text{C}_{24}\text{H}_{28}\text{N}_4\text{O}_7$ requires 483.1875).

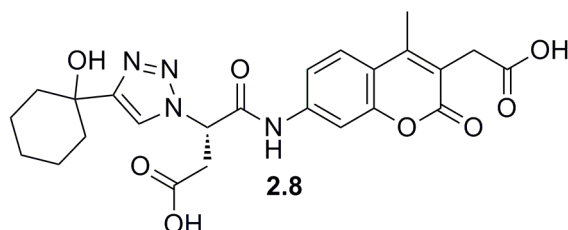


Substrate 2.6: ^1H NMR (400 MHz, DMSO *d*-6): δ 2.36 (s, 3), 2.57-2.61 (t, 2, $J = 7.6$), 2.84-2.87 (t, 2, $J = 7.6$), 3.21-3.39 (m, 2), 3.58 (s, 2), 5.73-5.77 (t, 1, $J = 7.4$), 7.48-

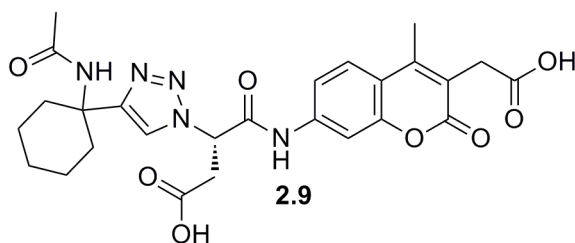
7.50 (d, 1, $J = 8.8$), 7.71 (s, 1), 7.78-7.80 (d, 1, $J = 8.8$), 8.04 (s, 1), 11.01 (s, 1). HRMS (FAB+) m/z : 473.1309 (MH^+ $C_{21}H_{21}N_4O_7$ requires 473.1315).



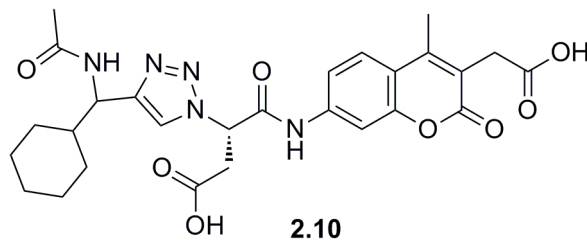
Substrate 2.7: 1H NMR (400 MHz, DMSO d_6): δ 1.40-1.41 (d, 3, $J = 6.4$), 2.37 (s, 3), 3.25-3.41 (m, 2), 3.59 (s, 2), 4.82-4.85 (t, 1, $J = 6.4$), 5.76-5.79 (t, 1, $J = 7.2$), 7.49-7.51 (d, 1, $J = 8.8$), 7.71 (s, 1), 7.79-7.81 (d, 1, $J = 8.8$), 8.09 (s, 1), 11.00 (s, 1). HRMS (FAB+) m/z : 445.1359 (MH^+ $C_{20}H_{21}N_4O_8$ requires 445.1356).



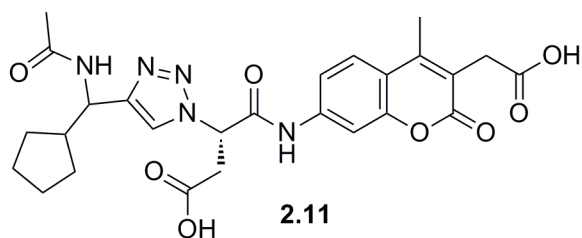
Substrate 2.8: 1H NMR (400 MHz, DMSO d_6): δ 1.25-1.40 (m, 4), 1.50-1.67 (m, 4), 1.82-1.84 (m, 2), 2.37 (s, 3), 3.28-3.37 (m, 2), 3.54 (s, 2), 5.74-5.77 (t, 1, $J = 7.2$), 7.49-7.51 (d, 1, $J = 8.8$), 7.72 (s, 1), 7.80-7.82 (d, 1, $J = 8.8$), 8.04 (s, 1), 11.00 (s, 1). HRMS (FAB+) m/z : 521.1648 (MNa^+ $C_{24}H_{26}N_4O_8Na$ requires 521.1641).



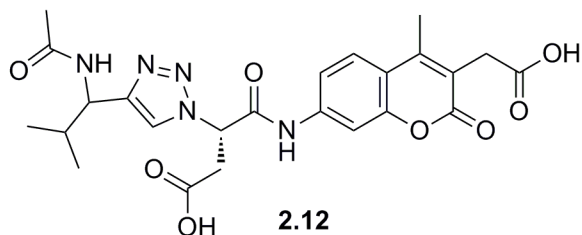
Substrate 2.9: 1H NMR (400 MHz, DMSO d_6): δ 1.24-1.43 (m, 6), 1.52-1.79 (m, 2), 1.82 (s, 3), 2.27-2.34 (m, 2), 2.36 (s, 3), 3.25-3.33 (m, 2), 3.58 (s, 2), 5.69-5.73 (t, 1, $J = 7.2$), 7.48-7.50 (d, 1, $J = 8.8$), 7.71 (s, 1), 7.75 (s, 1), 7.79-7.81 (d, 1, $J = 8.8$), 7.96 (s, 1), 10.99 (s, 1). HRMS (FAB+) m/z : 540.2094 (MH^+ $C_{26}H_{29}N_5O_8$ requires 540.2102).



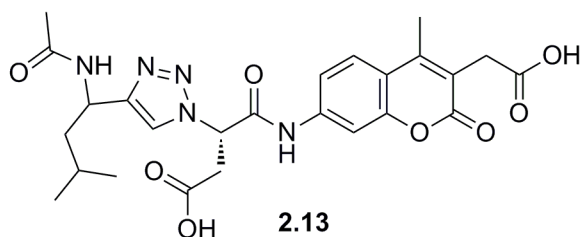
Substrate 2.10: LRMS calculated for MH^+ $\text{C}_{27}\text{H}_{31}\text{N}_5\text{O}_8$ 554.2, found 554.1.



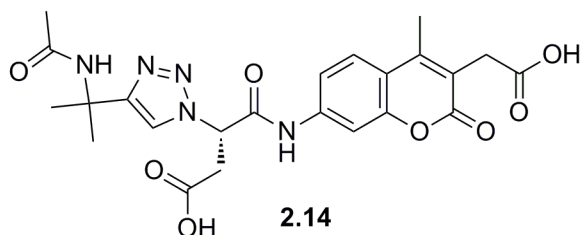
Substrate 2.11: LRMS calculated for MH^+ $\text{C}_{26}\text{H}_{29}\text{N}_5\text{O}_8$ 540.2, found 540.1.



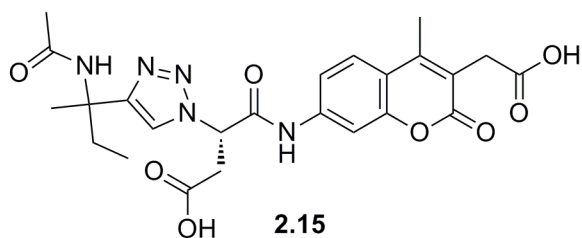
Substrate 2.12: LRMS calculated for MH^+ $\text{C}_{24}\text{H}_{27}\text{N}_5\text{O}_8$ 514.2, found 514.1.



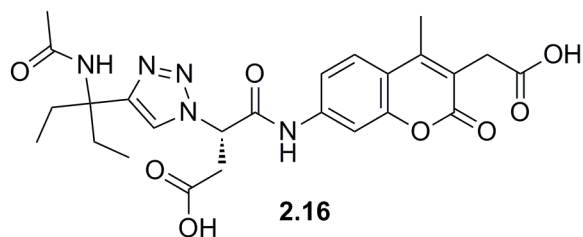
Substrate 2.13: LRMS calculated for MH^+ $\text{C}_{25}\text{H}_{29}\text{N}_5\text{O}_8$ 528.2, found 528.1.



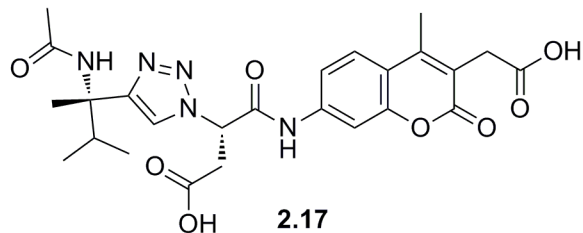
Substrate 2.14: LRMS calculated for MH^+ $\text{C}_{23}\text{H}_{25}\text{N}_5\text{O}_8$ 500.2, found 500.1.



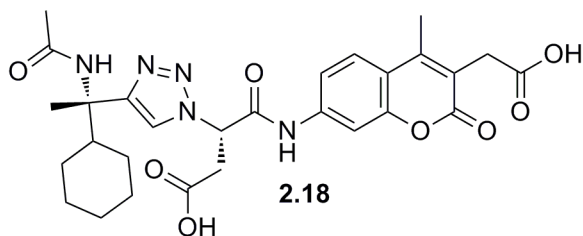
Substrate 2.15: LRMS calculated for MH^+ $\text{C}_{24}\text{H}_{27}\text{N}_5\text{O}_8$ 514.2, found 514.1.



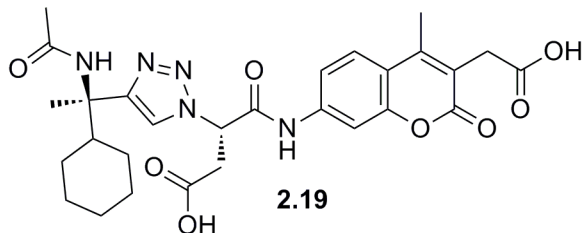
Substrate 2.16: LRMS calculated for MH^+ $\text{C}_{25}\text{H}_{29}\text{N}_5\text{O}_8$ 528.2, found 528.2.



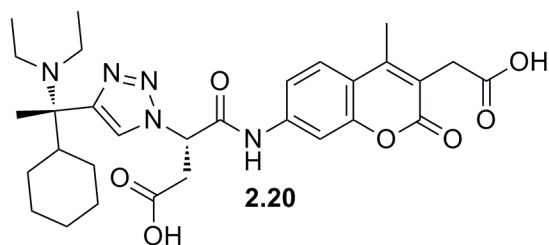
Substrate 2.17: LRMS calculated for MH^+ $\text{C}_{25}\text{H}_{29}\text{N}_5\text{O}_8$ 528.2, found 528.2.



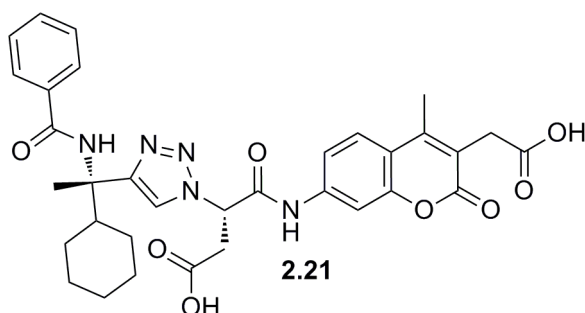
Substrate 2.18: ^1H NMR (400 MHz, $\text{DMSO } d_6$): δ 0.79-1.12 (m, 6) 1.32-1.35 (m, 2), 1.58 (s, 3), 1.67-1.70 (m, 2), 1.80 (s, 3), 2.01-2.03 (m, 1), 2.36 (s, 3), 3.21-3.46 (m, 2), 3.58 (s, 2), 5.70-5.73 (t, 1, $J = 7.4$), 7.47-7.49 (d, 1, $J = 8.8$), 7.66 (s, 1), 7.70 (s, 1), 7.79-7.81 (d, 1, $J = 8.8$), 8.00 (s, 1), 10.99 (s, 1). HRMS (FAB+) m/z : 568.2407 (MH^+ $\text{C}_{28}\text{H}_{34}\text{N}_5\text{O}_8$ requires 568.2415).



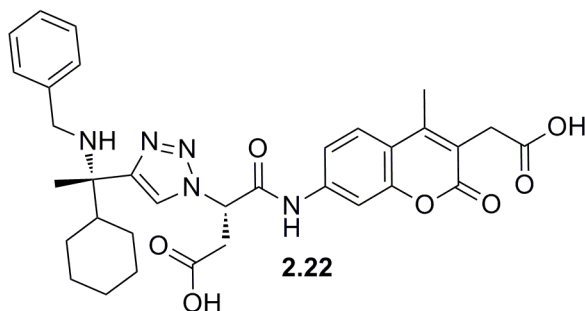
Substrate 2.19: ^1H NMR (400 MHz, $\text{DMSO } d_6$): δ 0.79-1.04 (m, 6) 1.30-1.33 (m, 2), 1.58 (s, 3), 1.66-1.69 (m, 2), 1.80 (s, 3), 2.00-2.03 (m, 1), 2.36 (s, 3), 3.26-3.58 (m, 2), 3.58 (s, 2), 5.71-5.74 (t, 1, $J = 7.4$), 7.47-7.49 (d, 1, $J = 8.8$), 7.68 (s, 1), 7.70 (s, 1), 7.78-7.80 (d, 1, $J = 8.8$), 8.01 (s, 1), 10.99 (s, 1). HRMS (FAB+) m/z : 590.2227 (MNa^+ $\text{C}_{28}\text{H}_{33}\text{N}_5\text{O}_8\text{Na}$ requires 590.2224).



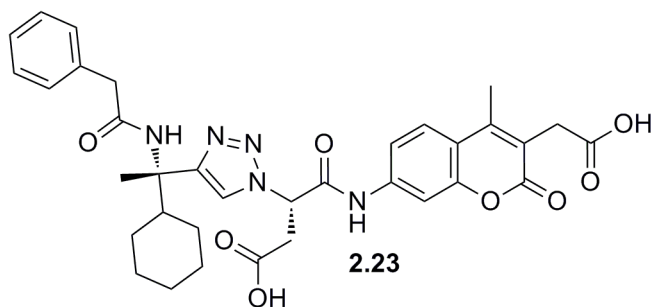
Substrate 2.20: $^1\text{H NMR}$ (400 MHz, DMSO *d*-6): δ 0.96-0.99 (m, 4) 1.11-1.30 (m, 10), 1.62-1.65 (m, 2), 1.68 (s, 3), 1.73-1.77 (m, 1), 2.36 (s, 3), 3.05-3.19 (m, 4), 3.21-3.39 (m, 2), 3.58 (s, 2), 5.85-5.89 (t, 1, $J = 7.4$), 7.46-7.48 (d, 1, $J = 8.8$), 7.71 (s, 1), 7.79-7.81 (d, 1, $J = 8.8$), 8.57 (s, 1), 11.00 (s, 1). HRMS (FAB+) m/z : 582.2928 (MH^+ $\text{C}_{30}\text{H}_{40}\text{N}_5\text{O}_7$ requires 582.2932).



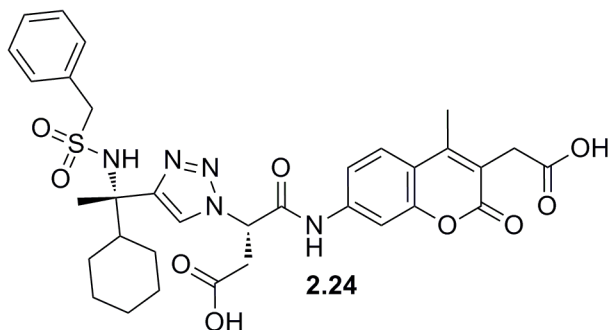
Substrate 2.21: $^1\text{H NMR}$ (400 MHz, DMSO *d*-6): δ 0.81-1.19 (m, 6) 1.57-1.60 (m, 2), 1.72 (s, 3), 1.78-1.81 (m, 2), 2.27-2.29 (m, 1), 2.36 (s, 3), 3.27-3.41 (m, 2), 3.58 (s, 2), 5.72-5.75 (t, 1, $J = 7.4$), 7.43-7.50 (m, 4), 7.69 (s, 1), 7.73-7.75 (d, 2, $J = 8.0$), 7.79-7.81 (d, 1, $J = 8.8$), 8.04 (s, 1), 8.12 (s, 1), 11.00 (s, 1). HRMS (FAB+) m/z : 652.2383 (MNa^+ $\text{C}_{33}\text{H}_{35}\text{N}_5\text{O}_8\text{Na}$ requires 652.2368).



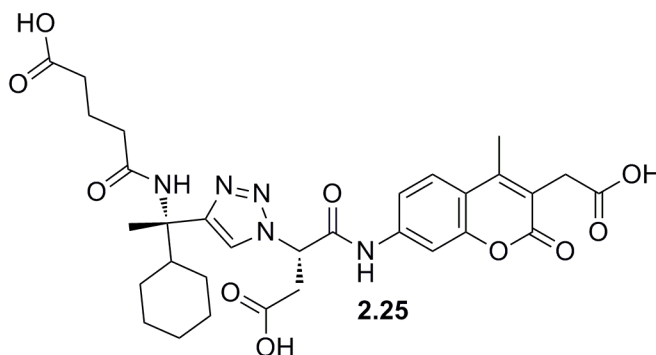
Substrate 2.22: $^1\text{H NMR}$ (400 MHz, DMSO *d*-6): δ 0.94-1.15 (m, 8), 1.61 (s, 3), 1.77-1.87 (m, 2), 2.21-2.23 (m, 1), 2.36 (s, 3), 3.25-3.41 (m, 2), 3.58 (s, 2), 3.93 (s, 2), 5.87-5.91 (t, 1, $J = 7.6$), 7.29-7.34 (m, 5), 7.48-7.50 (d, 1, $J = 8.8$), 7.73 (s, 1), 7.80-7.82 (d, 1, $J = 8.8$), 8.49 (s, 1), 10.99 (s, 1). HRMS (FAB+) m/z : 616.2771 (MH^+ $\text{C}_{33}\text{H}_{38}\text{N}_5\text{O}_8$ requires 616.2764).



Substrate 2.23: $^1\text{H NMR}$ (400 MHz, DMSO *d*-6): δ 0.76-1.11 (m, 6) 1.30-1.33 (m, 2), 1.59 (s, 3), 1.65-1.70 (m, 4), 2.00-2.03 (m, 1), 2.37 (s, 3), 3.20-3.43 (m, 2), 3.58 (s, 2), 5.67-5.71 (t, 1, $J = 7.6$), 7.17-7.27 (m, 5), 7.47-7.49 (d, 1, $J = 7.2$), 7.71 (s, 1), 7.79-7.81 (d, 1, $J = 8.8$), 7.84 (s, 1), 7.94 (s, 1), 11.00 (s, 1). HRMS (FAB+) m/z : 666.2540 ($\text{MNa}^+ \text{C}_{34}\text{H}_{37}\text{N}_5\text{O}_8\text{Na}$ requires 666.2535).

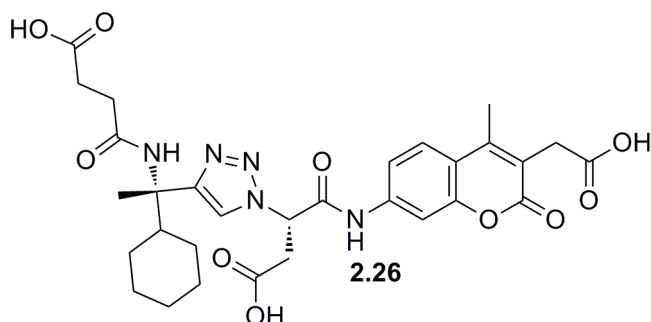


Substrate 2.24: $^1\text{H NMR}$ (400 MHz, DMSO *d*-6): δ 0.81-1.16 (m, 6) 1.54-1.57 (m, 5), 1.71-1.73 (m, 1), 1.91-1.94 (m, 1), 2.05-2.10 (m, 1), 2.34 (s, 3), 3.29-3.34 (m, 2), 3.42-3.46 (m, 1), 3.57 (s, 2), 3.63-3.67 (m, 1), 5.76-5.80 (t, 1, $J = 7.6$), 7.12-7.14 (m, 2 H), 7.20-7.22 (m, 4 H), 7.40-7.43 (d, 1, $J = 7.2$), 7.66-7.64 (d, 1, $J = 7.2$), 7.72-7.74 (d, 1, $J = 8.8$), 8.23 (s, 1), 10.89 (s, 1). HRMS (FAB+) m/z : 702.2210 ($\text{MNa}^+ \text{C}_{33}\text{H}_{37}\text{N}_5\text{O}_9\text{S}$ requires 702.2202).

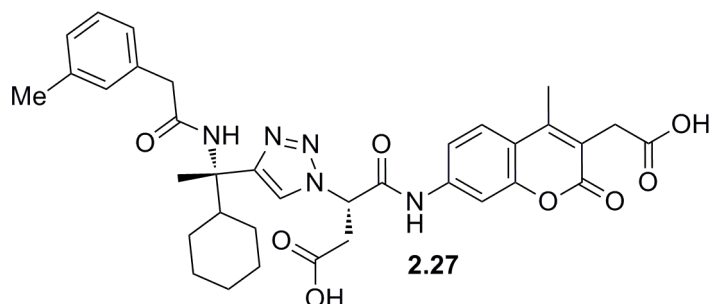


Substrate 2.25: $^1\text{H NMR}$ (400 MHz, DMSO *d*-6): δ 0.72-1.13 (m, 6) 1.32-1.36 (m, 2), 1.59 (s, 3), 1.61-1.67 (m, 4), 1.98-2.02 (m, 1), 2.10-2.17 (m, 4), 2.37 (s, 3), 3.26-3.43 (m, 2), 3.59 (s, 2), 5.70-5.74 (t, 1, $J = 7.4$), 7.49-7.51 (d, 1, $J = 8.8$), 7.60 (s, 1), 7.70

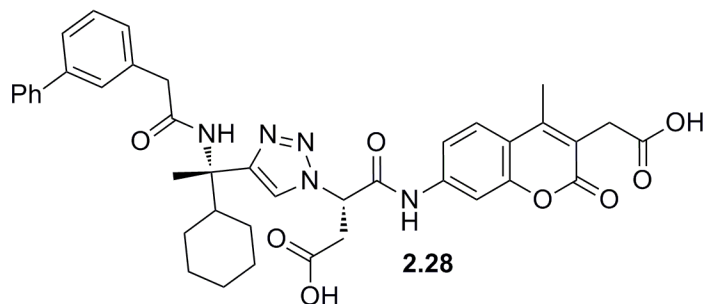
(s, 1), 7.80-7.82 (d, 1, $J = 8.8$), 8.00 (s, 1), 11.00 (s, 1). HRMS (FAB+) m/z : 662.2438 ($MNa^+ C_{31}H_{37}N_5O_{10}Na$ requires 662.2427).



Substrate 2.26: 1H NMR (400 MHz, DMSO d_6): δ 0.98-1.11 (m, 6) 1.37-1.39 (m, 2), 1.58 (s, 3), 1.63-1.66 (m, 6), 1.99-2.01 (m, 1), 2.36 (s, 3), 3.25-3.43 (m, 2), 3.58 (s, 2), 5.68-5.72 (t, 1, $J = 7.4$), 7.48-7.50 (d, 1, $J = 8.8$), 7.65 (s, 1), 7.70 (s, 1) 7.79-7.81 (d, 1, $J = 8.8$), 7.98 (s, 1), 11.00 (s, 1). HRMS (FAB+) m/z : 648.2282 ($MNa^+ C_{30}H_{35}N_5O_{10}Na$ requires 648.2272).

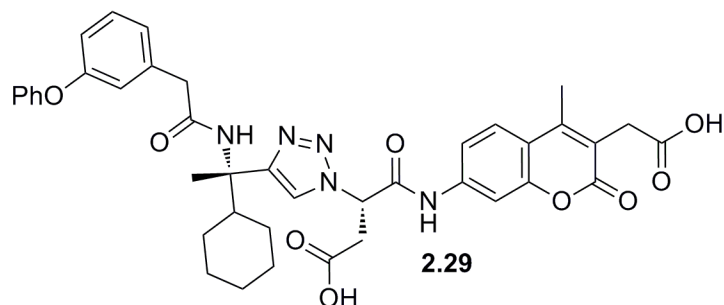


Substrate 2.27: 1H NMR (400 MHz, DMSO d_6): δ 0.75-1.13 (m, 6) 1.34-1.37 (m, 2), 1.60 (s, 3), 1.67-1.69 (m, 2), 2.02-2.07 (m, 1), 2.25 (s, 3), 2.37 (s, 3), 3.23-3.42 (m, 4), 3.59 (s, 2), 5.68-5.72 (t, 1, $J = 7.4$), 6.98-7.03 (m, 3), 7.12-7.16 (t, 1, $J = 7.6$), 7.47-7.50 (d, 1, $J = 8.8$), 7.72 (s, 1), 7.79 (s, 1), 7.81 (s, 1), 7.96 (s, 1), 11.01 (s, 1). HRMS (FAB+) m/z : 680.2696 ($MNa^+ C_{35}H_{39}N_5O_8Na$ requires 680.2710).

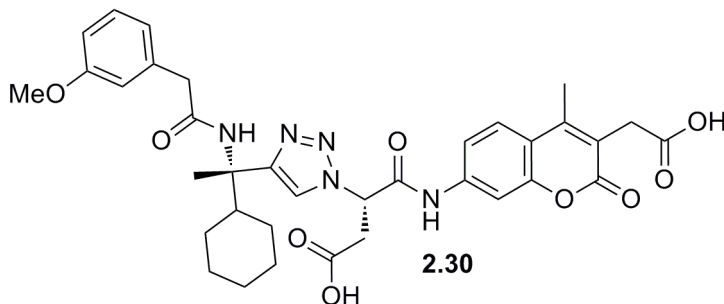


Substrate 2.28: 1H NMR (400 MHz, DMSO d_6): δ 0.72-1.11 (m, 6) 1.34-1.37 (m, 2), 1.56 (s, 3), 1.58-1.61 (m, 2), 2.03-2.08 (m, 1), 2.37 (s, 3), 3.23-3.52 (m, 4), 3.59 (s, 2), 5.70-5.74 (t, 1, $J = 7.4$), 7.21-7.22 (d, 1, $J = 7.2$), 7.34-7.36 (m, 2), 7.43-7.49 (m,

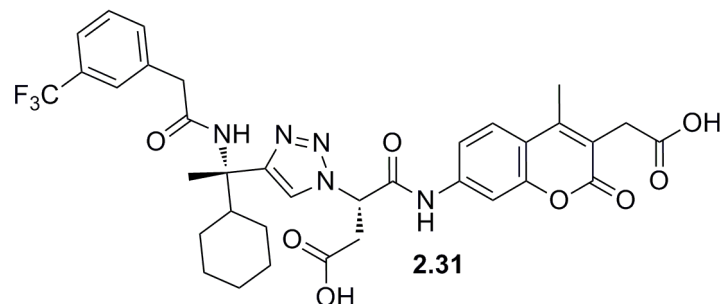
3), 7.55 (s, 1), 7.60-7.62 (d, 2, $J = 7.2$), 7.71 (s, 1), 7.78-7.81 (d, 1, $J = 8.8$), 7.91 (s, 1), 7.99 (s, 1), 10.99 (s, 1). HRMS (FAB+) m/z : 720.3033 (MH^+ $C_{40}H_{42}N_5O_8$ requires 720.3044).



Substrate 2.29: 1H NMR (400 MHz, DMSO d_6): δ 0.75-1.10 (m, 6) 1.30-1.35 (m, 2), 1.57 (s, 3), 1.61-1.66 (m, 2), 2.00-2.05 (m, 1), 2.37 (s, 3), 3.23-3.46 (m, 4), 3.59 (s, 2), 5.72-5.77 (t, 1, $J = 7.4$), 6.84-6.86 (m, 2), 6.92 (s, 1), 6.97-6.99 (d, 2, $J = 7.6$), 7.11-7.13 (m, 1), 7.27-7.30 (t, 1, $J = 7.6$), 7.34-7.38 (t, 2, $J = 7.6$), 7.48-7.50 (d, 1, $J = 8.8$), 7.71 (s, 1), 7.79-7.81 (d, 2, $J = 8.8$), 7.96 (s, 1), 11.00 (s, 1). HRMS (FAB+) m/z : 758.2802 (MNa^+ $C_{40}H_{41}N_5O_9Na$ requires 758.2810).

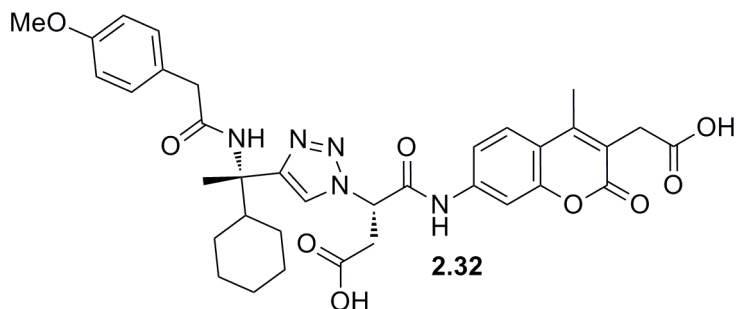


Substrate 2.30: 1H NMR (400 MHz, DMSO d_6): δ 0.78-1.13 (m, 6) 1.32-1.37 (m, 2), 1.60 (s, 3), 1.66-1.70 (m, 2), 2.01-2.06 (m, 1), 2.38 (s, 3), 3.22-3.42 (m, 4), 3.59 (s, 2), 3.71 (s, 3), 5.69-5.73 (t, 1, $J = 7.4$), 6.74-6.82 (m, 3), 7.13-7.17 (t, 1, $J = 7.6$), 7.48-7.50 (d, 1, $J = 8.8$), 7.72 (s, 1), 7.80 (s, 1), 7.82 (s, 1), 7.97 (s, 1), 11.00 (s, 1). HRMS (FAB+) m/z : 674.2826 (MH^+ $C_{35}H_{40}N_5O_9Na$ requires 674.2819).

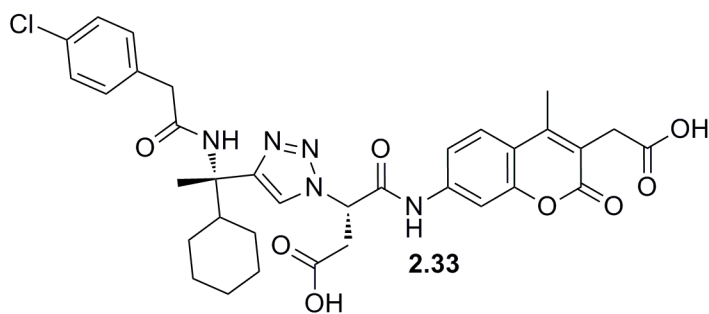


Substrate 2.31: 1H NMR (400 MHz, DMSO d_6): δ 0.77-1.12 (m, 6) 1.33-1.37 (m, 1), 1.60 (s, 3), 1.65-1.69 (m, 2), 2.02-2.06 (m, 2), 2.37 (s, 3), 3.19-3.47 (m, 4), 3.59 (s, 2), 5.70-5.74 (t, 1, $J = 7.4$), 7.47-7.55 (m, 4), 7.61 (s, 1), 7.71 (s, 1), 7.79-7.82 (d, 1, J

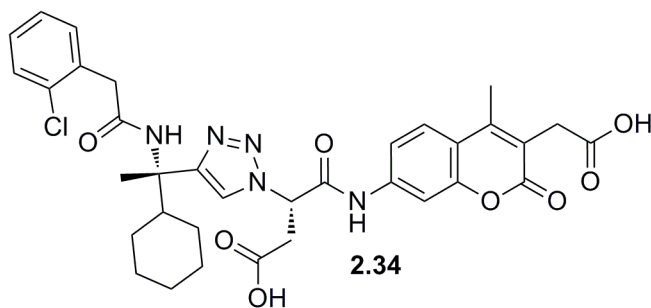
= 8.8), 7.97 (s, 1), 8.00 (s, 1), 11.00 (s, 1). HRMS (FAB+) m/z : 712.2594 (MH^+ $C_{35}H_{37}N_5O_8$ requires 712.2590).



Substrate 2.32: 1H NMR (400 MHz, DMSO d_6): δ 0.74-1.12 (m, 6) 1.34-1.37 (m, 2), 1.59 (s, 3), 1.62-1.67 (m, 2), 2.01-2.06 (m, 1), 2.37 (s, 3), 3.19-3.45 (m, 4), 3.59 (s, 2), 3.69 (s, 3), 5.70-5.74 (t, 1, $J = 7.4$), 6.80-6.83 (d, 2, $J = 8.4$), 7.12-7.14 (d, 2, $J = 8.4$), 7.48-7.50 (d, 1, $J = 8.8$), 7.72 (s, 1), 7.76 (s, 1), 7.79-7.82 (d, 1, $J = 8.8$), 7.95 (s, 1), 11.00 (s, 1). HRMS (FAB+) m/z : 674.2826 (MH^+ $C_{35}H_{40}N_5O_9Na$ requires 674.2828).

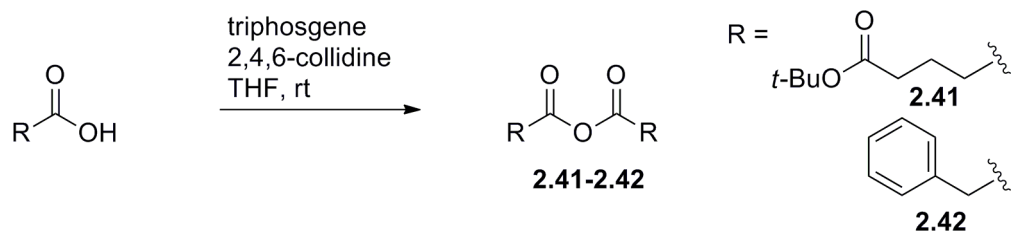


Substrate 2.33: 1H NMR (400 MHz, DMSO d_6): δ 0.74-1.12 (m, 6) 1.31-1.34 (m, 2), 1.59 (s, 3), 1.66-1.69 (m, 2), 2.01-2.05 (m, 1), 2.34 (s, 3), 3.20-3.44 (m, 4), 3.51 (s, 2), 5.71-5.74 (t, 1, $J = 7.4$), 6.97 (s, 1), 7.21-7.23 (d, 2, $J = 7.6$), 7.29-7.31 (d, 2, $J = 7.6$), 7.47-7.49 (d, 1, $J = 8.8$), 7.77-7.80 (d, 1, $J = 8.8$), 7.89 (s, 1), 7.98 (s, 1), 10.98 (s, 1). LRMS calculated for MH^+ $C_{34}H_{39}ClN_5O_8$ 678.2, found 678.2.

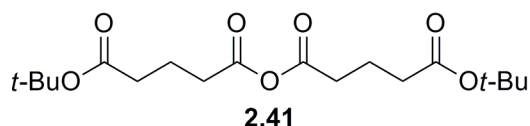


Substrate 2.34: LRMS calculated for MH^+ $C_{34}H_{39}ClN_5O_8$ 678.2, found 678.2.

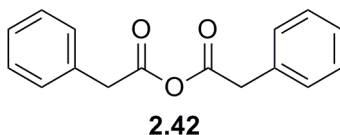
Synthesis of Aryloxy-methyl Ketones and Intermediates



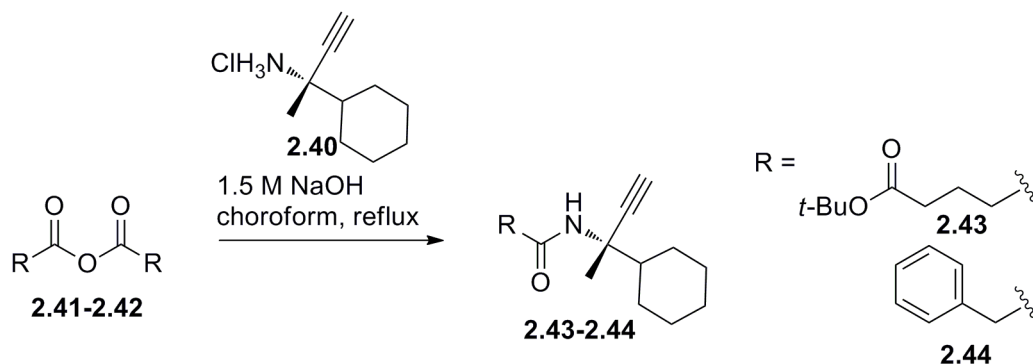
General Synthesis of Symmetric Anhydrides 2.41-2.42 (Procedure A). Triphosgene (1 equiv) was dissolved in THF in a flame dried round-bottom flask and placed under nitrogen. The solution was stirred and cooled in an ice-water bath. The carboxylic acid (5 equiv) was added to the above solution. After the acid dissolved, 2,4,6-collidine (10 equiv) was added slowly. The round-bottom flask was removed from the ice-water bath and the reaction mixture was stirred at rt for 15 min. The reaction mixture was transferred to a separatory funnel and EtOAc (250 mL) was added. The organic layer was washed with water (120 mL), 1.0M aqueous hydrochloric acid solution (120 mL x 2), water (120 mL), 1.0M aqueous sodium hydroxide solution (120 mL x 2), and water (120 mL x 2). The organic layer was dried over anhydrous sodium sulfate, filtered, and concentrated under reduced pressure to obtain the desired product.



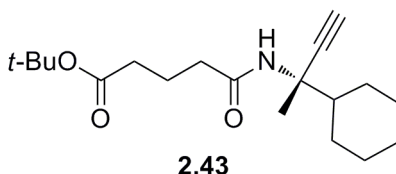
5-(*tert*-butoxy)-5-oxopentanoic anhydride 2.41. Procedure A was used to prepare 5-(*tert*-butoxy)-5-oxopentanoic anhydride (1.61 g, 76%) from 5-(*tert*-butoxy)-5-pentanoic acid (1.88 g, 10.0 mmol), which was prepared from glutaric anhydride according to a previous literature procedure⁴⁵, triphosgene (0.590 g, 2.00 mmol), and 2,4,6-collidine (2.64 mL, 20.0 mmol). ¹H NMR (400 MHz, CDCl₃, δ): 1.41 (s, 18 H), 1.88-1.92 (t, 4H, $J = 7.2$ Hz), 2.26-2.30 (t, 4H, $J = 7.2$ Hz), 2.47-2.51 (t, 4H, $J = 7.2$ Hz). ¹³C NMR (100 MHz, CDCl₃, δ): 19.7, 28.3, 34.2, 34.4, 80.8, 169.0, 172.2. HRMS-FAB (m/z): [M + Na]⁺ calcd for C₁₈H₃₀O₇Na, 381.1889; found, 381.1882.



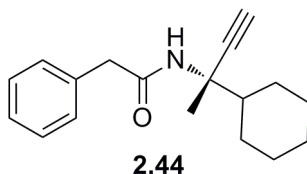
Phenylacetic acid anhydride 2.42. Procedure A was used to prepare phenylacetic acid anhydride (1.34 g, 88%) from phenylacetic acid (1.36 g, 10.0 mmol), triphosgene (0.59 g, 2.00 mmol), and 2,4,6-collidine (2.64 mL, 20.0 mmol). ¹H NMR (400 MHz, CDCl₃): δ 3.74 (s, 4), 7.22-7.27 (m, 4), 7.31-7.35 (m, 6). ¹³C NMR (100 MHz, CDCl₃): δ 42.2, 127.8, 129.0, 129.6, 132.1, 167.1. HRMS (FAB⁺) m/z : 255.1021 (MH⁺ C₁₆H₁₅O₃ requires 255.1026).



General Synthesis of Propargyl amides 2.43-2.44 (Procedure B). A 1.50 M sodium hydroxide solution was added to the hydrochloride salt of (*S*)-2-amino-2-cyclohexyl-3-butyne **2.40** (1 equiv). A solution of anhydride (0.17 M, 1 equiv) in chloroform was added to the above solution and heated at reflux for 24 h. The reaction mixture was transferred to a separatory funnel, and EtOAc (150 mL) and water (15 mL) were added. The organic layer was washed with brine (25 mL), 10 M aqueous sodium hydroxide solution (25 mL x 4), brine (25 mL x 4), and water (25 mL x 2). The organic layer was dried over anhydrous sodium sulfate, filtered, and concentrated under reduced pressure. The product was purified by flash chromatography (1:1 hexanes:EtOAc) to afford the desired product.

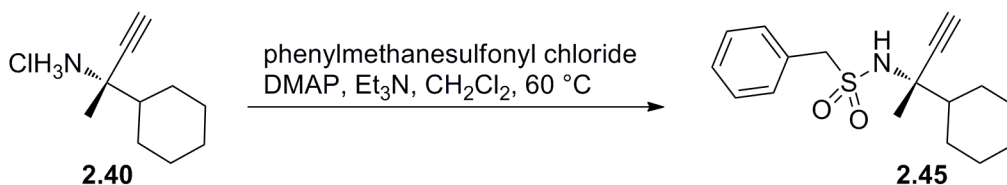


Propargyl amide 2.43. Amide **2.43** (0.100 g, 71%) was prepared from 0.099g (0.530 mmol) of hydrochloride salt of (*S*)-2-amino-2-cyclohexyl-3-butyne **2.40** and phenylacetic acid anhydride (0.17M, 0.102 g, 0.530 mmol, 1 equiv) in chloroform (3.10 mL) using Procedure B. ^1H NMR (400 MHz, CDCl_3): δ 0.95-1.05 (m, 4), 1.06-1.09 (m, 2), 1.57 (s, 3), 1.62-1.74 (m, 5), 1.90-2.05 (t, 2, $J = 12.0$), 2.31 (s, 1), 3.54 (s, 2), 5.43 (br s, 1), 7.25-7.31 (dd, 3, $J = 7.6, 7.2$), 7.35-7.38 (m, 2). ^{13}C NMR (100 MHz, CDCl_3): δ 24.4, 26.3, 27.5, 27.7, 44.4, 44.8, 55.7, 71.5, 85.4, 127.5, 129.2, 129.5, 135.2, 169.8. HRMS (FAB+) m/z : 270.1858 (MH^+ $\text{C}_{18}\text{H}_{24}\text{NO}$ requires 270.1853).

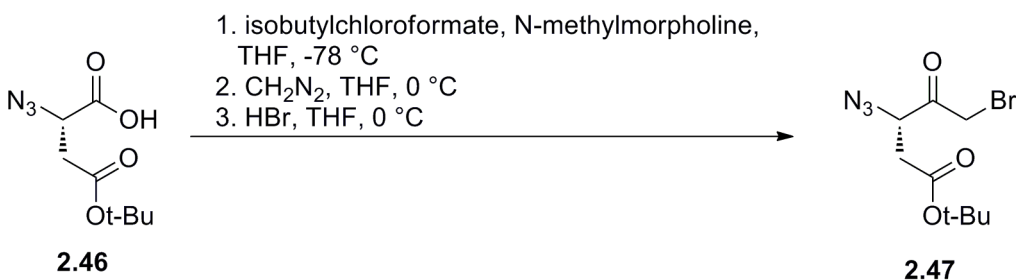


Propargyl amide 2.44. Amide **2.44** (0.41 g, 70%) was prepared from 0.34 g (1.80 mmol) of hydrochloride salt of (*S*)-2-amino-2-cyclohexyl-3-butyne **2.40** and 5-(*tert*-butoxy)-5-oxopentanoic anhydride (0.17 M, 1.80 mmol, 1 equiv) in chloroform (10.6

mL) using Procedure B. ^1H NMR (400 MHz, CDCl_3 , δ): 1.16-1.25 (m, 6H), 1.42 (s, 9H), 1.52 (s, 3H), 1.67-1.76 (m, 5H), 1.87-1.91 (t, 2H, $J = 7.2$), 2.15-2.19 (t, 2H, $J = 7.2$), 2.23-2.27 (t, 2H, $J = 7.2$), 2.32 (s, 1H). ^{13}C NMR (100 MHz, CDCl_3 , δ): 21.3, 24.5, 25.4, 26.4, 27.7, 27.9, 28.3, 34.6, 36.4, 44.2, 55.9, 71.5, 80.6, 171.3, 172.9. HRMS-FAB (m/z): $[\text{M} + \text{Na}]^+$ calcd for $\text{C}_{19}\text{H}_{31}\text{NO}_3\text{Na}$, 344.2202; found, 344.2197.

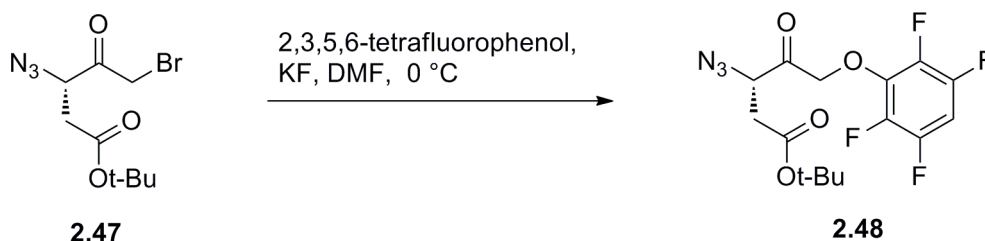


Propargyl sulfonamide 2.45. To a flame-dried tube was added the hydrochloride salt of (*S*)-2-amino-2-cyclohexyl-3-butyne **2.40** (0.20M, 0.25 g, 1.32 mmol, 1 equiv), phenylmethanesulfonyl chloride (0.27 g, 1.45 mmol, 1.10 equiv), and DMAP (0.031 g, 0.26 mmol, 0.2 equiv) in CH_2Cl_2 (6.6 mL) and the resulting mixture was stirred. To the solution was added NEt_3 (0.40 mL, 2.9 mmol, 2.2 equiv), and the mixture was then stirred in a sealed tube, which was heated in a 60°C oil bath for 18 h. The reaction mixture was transferred to a separatory funnel, and aqueous NH_4Cl (10 mL) was added followed by extraction with CH_2Cl_2 (30 mL x 3). The organic layer was dried over anhydrous sodium sulfate, filtered, and concentrated under reduced pressure. The product was purified by flash chromatography (7:3 hexanes:EtOAc) to afford the desired product as an orange solid (0.235 g, 59%). ^1H NMR (400 MHz, CDCl_3 , δ): 1.00-1.12 (m, 5H), 1.53 (s, 3H), 1.58-1.61 (m, 2H), 1.76-1.87 (m, 2H), 1.89-2.02 (m, 2H), 2.63 (s, 1H), 4.14 (s, 1H), 4.48 (s, 2H), 7.34-7.35 (m, 3H), 7.43-7.44 (d, 2H, $J = 4.8$). ^{13}C NMR (100 MHz, CDCl_3 , δ): 26.1, 26.3, 27.0, 28.0, 48.4, 57.4, 60.1, 74.3, 84.6, 128.8, 129.9, 131.3. HRMS-FAB (m/z): $[\text{M} + \text{H}]^+$ calcd for $\text{C}_{17}\text{H}_{23}\text{NO}_2\text{S}$, 305.1450; found, 305.1457.

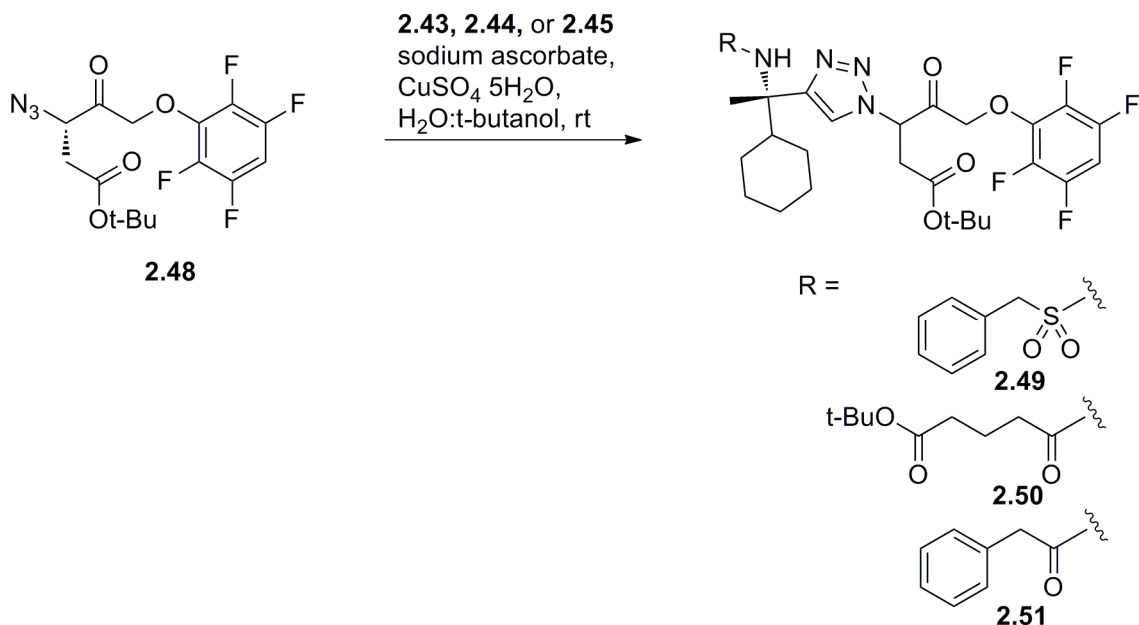


Bromomethyl ketone 2.47. The following method was adapted from a previous literature procedure.⁴⁶ Azido acid **2.46** was prepared from Asp(*Ot*-Bu)-OH according to a previously reported literature procedure.⁴⁷ To a 0.1M solution of azido acid **2.46** (1.00 g, 4.65 mmol) and *N*-methylmorpholine (0.56 mL, 5.12 mmol) in THF (46.5 mL) at -78°C was added isobutylchloroformate (0.66 mL, 5.12 mmol). The reaction mixture was stirred for 15 min and the resulting heterogenous mixture was canula filtered into a flask at -78°C . Diazomethane, prepared from Diazald (3.01g, 14.14 mmol), was bubbled slowly while the reaction mixture was maintained at -78°C . After addition of

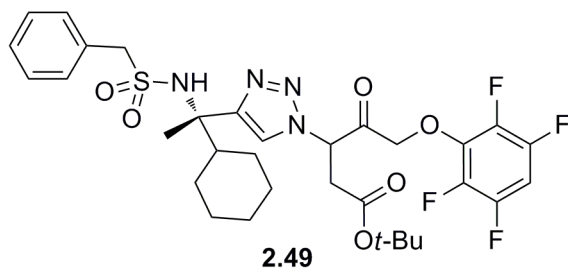
diazomethane was complete, the reaction flask was stoppered and kept in the refrigerator at -4 °C overnight. The reaction mixture was then treated with 40% aqueous HBr (0.953 mL) and stirred for 15 min at 0 °C. The reaction mixture was diluted with EtOAc (50 mL) and washed with 10 wt% aqueous citric acid (2 x 10 mL), saturated aqueous NaHCO₃ (2 x 10 mL), and aqueous saturated NaCl (10 mL). The organic layer was dried with Na₂SO₄, filtered, and concentrated under reduced pressure to afford **2.47** as a yellow oil (81%). The crude material was used for the subsequent reaction. ¹H NMR (400 MHz, CDCl₃): δ 1.45 (s, 9), 2.74-2.94 (m, 2), 4.09-4.27 (m, 2), 4.48-4.51 (t, 1, *J* = 6.0). ¹³C NMR (100 MHz, CDCl₃): δ 28.2, 32.4, 37.6, 62.1, 82.6, 169.0, 198.2. HRMS (FAB+) *m/z*: 298.0379 (MLi⁺ C₉H₁₄N₃O₃Li requires 298.0383).



α -Azido methyl ketone 2.48. A solution of 2,3,4,6-tetrafluorophenol (0.45 g, 0.57 M, 2.73 mmol, 3.2 equiv) and potassium fluoride (0.22 g, 8.73 mmol, 3.2 equiv) in DMF was added to a flame-dried reaction vessel under nitrogen. The reaction mixture was cooled to 0° C in an ice-water bath and (*S*)-*tert*-butyl-3-azido-5-bromo-4-oxopentanoate **1.47** (0.80 g, 2.73 mmol, 1 equiv) was added dropwise. After stirring at 0 °C for 1.5 h, the mixture was diluted with diethyl ether (125 mL) and transferred to a separatory funnel. The organic layer was washed with aqueous sodium bicarbonate (75 mL x 2) and brine (75 mL). The organic layer was dried over anhydrous sodium sulfate, filtered, and concentrated under reduced pressure. The product was purified by flash chromatography (7:3 hexanes:EtOAc) to afford the desired product **2.48** as a pale yellow oil (0.560 g, 55%). ¹H NMR (400 MHz, CDCl₃): δ 1.41 (s, 9), 2.75-2.81 (m, 2), 4.41-4.45 (t, 1, *J* = 5.6), 5.18 (s, 2), 6.74-6.80 (m, 1). HRMS (FAB+) *m/z*: 400.0896 (MNa⁺ C₁₅H₁₅N₃O₄F₄Na requires 400.0893).

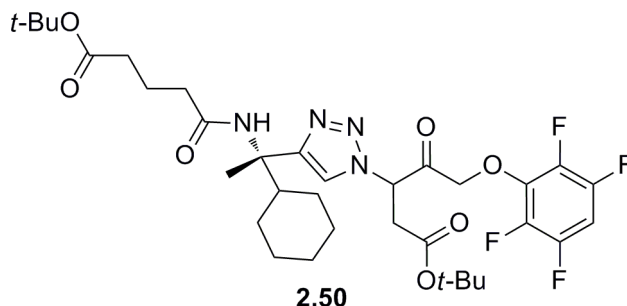


General Procedure for Copper(I)-Catalyzed Synthesis of 1,4-Disubstituted 1,2,3-Triazoles 2.49, 2.50, and 2.51 (Procedure C). The following procedure was adapted from a previous literature procedure.⁴⁸ To a solution of azido-aryloxy methyl ketone **2.48** (0.25 M, 1 equiv) and propargyl amide **2.43**, **2.44**, and **2.45** (1 equiv) in 1:1 water/tert-butanol was added sodium ascorbate (1 equiv of freshly prepared 1.0 M aqueous solution). A solution of copper(II) sulfate pentahydrate (0.10 equiv of a freshly prepared 0.3M aqueous solution) was added to the reaction mixture and was vigorously stirred overnight. The reaction mixture was diluted with 10 mL of water and was extracted with EtOAc (3 x 10 mL). The organic layer was washed with brine (15 mL) and dried over sodium sulfate, filtered, and concentrated under reduced pressure. The product was purified by flash chromatography (7:3 hexanes:ethyl acetate) to afford the desired product.

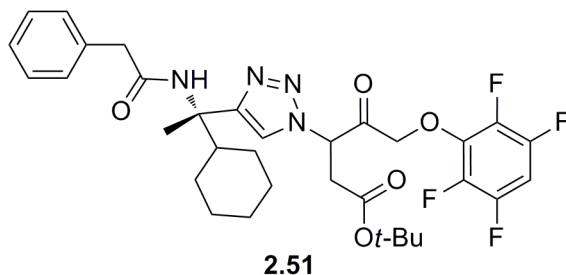


Aryloxy methyl ketone-ester 2.49. Procedure C was followed using azido-aryloxy methyl ketone **2.48** (0.07 g, 0.200 mmol), propargyl sulfonamide **2.45** (0.06 g, 0.200 mmol), 1.0 M sodium ascorbate (0.02 mL, 0.200 mmol), and 0.3 M copper(II) sulfate pentahydrate (0.07 mL, 0.02 mmol). After chromatography the product was obtained as a pale yellow solid (0.09 g, 65%). ¹H NMR (400 MHz, CDCl₃, δ): 0.86-1.14 (m, 6H), 1.48 (s, 9H), 1.74 (s, 3H), 1.75-1.88 (m, 3H), 1.91-1.98 (m, 2H), 3.10-3.16 (m,

2H, $J = 7.2, 17.2$), 3.87-4.05 (m, 2H), 4.78 (s, 1H), 4.87-4.92 (m, 2H), 5.87-5.90 (t, 1H, $J = 6.8$), 6.71-6.79 (m, 1H), 7.30-7.33 (m, 5H), 7.62 (s, 1H). HRMS (FAB+) m/z : 705.2351 ($MNa^+ C_{32}H_{38}N_4O_6F_4SNa$ requires 705.2346).



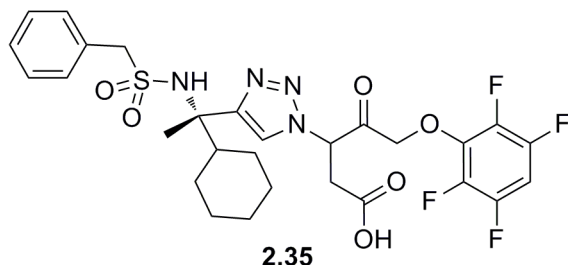
Aryloxy methyl ketone 2.50. Procedure C was followed using azido-aryloxy methyl ketone **2.48** (0.15 g, 0.400 mmol), propargyl amide **2.43** (0.13 g, 0.400 mmol), 1.0 M sodium ascorbate (0.40 mL, 0.400 mmol), and 0.3 M copper(II) sulfate pentahydrate (0.13 mL, 0.04 mmol). After chromatography the product was obtained as a pale yellow solid (0.165 g, 60%). 1H NMR (400 MHz, $CDCl_3$, δ): 0.75-0.96 (m, 3H), 1.13-1.25 (m, 3H), 1.38 (s, 9H), 1.41 (s, 9H), 1.56-1.64 (m, 5H), 1.71 (s, 3H), 1.82-1.87 (t, 2H, $J = 7.2$), 2.18-2.24 (m, 4H), 3.07-3.61 (m, 2H), 4.89 (s, 2H), 5.81-5.86 (dd, 1H, $J = 7.2, 13.6$), 6.51 (s, 1H), 6.75-6.79 (m, 1H), 7.59 (s, 1H). HRMS (FAB+) m/z : 721.3193 ($MNa^+ C_{34}H_{46}N_4O_7F_4Na$ requires 721.3200).



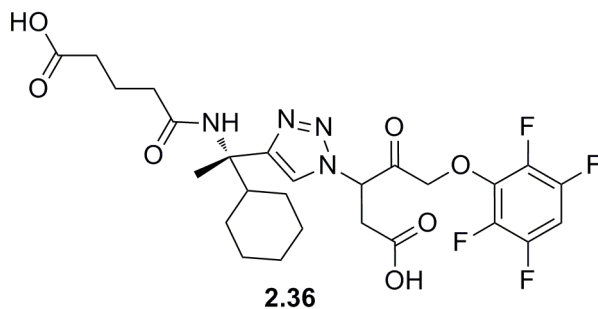
Aryloxy methyl ketone 2.51. Procedure C was followed using azido-aryloxy methyl ketone **2.48** (0.11 g, 0.300 mmol), propargyl amide **2.44** (0.08g, 0.300 mmol), 1.0 M sodium ascorbate (0.30 mL, 0.300 mmol), and 0.3 M copper(II) sulfate pentahydrate (0.10 mL, 0.03 mmol). After chromatography the product was obtained as a pale yellow solid (0.095 g, 49%). 1H NMR (400 MHz, $CDCl_3$, δ): 0.62-0.86 (m, 3H), 1.10-1.19 (m, 2H), 1.41 (s, 9H), 1.50-1.66 (m, 4H), 1.71 (s, 3H), 2.14-2.2 (t, 1H, $J = 12.0$), 3.03-3.37 (m, 2H), 3.52 (s, 2H), 4.85-4.92 (m, 2H), 5.80-5.84 (t, 1H, $J = 7.2$), 6.26 (s, 1), 6.77-6.82 (m, 1H), 7.26-7.30 (m, 3H), 7.34-7.38 (m, 2H), 7.53 (s, 1H). HRMS (FAB+) m/z : 647.2857 ($MNa^+ C_{33}H_{39}N_4O_5F_4$ requires 647.2858).

General Procedure for Deprotection of *tert*-butyl esters (Procedure D). To a 0.33 M solution of aryloxy methyl ketone-ester in CH_2Cl_2 was added a solution of 95% trifluoroacetic acid (TFA):2.5% H_2O :2.5% triisopropylsilane. The reaction mixture was stirred for 1 h at rt. The crude reaction mixture was purified by HPLC [preparatory

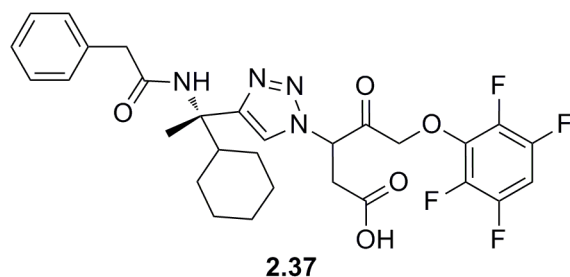
reverse phase C₁₈ column (24.1 x 250 mm), CH₃CN/H₂O -0.1% TFA, 5:95 to 95:5 over 55 min; 10 mL/min, 254 nm detection] and lyophilized to afford the pure product.



Aryloxy methyl ketone inhibitor 2.35. Procedure D was followed using aryloxy methyl ketone-ester **2.49** (0.06 g, 0.100 mmol) and 95% TFA:2.5% H₂O:2.5% triisopropylsilane (0.70 mL) in CH₂Cl₂ (0.30 mL) to afford inhibitor **2.35** as a white solid (0.030 g, 49%). ¹H NMR (400 MHz, DMSO-d₆, δ): 0.83-1.16 (m, 8H), 1.52 (s, 3H), 1.72-1.75 (m, 1H), 1.91-2.00 (m, 2H), 3.26-3.31 (m, 2H), 3.62-3.82 (m, 2H), 4.89-4.93 (d, 1H, *J* = 18.0), 5.17-5.23 (dd, 1H, *J* = 6.4, 18.0), 5.96-5.98 (m, 1H), 7.24-7.28 (m, 5H), 7.56-7.76 (m, 1H), 8.09 (s, 1H). HRMS (FAB+) *m/z*: 649.1724 (MNa⁺ C₂₈H₃₀N₄O₆F₄Na requires 649.1720).



Aryloxy methyl ketone inhibitor 2.36. Procedure D was followed using aryloxy methyl ketone-ester **2.50** (0.70g, 0.100 mmol) and 95% TFA:2.5% H₂O:2.5% triisopropylsilane (1.00 mL) in CH₂Cl₂ (0.43 mL) to afford inhibitor **2.36** as a white solid (0.050 g, 58%). ¹H NMR (400 MHz, CD₃OD, δ): 0.70-1.15 (m, 8H), 1.31-1.50 (m, 2H), 1.53 (s, 3H), 1.56-1.58 (m, 2H), 1.67-1.72 (m, 1H), 1.87-1.94 (m, 2H), 2.08-2.13 (dd, 2H, *J* = 7.2, 14.4), 2.16-2.22 (dd, 2H, *J* = 7.2, 14.4), 3.09-3.19 (m, 2H), 4.06-4.21 (m, 2H), 5.34-5.37 (t, 1H, *J* = 5.2), 7.01-7.05 (m, 1H), 7.69 (s, 1H). HRMS (FAB+) *m/z*: 609.1946 (MNa⁺ C₂₆H₃₀N₄O₇F₄Na requires 609.1948).



Aryloxy methyl ketone inhibitor 2.37. Procedure D was followed using aryloxy methyl ketone-ester **2.51** (0.096 g, 0.150 mmol) and 95% TFA:2.5% H₂O:2.5% triisopropylsilane (1.05 mL) in CH₂Cl₂ (0.45 mL) to afford inhibitor **2.37** as a white solid (0.030 g, 32%). ¹H NMR (400 MHz, DMSO-d₆, δ): 0.76-1.16 (m, 8H), 1.59 (s, 3H), 1.66-1.70 (m, 2H), 2.01-2.05 (m, 1H), 3.19-3.49 (m, 4H), 4.89-4.93 (d, 1H, *J* = 18.0), 5.17-5.23 (dd, 1H, *J* = 6.4, 18.0), 5.86-5.90 (t, 1H, *J* = 8.0), 7.17-7.27 (m, 5H), 7.53-7.59 (m, 1H), 7.96 (s, 1H), 8.18 (s, 1H). HRMS (FAB+) *m/z*: 591.2231 (MH⁺ C₂₉H₃₁N₄O₅F₄ requires 591.2239).

AMCA Substrate and Irreversible Inhibitor Assays

General Procedure for Assays. Caspases-3, -6, -7, -8, and -9 were obtained by expression in *E. coli* as previously described.⁴⁹ Caspase-1, cathepsin B, L, and V were purchased from EMD Biosciences (San Diego, CA), caspase-2 was purchased from Biomol International (Plymouth Meeting, PA) and Legumain was purchased from R&D Systems (Minneapolis, MN). Caspase substrates Ac-DEVD-AMC, Ac-VDVAD-AFC, and Ac-LEHD-AFC were purchased from EMD Biosciences (San Diego, CA) and Ac-VDVAD-AMC was purchased from Biomol International (Plymouth Meeting, PA). Cathepsin substrate Cbz-FR-AMC was purchased from EMD Biosciences (San Diego, CA). Cathepsin S substrate Cbz-LR-AMC and legumain substrate Cbz-AAN-AMC were purchased from Bachem (Torrance, CA). The proteolytic cleavage of *N*-acyl aminocoumarins by caspases was conducted in Dynatech Microfluor fluorescence 96-well microtiter plates, and readings were taken on a Molecular Devices Spectra Max Gemini XS instrument. The excitation wavelength was 370 nm and the emission wavelength was 455 nm for AMCA substrates, the excitation wavelength was 355 nm and the emission wavelength was 450 nm for peptidyl AMC substrates, and the excitation wavelength was 430 nm and the emission wavelength was 535 nm for peptidyl AFC substrates.

Assay Procedure for AMCA substrates. Assays were conducted at 37 °C in duplicate with and without the enzyme according to previously reported protocols (Wood et al.). In each well was placed 38 μL of enzyme solution and 2 μL of a DMSO substrate solution. Relative fluorescent units (RFU) were measured at regular intervals over a period of time (maximum 15 min). A plot of RFU versus time was made for each substrate with and without caspase-3 or caspase-6. The slope of the plotted line gave relative $k_{\text{cat}}/K_{\text{m}}$ of each substrate for caspase-3 or caspase-6.

Assay Procedure for Irreversible Inhibitors. The k_{inact}/K_i for inhibitors were determined under pseudo-first order conditions using the progress curve method.^{50,51} Assay wells contained a mixture of inhibitor and AMC or AFC substrate in buffer. Aliquots of caspase were added to each well to initiate the assay. Hydrolysis of the AMC or AFC substrate was monitored fluorometrically for 45 min. To determine the inhibition parameters, time points for which the control ($[I] = 0$) was linear were used. For each inhibitor, a k_{obs} was calculated for at least four different concentrations of inhibitors via a nonlinear regression of the data according to the equation $P = (v_i/k_{\text{obs}})[1 - \exp(-k_{\text{obs}}t)]$ (where product formation = P, initial rate = v_i , time = t, and the first-order rate constant = k_{obs}). If k_{obs} varied linearly with $[I]$, then the association constant k_{ass} was determined by linear regression analysis using $k_{\text{obs}} = (k_{\text{ass}}[I]) / (1 + [S]/K_m)$ where $[S]$ is the concentration of the substrate. If k_{obs} varied hyperbolically with $[I]$, then non-linear regression analysis was performed to determine k_{inact}/K_i using $k_{\text{obs}} = k_{\text{inact}}[I] / ([I] + K_i * (1 + [S]/K_m))$. Inhibition was measured in duplicate and the average is reported.

Caspase-1. Caspase-1 kinetic assays were performed using Ac-WEHD-AMC ($K_m = 4.0 \mu\text{M}$) as the substrate. The assay buffer was 100 mM HEPES, 20% (w/v) glycerol, 10% (w/v) sucrose, 0.1% (w/v) CHAPS, and 10 mM DTT solution in H₂O at pH 7.5. The concentration of the enzyme stock solution was 20 nM in the assay buffer. The concentrations of inhibitor stock solutions in DMSO ranged from (5.00×10^{-7} to 1.12×10^{-4}). The concentration of the substrate stock solution was 80 μM in assay buffer. The reaction was started by adding 140 μL of assay buffer, 10 μL of various amounts of inhibitor (final concentrations ranging from 2.50×10^{-8} M to 5.60×10^{-6} M), 10 μL of substrate (final concentration 4.0 μM). Then 40 μL of Caspase-1 (final concentration of 4 nM) was added to the mixture after incubating for 5 min at 37 °C.

Caspase-2. Caspase-2 kinetic assays were performed using Ac-VDVAD-AMC ($K_m = 80.2 \mu\text{M}$) as the substrate and with the same conditions as described for Caspase-1 using the following modifications: The assay buffer was 20 mM Pipes, 200 mM NaCl, 0.2% (w/v) CHAPS, 20% (w/v) sucrose, 20 mM DTT, and 2mM EDTA solution in H₂O at pH 7.2. The concentration of the substrate stock solution was 1.60 mM in assay buffer (final concentration: 80.2 μM). The inhibitor stock solutions ranged from 0.02 M to 3.12×10^{-5} M in DMSO (final concentration ranging from 1.00×10^{-3} M to 1.56×10^{-6}). The concentration of the enzyme stock solution was 150 nM in assay buffer (final concentration: 30.0 nM).

Caspase-3. Caspase-3 kinetic assays were performed using Ac-DEVD-AMC ($K_m = 9.7 \mu\text{M}$) as the substrate and with the same conditions as described for Caspase-2. The concentration of the substrate stock solution was 194 μM in assay buffer (final concentration: 9.7 μM). The inhibitor stock solutions ranged from 1.50×10^{-8} M to 2.88×10^{-4} M in DMSO (final concentration ranging from 7.50×10^{-9} M to 1.44×10^{-5} M).

The concentration of the enzyme stock solution was 3.75 nM in assay buffer (final concentration: 0.75 nM).

Caspase-6. Caspase-6 kinetic assays were performed using Ac-DEVD-AMC ($K_m = 236.35 \mu\text{M}$) as the substrate and with the same conditions as described for Caspase-3. The concentration of the substrate stock solution was 4.72 mM in assay buffer (final concentration: 236.35 μM). The inhibitor stock solutions ranged from $4.00 \times 10^{-7} \text{ M}$ to $4.80 \times 10^{-4} \text{ M}$ in DMSO (final concentration ranging from $2.00 \times 10^{-8} \text{ M}$ to $1.60 \times 10^{-6} \text{ M}$). The concentration of the enzyme stock solution was 18.75 nM in assay buffer (final concentration: 3.75 nM).

Caspase-7. Caspase-7 kinetic assays were performed using Ac-DEVD-AMC ($K_m = 20.2 \mu\text{M}$) as the substrate and with the same conditions as described for Caspase-3. The concentration of the substrate stock solution was 404 μM in assay buffer (final concentration: 20.2 μM). The inhibitor stock solutions ranged from $4.00 \times 10^{-7} \text{ M}$ to $1.28 \times 10^{-4} \text{ M}$ in DMSO (final concentration ranging from $2.00 \times 10^{-8} \text{ M}$ to $6.40 \times 10^{-6} \text{ M}$). The concentration of the enzyme stock solution was 18.75 nM in assay buffer (final concentration: 3.75 nM).

Caspase-8. Caspase-8 kinetic assays were performed using Ac-DEVD-AMC ($K_m = 6.79 \mu\text{M}$) as the substrate and with the same conditions as described for Caspase-3. The concentration of the substrate stock solution was 135.8 μM in assay buffer (final concentration: 6.79 μM). The inhibitor stock solutions ranged from $3.60 \times 10^{-6} \text{ M}$ to $2.30 \times 10^{-4} \text{ M}$ in DMSO (final concentration ranging from $1.80 \times 10^{-7} \text{ M}$ to $1.15 \times 10^{-5} \text{ M}$). The concentration of the enzyme stock solution was 187.5 nM in assay buffer (final concentration: 32 nM).

Caspase-9. Caspase-9 kinetic assays were performed using Ac-LEHD-AFC ($K_m = 114 \mu\text{M}$) as the substrate and with the same conditions as described for Caspase-1 using the following: The assay buffer was 200 mM HEPES, 100 mM NaCl, 0.01% (w/v) CHAPS, 20% (w/v) sucrose, 20 mM DTT, and 2 mM EDTA in H_2O at pH 7.0 and supplemented with 0.7 M sodium citrate. The concentration of the substrate stock solution was 2.28 mM in assay buffer (final concentration: 114 μM). The inhibitor stock solutions ranged from $4.80 \times 10^{-6} \text{ M}$ to $6.40 \times 10^{-4} \text{ M}$ in DMSO (final concentration ranging from $2.40 \times 10^{-7} \text{ M}$ to $3.20 \times 10^{-5} \text{ M}$). The concentration of the enzyme stock solution was 200 nM in assay buffer (final concentration: 40.0 nM).

Cathepsin B. Cathepsin B kinetic assays were performed using Cbz-FR-AMC as the substrate. The assay buffer was 100 mM phosphate, 0.1% (w/v) polyglycerol, 1 mM DTT, 1mM EDTA, 0.01 % Brij 35 solution in H_2O at pH 6.0. The concentration of the enzyme stock solution was 760 nM in the assay buffer. The concentrations of inhibitor stock solutions in DMSO ranged from ($1.25 \times 10^{-7} \text{ M}$ to 8.00×10^{-3}). The concentration of the substrate stock solution was 200 μM in assay buffer. The reaction was started by

adding 140 μL of assay buffer, 10 μL of various amounts of inhibitor (final concentrations ranging from $6.25 \times 10^{-8} \text{ M}$ to $4.00 \times 10^{-4} \text{ M}$) and 40 μL of cathepsin B (final concentration of 150 nM). Then, 10 μL of substrate (final concentration 10 μM) was added to the mixture after incubating for 5 min at 37 $^{\circ}\text{C}$.

Cathepsin S. Cathepsin S kinetic assays were performed using Cbz-LR-AMC ($K_m = 23 \mu\text{M}$) as the substrate and with the same conditions as described for cathepsin B using the following: The assay buffer was 100 mM phosphate, 0.1% (w/v) polyglycerol, 1 mM DTT, 1mM EDTA solution in H_2O at pH 6.0. The concentration of the substrate stock solution was 200 μM in assay buffer (final concentration: 10 μM). The inhibitor stock solutions ranged from $3.20 \times 10^{-3} \text{ M}$ to $1.25 \times 10^{-5} \text{ M}$ in DMSO (final concentration ranging from $1.60 \times 10^{-4} \text{ M}$ to $1.00 \times 10^{-6} \text{ M}$). The concentration of the enzyme stock solution was 13.3 nM in assay buffer (final concentration: 2.1 nM).

Cathepsin V. Cathepsin V kinetic assays were performed using Cbz-FR-AMC as the substrate and with the same conditions as described for cathepsin B using the following: The assay buffer was 100 mM acetate buffer, 0.1% (w/v) polyglycerol, 1 mM DTT, 1mM EDTA solution in H_2O at pH 5.5. The concentration of the substrate stock solution was 200 μM in assay buffer (final concentration: 10 μM). The inhibitor stock solutions ranged from 8.00×10^{-3} to $1.25 \times 10^{-4} \text{ M}$ in DMSO (final concentration ranging from $4.00 \times 10^{-4} \text{ M}$ to $6.25 \times 10^{-6} \text{ M}$). The concentration of the enzyme stock solution was 1.51 μM in assay buffer (final concentration: 300 nM).

Legumain. To activate Legumain, the enzyme was incubated in 50 mM Sodium acetate, 100 mM NaCl at pH 4.0 for 4 h at 37 $^{\circ}\text{C}$ (concentration in activation buffer: 100 $\mu\text{g}/\text{mL}$). Legumain kinetic assays were performed using Cbz-AAN-AMC as the substrate. The assay buffer was 39.5 mM citric acid/121 mM sodium phosphate dibasic buffer, 2 mM DTT solution in H_2O at pH 5.8. The concentration of the enzyme stock solution was 0.76 $\mu\text{g}/\text{mL}$ in the assay buffer. The concentrations of inhibitor stock solutions in DMSO ranged from ($1.25 \times 10^{-7} \text{ M}$ to 8.00×10^{-3}). The concentration of the substrate stock solution was 200 μM in assay buffer. The reaction was started by adding 140 μL of assay buffer, 10 μL of various amounts of inhibitor (final concentrations ranging from $6.25 \times 10^{-8} \text{ M}$ to $4.00 \times 10^{-4} \text{ M}$) and 40 μL of legumain (final concentration of 0.15 $\mu\text{g}/\text{mL}$). Then, 10 μL of substrate (final concentration 10 μM) was added to the mixture after incubating for 15 min at 30 $^{\circ}\text{C}$. Since very weak inhibition was observed at the above inhibitor concentrations, IC_{50} values were calculated by plotting the the relative (RFU)/min against the inhibitor concentration (μM).

Huntingtin Neopeptide Antibody Production. Antibodies specific for the C-terminal ends of Htt caspase cleavage products ending at amino acid 513, 552 and 586 were prepared using the immunizing peptides KLH-DHTLQADSVD, KLH-DSDPAMDLD and KLH-COSDSSEIVLD. Peptide sequences were injected into

rabbits, antibody was purified to the injected peptide and a bridging peptide was used to remove antibodies reacting to full-length Htt (Open Biosystems). Antibodies were affinity purified as previously described with minor modifications.^{52,53}

Htt Constructs. Htt expression constructs used in these studies included a normal (23Q) and expanded (148Q) full-length Htt construct.

Cell Culture. Superfect reagent (Qiagen) was used for transient transfections of human embryonic kidney (HEK) 293T cells with Htt constructs. Cells were collected 60 h post-transfection for analysis. 293T cells or striatal Hdh^{7Q/7Q} and Hdh^{111Q/111Q} cells were cultured in Dulbecco's modified eagle medium (DMEM; Cellgro) with 10% fetal bovine serum (FBS) and 100 U/mL penicillin and 100 ug/mL streptomycin.

Western Analysis. 293T cell pellets were lysed in M-PER (Mammalian Protein Extraction Reagent, Pierce) with protease inhibitors (Mini Complete, Roche), lysates were sonicated and then spun to remove debris (16,000Xg, 20 min). Protein concentration was determined by BCA Protein Assay kit (Pierce). Htt-expressing lysates were in some cases treated exogenously with caspases-2, -3 or -6 (ENZO, 100 U, 2 h, 37 °C) with and without inhibitors **2.35**, **2.36** and **2.37**. Samples were resolved by SDS-PAGE on NuPAGE 4-12% BisTris gel (Invitrogen) in MES running buffer (Invitrogen) for 55 min at 200V. Proteins were transferred to Optitran BA-S nitrocellulose (Schleicher & Schuell) for 14 h at 20 V at 4 °C. Membranes were blocked in 5% milk in Tris-buffered saline Tween-20 and probed overnight with polyclonal neoHtt513, neoHtt552 and neoHtt586 (Open Biosystems; 1:1000 or 1:100 respectively, produced in collaboration with CHDI/Open Biosystems) or monoclonal α -Huntingtin 2166 (Chemicon, 1:1000). Secondary anti-rabbit or anti-mouse antibodies (1:3000, Amersham Biosciences/GE Healthcare) and enhanced chemiluminescence (ECL) reagent (Pierce) were used for detection. We utilized anti-GAPDH as the loading control (Fitzgerald #10R-G109a, 1:1000).

Kcat/Km of Htt with Caspases. 293T cells over-expressing myc-tagged 23Q human full-length Htt were lysed in M-PER (Mammalian Protein Extraction Reagent, Pierce), sonicated and spun to remove debris (16,000Xg, 20 min). Protein was determined using a BCA assay kit (Pierce). Purified human poly-(ADP-ribose) polymerase (PARP) was obtained from Trevigen (Gaithersburg, MD). Htt lysate (15 ug) was incubated with caspase-3 (4 nM; ENZO) or caspase-6 (48 nM, ENZO) for 60 min at 37°C in caspase assay buffer (20 mM PIPES, pH 7.2, 100 mM NaCl, 1% CHAPS, 10% sucrose). Purified PARP (35 ng) was incubated with caspase-3 (7.2-144 nM) under identical conditions. NuPAGE LDS sample buffer (Invitrogen) and 50 mM DTT were added and samples were boiled and separated using SDS-PAGE. Following transfer to nitrocellulose membranes, Htt protein blots were incubated in monoclonal Htt 2166 (1:500; Millipore), PARP protein blots were incubated in polyclonal PARP 253 (1:300; ENZO) and densitometry of bands was performed. All reactions were carried out using subsaturating levels of substrate, where the cleavage is assumed to be a first order

process. Values of k_{cat}/K_m were calculated from the relationship $S_t/S_o = e^{-k_{obs} * t}$ where S_t =concentration of substrate remaining at time t , S_o =initial substrate concentration and $k_{obs} = k_{cat} * [enzyme]/K_m$ (Gervais *et al.*, 1998).

Caspase Activity in Striatal *Hdh*^{7Q/7Q} and *Hdh*^{111Q/111Q} cells. Striatal *Hdh*^{7Q/7Q} and *Hdh*^{111Q/111Q} cells were maintained at 33 °C in a humidified atmosphere of 95% air and 5% CO₂, in DMEM supplemented with 10% FBS, 100 U/mL penicillin and 100 µg/mL streptomycin. Cells were fed with fresh medium every 2–3 d. Striatal cells were plated at 5000 cells/well in collagen coated 96-well plates and were grown for 48 h. Cells were maintained in serum DMEM for 24 h with or without caspase inhibitors and an additional 24 h without serum with same inhibitor treatment. Caspase 3/7 activity was measured using kit as per manufacturer's direction (Mountain View, CA) and normalized by protein concentration. Briefly, cells were lysed in working cell lysis buffer (50 µL, 1:1 lysis buffer: serum free DMEM) by shaking at 700 rpm for 5 min and a 20 µL aliquot was measured for protein concentration. Afterwards 70 uL of working lysis buffer with DTT (15 mM), and caspase substrate (1x) was added to remaining lysed cells, shaken briefly and then read continuously at 37 °C for 90 minutes with excitation at 488nm and emission at 530nm.

Immunocytochemistry. Striatal *Hdh*^{7Q/7Q} and *Hdh*^{111Q/111Q} cells cultured on cover slips with or without serum withdrawal were fixed with 4% paraformaldehyde for 20 min at room temperature. The fixed cells were then permeabilized with 0.1% TritonX-100 for 10 min and blocked with 5% donkey serum for 45 min. The incubation with the primary antibody (rabbit polyclonal neoHtt513, 1:100) at 4°C overnight was followed by secondary antibody (donkey anti rabbit Alexa546, 1:1000, Invitrogen) incubation at room temperature for 1.5 h. Finally cells were mounted to a slide with droplets of Prolong Gold with DAPI (Invitrogen) on it before microscopy.

Primary cortico-striatal co-culture. Striatum and cortex from E18 rat embryos were micro-dissected, enzymatically treated with papain and dissociated. Five million cells of each type were electroporated separately (Amaxa Biosystems) with DNA constructs expressing either YFP in striatal neurons or mCherry in cortical neurons together with a plasmid expressing mutant polyQ expanded Htt exon1 (HttN90Q73), then plated together on a layer of astrocytes which was prepared three days prior. Our method for assessing culture health in experiments is by determining the numbers and morphology of GFP expressing cells. In developing the assay we found with vital stains that about 50% of cells die immediately after the electroporation. The neurons that survive the electroporation appear to be healthy, extending neurites and forming functional synapses as assessed by synaptic marker staining and electrophysiology. Neurons and astrocytes were grown in Neurobasal media (Invitrogen) supplemented with 5% fetal calf serum (Sigma), 2 mM glutamine (glutamax, Invitrogen), 10 mM potassium chloride and 5 ug/ml gentamycin. Astrocytes were isolated from E18 embryos and expanded for three passages before plating into 96-well plates. Co-cultures were incubated in 95% O₂/5% CO₂ at 37°C for six days before analysis. Compounds were

dissolved in DMSO and dosed as a single dose shortly after neuron plating. The control condition was HttN90Q73 with DMSO alone. For quantification of neurons using the Cellomics ArrayScan VTI, fluorescent images were acquired at 10x magnification from 9 fields per well using YFP and dsRED filter sets and analyzed using the Target Activation algorithm. The algorithm was optimized for object size, object shape and fluorescence intensity to identify specific neuron cell bodies. Healthy neurons are easily identified by the size of the cell body and neuritic morphology. Graphical analysis and statistical computations were performed with GraphPad Prism.

References

- (1) HDCRG *Cell* **1993**, *72*, 971.
- (2) Arrasate, M.; Mitra, S.; Schweitzer, E. S.; Segal, M. R.; Finkbeiner, S. *Nature* **2004**, *431*, 805.
- (3) Sawada, H.; Ishiguro, H.; Nishii, K.; Yamada, K.; Tsuchida, K.; Takahashi, H.; Goto, J.; Kanazawa, I.; Nagatsu, T. *Neuroscience Research* **2007**, *57*, 559.
- (4) Dunah, A. W.; Jeong, H.; Griffin, A.; Kim, Y.-M.; Standaert, D. G.; Hersch, S. M.; Mouradian, M. M.; Young, A. B.; Tanese, N.; Krainc, D. *Science* **2002**, *296*, 2238.
- (5) Li, S.-H.; Cheng, A. L.; Zhou, H.; Lam, S.; Rao, M.; Li, H.; Li, X.-J. *Molecular and Cellular Biology* **2002**, *22*, 1277.
- (6) Zhai, W.; Jeong, H.; Cui, L.; Krainc, D.; Tjian, R. *Cell* **2005**, *123*, 1241.
- (7) Charvin, D.; Roze, E.; Perrin, V.; Deyts, C.; Betuing, S.; Pages, C.; Regulier, E.; Luthi-Carter, R.; Brouillet, E.; Deglon, N.; Caboche, J. *Neurobiology of Disease* **2008**, *29*, 22.
- (8) Fan, M. M. Y.; Raymond, L. A. *Progress in Neurobiology* **2007**, *81*, 272.
- (9) Stack, E. C.; Dedeoglu, A.; Smith, K. M.; Cormier, K.; Kubilus, J. K.; Bogdanov, M.; Matson, W. R.; Yang, L.; Jenkins, B. G.; Luthi-Carter, R.; Kowall, N. W.; Hersch, S. M.; Beal, M. F.; Ferrante, R. J. *Journal of Neuroscience* **2007**, *27*, 12908.
- (10) Gutekunst, C.-A.; Li, S.-H.; Yi, H.; Mulroy, J. S.; Kuemmerle, S.; Jones, R.; Rye, D.; Ferrante, R. J.; Hersch, S. M.; Li, X.-J. *Journal of Neuroscience* **1999**, *19*, 2522.
- (11) Davies, S. W.; Turmaine, M.; Cozens, B. A.; DiFiglia, M.; Sharp, A. H.; Ross, C. A.; Scherzinger, E.; Wanker, E. E.; Mangiarini, L.; Bates, G. P. *Cell* **1997**, *90*, 537.
- (12) DiFiglia, M.; Sapp, E.; Chase, K. O.; Davies, S. W.; Bates, G. P.; Vonsattel, J. P.; Aronin, N. *Science* **1997**, *277*, 1990.
- (13) Goldberg, Y. P.; Nicholson, D. W.; Rasper, D. M.; Kalchman, M. A.; Koide, H. B.; Graham, R. K.; Bromm, M.; Kazemi-Esfarjani, P.; Thornberry, N. A.; et al. *Nature Genetics* **1996**, *13*, 442.

- (14) Martindale, D.; Hackam, A.; Wieczorek, A.; Ellerby, L.; Wellington, C.; McCutcheon, K.; Singaraja, R.; Kazemi-Esfarjani, P.; Devon, R.; Kim, S. U.; Bredesen, D. E.; Tufaro, F.; Hayden, M. R. *Nature Genetics* **1998**, *18*, 150.
- (15) Gafni, J.; Ellerby, L. M. *Journal of Neuroscience* **2002**, *22*, 4842.
- (16) Gafni, J.; Hermel, E.; Young, J. E.; Wellington, C. L.; Hayden, M. R.; Ellerby, L. M. *Journal of Biological Chemistry* **2004**, *279*, 20211.
- (17) Lunkes, A.; Lindenberg, K. S.; Ben-Haiem, L.; Weber, C.; Devys, D.; Landwehrmeyer, G. B.; Mandel, J.-L.; Trotter, Y. *Molecular Cell* **2002**, *10*, 259.
- (18) Wellington, C. L.; Ellerby, L. M.; Hackam, A. S.; Margolis, R. L.; Trifiro, M. A.; Singaraja, R.; McCutcheon, K.; Salvesen, G. S.; Propp, S. S.; Bromm, M.; Rowland, K. J.; Zhang, T.; Rasper, D.; Roy, S.; Thornberry, N.; Pinsky, L.; Kakizuka, A.; Ross, C. A.; Nicholson, D. W.; Bredesen, D. E.; Hayden, M. R. *Journal of Biological Chemistry* **1998**, *273*, 9158.
- (19) Pop, C.; Salvesen, G. S. *Journal of Biological Chemistry* **2009**, *284*, 21777.
- (20) Reed John, C. *Nature reviews. Drug discovery* **2002**, *1*, 111.
- (21) Wellington, C. L.; Singaraja, R.; Ellerby, L.; Savill, J.; Roy, S.; Leavitt, B.; Cattaneo, E.; Hackam, A.; Sharp, A.; Thornberry, N.; Nicholson, D. W.; Bredesen, D. E.; Hayden, M. R. *Journal of Biological Chemistry* **2000**, *275*, 19831.
- (22) Graham, R. K.; Deng, Y.; Slow, E. J.; Haigh, B.; Bissada, N.; Lu, G.; Pearson, J.; Shehadeh, J.; Bertram, L.; Murphy, Z.; Warby, S. C.; Doty, C. N.; Roy, S.; Wellington, C. L.; Leavitt, B. R.; Raymond, L. A.; Nicholson, D. W.; Hayden, M. R. *Cell* **2006**, *125*, 1179.
- (23) Hermel, E.; Gafni, J.; Propp, S. S.; Leavitt, B. R.; Wellington, C. L.; Young, J. E.; Hackam, A. S.; Logvinova, A. V.; Peel, A. L.; Chen, S. F.; Hook, V.; Singaraja, R.; Krajewski, S.; Goldsmith, P. C.; Ellerby, H. M.; Hayden, M. R.; Bredesen, D. E.; Ellerby, L. M. *Cell Death and Differentiation* **2004**, *11*, 424.
- (24) Schulz, J. B.; Weller, M.; Matthews, R. T.; Heneka, M. T.; Groscurth, P.; Martinou, J.-C.; Lommatzsch, J.; Von Coelln, R.; Wullner, U.; Loschmann, P. A.; Beal, M. F.; Dichgans, J.; Klockgether, T. *Cell Death and Differentiation* **1998**, *5*, 847.
- (25) Toulmond, S.; Tang, K.; Bureau, Y.; Ashdown, H.; Degen, S.; O'Donnell, R.; Tam, J.; Han, Y.; Colucci, J.; Giroux, A.; Zhu, Y.; Boucher, M.; Pikounis, B.; Xanthoudakis, S.; Roy, S.; Rigby, M.; Zamboni, R.; Robertson, G. S.; Ng, G. Y. K.; Nicholson, D. W.; Flueckiger, J.-P. *British Journal of Pharmacology* **2004**, *141*, 689.
- (26) Chen, M.; Ona, V. O.; Li, M.; Ferrante, R. J.; Fink, K. B.; Zhu, S.; Bian, J.; Guo, L.; Farrell, L. A.; Hersch, S. M.; Hobbs, W.; Vonsattel, J.-P.; Cha, J.-H. J.; Friedlander, R. M. *Nature Medicine* **2000**, *6*, 797.
- (27) Cornelis, S.; Kersse, K.; Festjens, N.; Lamkanfi, M.; Vandenabeele, P. *Current Pharmaceutical Design* **2007**, *13*, 367.
- (28) O'Brien, T.; Lee, D. *Mini-Reviews in Medicinal Chemistry* **2004**, *4*, 153.

- (29) Talanian, R. V.; Quinlan, C.; Trautz, S.; Hackett, M. C.; Mankovich, J. A.; Banach, D.; Ghayur, T.; Brady, K. D.; Wong, W. W. *Journal of Biological Chemistry* **1997**, *272*, 9677.
- (30) Brak, K.; Doyle Patricia, S.; McKerrow James, H.; Ellman Jonathan, A. *Journal of the American Chemical Society* **2008**, *130*, 6404.
- (31) Inagaki, H.; Tsuruoka, H.; Hornsby, M.; Lesley Scott, A.; Spraggon, G.; Ellman Jonathan, A. *Journal of Medicinal Chemistry* **2007**, *50*, 2693.
- (32) Patterson, A. W.; Wood, W. J. L.; Hornsby, M.; Lesley, S.; Spraggon, G.; Ellman, J. A. *Journal of Medicinal Chemistry* **2006**, *49*, 6298.
- (33) Wood, W. J. L.; Patterson, A. W.; Tsuruoka, H.; Jain, R. K.; Ellman, J. A. *Journal of the American Chemical Society* **2005**, *127*, 15521.
- (34) Brik, A.; Alexandratos, J.; Lin, Y.-C.; Elder John, H.; Olson Arthur, J.; Wlodawer, A.; Goodsell David, S.; Wong, C.-H. *Chembiochem : a European journal of chemical biology* **2005**, *6*, 1167.
- (35) Thornberry, N. A.; Rano, T. A.; Peterson, E. P.; Rasper, D. M.; Timkey, T.; Garcia-Calvo, M.; Houtzager, V. M.; Nordstrom, P. A.; Roy, S.; Vaillancourt, J. P.; Chapman, K. T.; Nicholson, D. W. *Journal of Biological Chemistry* **1997**, *272*, 17907.
- (36) Linton, S. D.; Aja, T.; Allegrini, P. R.; Deckwerth, T. L.; Diaz, J.-L.; Hengerer, B.; Herrmann, J.; Jahangiri, K. G.; Kallen, J.; Karanewsky, D. S.; Meduna, S. P.; Nalley, K.; Robinson, E. D.; Roggo, S.; Rovelli, G.; Sauter, A.; Sayers, R. O.; Schmitz, A.; Smidt, R.; Ternansky, R. J.; Tomaselli, K. J.; Ullman, B. R.; Wiessner, C.; Wu, J. C. *Bioorganic & Medicinal Chemistry Letters* **2004**, *14*, 2685.
- (37) Linton, S. D.; Aja, T.; Armstrong, R. A.; Bai, X.; Chen, L.-S.; Chen, N.; Ching, B.; Contreras, P.; Diaz, J.-L.; Fisher, C. D.; Fritz, L. C.; Gladstone, P.; Groessler, T.; Gu, X.; Herrmann, J.; Hirakawa, B. P.; Hoglen, N. C.; Jahangiri, K. G.; Kalish, V. J.; Karanewsky, D. S.; Kodandapani, L.; Krebs, J.; McQuiston, J.; Meduna, S. P.; Nalley, K.; Robinson, E. D.; Sayers, R. O.; Sebring, K.; Spada, A. P.; Ternansky, R. J.; Tomaselli, K. J.; Ullman, B. R.; Valentino, K. L.; Weeks, S.; Winn, D.; Wu, J. C.; Yeo, P.; Zhang, C.-z. *Journal of Medicinal Chemistry* **2005**, *48*, 6779.
- (38) Baskin-Bey, E. S.; Washburn, K.; Feng, S.; Oltersdorf, T.; Shapiro, D.; Huyghe, M.; Burgart, L.; Garrity-Park, M.; van Vilsteren, F. G. I.; Oliver, L. K.; Rosen, C. B.; Gores, G. J. *American Journal of Transplantation* **2007**, *7*, 218.
- (39) Schweizer, A.; Briand, C.; Gruetter, M. G. *Journal of Biological Chemistry* **2003**, *278*, 42441.
- (40) Rozman-Pungercar, J.; Kopitar-Jerala, N.; Bogyo, M.; Turk, D.; Vasiljeva, O.; Stefe, I.; Vandenabeele, P.; Broemme, D.; Puizdar, V.; Fonovic, M.; Trstenjak-Prebanda, M.; Dolenc, I.; Turk, V.; Turk, B. *Cell Death and Differentiation* **2003**, *10*, 881.
- (41) Sexton, K. B.; Witte, M. D.; Blum, G.; Bogyo, M. *Bioorganic & Medicinal Chemistry Letters* **2007**, *17*, 649.

- (42) Trettel, F.; Rigamonti, D.; Hilditch-Maguire, P.; Wheeler, V. C.; Sharp, A. H.; Persichetti, F.; Cattaneo, E.; MacDonald, M. E. *Human Molecular Genetics* **2000**, *9*, 2799.
- (43) Patterson, A. W.; Ellman, J. A. *Journal of Organic Chemistry* **2006**, *71*, 7110.
- (44) Aschwanden, P.; Stephenson, C. R. J.; Carreira, E. M. *Organic Letters* **2006**, *8*, 2437.
- (45) Lelais, G.; Campo, M. A.; Kopp, S.; Seebach, D. *Helvetica Chimica Acta* **2004**, *87*, 1545.
- (46) Chino, M.; Wakao, M.; Ellman, J. A. *Tetrahedron* **2002**, *58*, 6305.
- (47) Lundquist, J. T. t.; Pelletier, J. C. *Organic Letters* **2001**, *3*, 781.
- (48) Rostovtsev, V. V.; Green, L. G.; Fokin, V. V.; Sharpless, K. B. *Angewandte Chemie, International Edition* **2002**, *41*, 2596.
- (49) Stennicke, H. R.; Salvesen, G. S. *Methods* **1999**, *17*, 313.
- (50) Bieth, J. G. *Methods in Enzymology* **1995**, *248*, 59.
- (51) Ekici Ozlem, D.; Li Zhao, Z.; Campbell Amy, J.; James Karen, E.; Asgian Juliana, L.; Mikolajczyk, J.; Salvesen Guy, S.; Ganesan, R.; Jelakovic, S.; Grutter Markus, G.; Powers James, C. *Journal of Medicinal Chemistry* **2006**, *49*, 5728.
- (52) Wellington, C. L.; Ellerby, L. M.; Gutekunst, C.-A.; Rogers, D.; Warby, S.; Graham, R. K.; Loubser, O.; van Raamsdonk, J.; Singaraja, R.; Yang, Y.-Z.; Gafni, J.; Bredesen, D.; Hersch, S. M.; Laevitt, B. R.; Roy, S.; Nicholson, D. W.; Hayden, M. R. *Journal of Neuroscience* **2002**, *22*, 7862.
- (53) Gervais, F. G.; Xu, D.; Robertson, G. S.; Vaillancourt, J. P.; Zhu, Y.; Huang, J.; LeBlanc, A.; Smith, D.; Rigby, M.; Shearman, M. S.; Clarke, E. E.; Zheng, H.; Van Der Ploeg, L. H. T.; Ruffolo, S. C.; Thornberry, N. A.; Xanthoudakis, S.; Zamboni, R. J.; Roy, S.; Nicholson, D. W. *Cell* **1999**, *97*, 395.

Chapter 3. Design of *Plasmodium falciparum* Dipeptidyl Aminopeptidase I Inhibitors and Development of Fragmenting Hybrid Approach for Anti-malarial Delivery.

The widespread resistance of malaria parasites to affordable drugs has made the identification of new targets an urgent issue. Dipeptidyl aminopeptidases (DPAPs) represent potentially viable new targets due to their involvement in hemoglobin degradation and parasite release. We report the use of homology modeling and computational docking to design and synthesize nonpeptidic DPAP1 inhibitors that kill Plasmodium falciparum at low nanomolar concentrations. Additionally, a fragmenting hybrid approach was developed as an alternative to artemisinin combination therapy (ACT), the current front-line treatment of malaria. Slow release of a secondary anti-malarial agent was achieved through a fragmenting hybrid containing a trioxolane agent conjugated to our lead nonpeptidic inhibitor of DPAP1. Overall, we validated DPAP1 as a valuable anti-malarial target and demonstrated that our fragmenting hybrid can be successfully used to deliver secondary anti-malarial agents into parasite-infected erythrocytes. The majority of this work has been published (Deu, E.; Leyva, M. J.; Albrow, V. E.; Rice, M. J.; Ellman, J. A.; Bogoy, M. Chemistry & Biology 2010, 17, 808-819).

Authorship

Dr. Hiroshi Nakagawa synthesized the initial dipeptidyl aminopeptidase I inhibitor. I hypothesized the optimization of the initial inhibitor structure that would increase binding interactions with the protease. I synthesized all nonpeptidic, dipeptidyl aminopeptidase I inhibitors. Computational modeling and all *in vitro* and *in vivo* studies on nonpeptidic inhibitors were conducted by Edgar Deu, Victoria E. Albrow, Mark J. Rice, Matthew Bogyo at the Department of Pathology at Stanford School of Medicine. Synthesis of trioxolane-based hybrid molecules and subsequent *in vitro* and *in vivo* studies were conducted by Sumit S. Mahajan and Adam R. Renslo at the Department of Pharmaceutical Chemistry at the University of California, San Francisco.

Introduction

Malaria is one of the most common infectious diseases caused by protozoan parasites and more than 40% of the world's population is at risk of contracting the disease.¹ Each year, a quarter of a billion malaria cases and about a million deaths occur. Malaria in humans is caused by four species of *Plasmodium* parasites that are transmitted by the *Anopheles* mosquito. No vaccine is currently available for malaria and the greatest obstacle to controlling the disease worldwide is the emerging widespread resistance of the *Plasmodium* species to chemotherapeutic agents. Studies have identified multi-antimalarial drug resistance in various areas of the world.²⁻⁴ More recently, resistance to the current first-line treatment, artemisinin-based combination therapy, is emerging in Southeast Asia.⁵⁻⁷ Therefore, there is an urgent need to develop new strategies to identify new drug targets to fight malaria.

Plasmodium falciparum is the most virulent of the four *Plasmodium* parasites and accounts for 90% of all malaria-related deaths. Completion of the *P. falciparum* genome in 2002 provided a basis for identifying new targets such as malarial proteases.⁸ Numerous proteases have been identified throughout the parasitic life cycle and play a role in various biological processes such as hemoglobin degradation, protein trafficking, parasite release or rupture, and erythrocyte invasion.⁹⁻¹² Inhibition of cysteine proteases result in disruption of parasite growth, egress from erythrocytes, and invasion with much of the studies on *P. falciparum* cysteine proteases focused on the falcipains (FPs). FP1 is expressed in the later stages of the erythrocytic cycle and is likely involved in host cell invasion while FP2, 2', 3 are located in the food vacuole and involved in hemoglobin degradation.^{13,14}

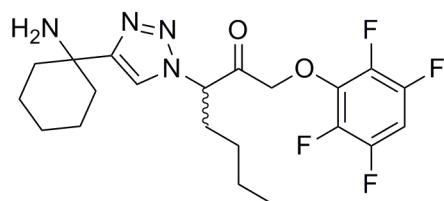
Recently, dipeptidyl aminopeptidases (DPAPs) were identified as key regulators of the *P. falciparum* erythrocytic life cycle.¹⁵ Unlike other proteases of the same family, DPAPs are composed of a papain-fold domain and an exclusion domain. The exclusion domain interacts with the N-terminal free amine of substrates, allowing proteolytic cleavage of dipeptides from the amino-terminus of polypeptides.^{16,17} DPAP1 is located in the food vacuole, an acidic organelle where protein degradation occurs, and is likely to be involved in the later stages of hemoglobin degradation. DPAP1 degrades oligopeptide products of upstream proteolysis, which can be further degraded into amino acids by

aminopeptidases.¹⁸⁻²⁰ DPAP3 was more recently identified as a key regulator of parasite release.²¹ DPAPs are potentially good targets due to their involvement in various biological processes at different stages of the parasite life cycle. Additionally, the closest human homolog to the DPAPs is cathepsin C, a protease that is not essential to mammals.²²⁻²⁴

We therefore, applied computational methods to design stable, nonpeptidic irreversible DPAP inhibitors. The most potent inhibitors killed *P. falciparum* in nanomolar concentrations in culture and were stable in mouse serum. Additionally, specific inhibition of DPAP1 prevented parasite growth *in vitro* and *in vivo*, which suggests that DPAP1 is a viable anti-malarial target. Finally, successful release of two anti-malarial agents with ACT-like activity was achieved by incorporating a fragmenting hybrid composed of a trioxolane analogue and one of our most potent irreversible DPAP inhibitors.

Computational Design, Synthesis, and Evaluation of Nonpeptidic Inhibitors

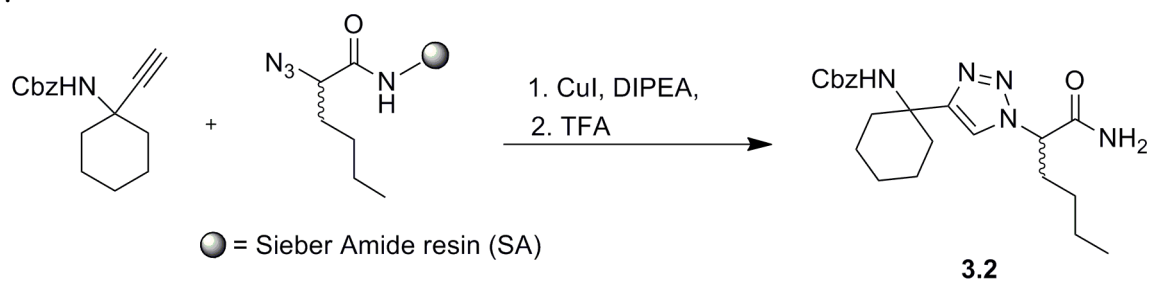
Inhibitors that were designed to target cathepsins,²⁵ with a 2,3,5,6-tetrafluorophenoxymethyl ketone pharmacophore and N-terminal free amine, were screened against DPAP1. Irreversible inhibitor **3.1** was the most potent inhibitor against DPAP1. To investigate the importance of the pharmacophore, we synthesized two analogs containing a nitrile and acyloxymethyl ketone pharmacophore. The synthesis of the reversible nitrile (**3.4**) was achieved by reacting Cbz-protected ethynylcyclohexylamine with racemic α -azido functionalized Sieber resin, followed by acidic cleavage from solid support yielded 1,2,3-triazole primary amide **3.2** (Scheme 3.1). Subsequent dehydration with 2,4,6-trichlorotriazine to afford nitrile **3.3**, and Cbz deprotection under acidic conditions yielded reversible inhibitor (**3.4**). Acyloxymethyl ketone **3.5** was synthesized by a formal 1,4-dipolar cycloaddition with racemic α -azido acyloxymethyl ketone and Boc-protected ethynylcyclohexylamine followed by acidic Boc-deprotection. After screening against DPAP1, the acyloxymethyl ketone (**3.2**) and nitrile (**3.3**) were 18-fold and 380-fold less potent than bench mark inhibitor **3.1** with a second order rate constant of inhibition (k_i) of $630 \pm 30 \text{ M}^{-1}\text{s}^{-1}$, respectively. The 2,3,5,6-tetrafluorophenoxymethyl ketone **3.1** has a half maximal inhibition ($\text{IC}_{50 \text{ DPAP1}}$) of 560 nM after 30 min of incubation in parasite lysates. To test whether DPAP1 inhibition results in parasite death, ring stage parasites were treated with inhibitor for ~75 h to yield the half maximal parasite growth ($\text{EC}_{50 \text{ POT}}$) value. Table 3.1 shows a correlation between DPAP1 inhibition and potency by comparing the k_i and $\text{EC}_{50 \text{ POT}}$ values. The more active an inhibitor is against DPAP1, the more potent it is at killing the parasite, which suggests that specific inhibition of DPAP1 directly correlates with parasite death.



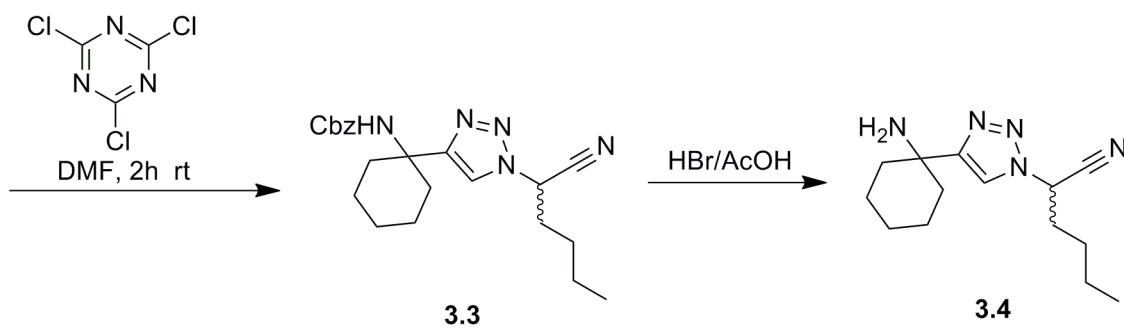
3.1

Figure 3.1. Benchmark DPAP1 aryloxymethyl ketone inhibitor (**3.1**).

Scheme 3.1. Synthesis of reversible nitrile inhibitor (**3.4**)



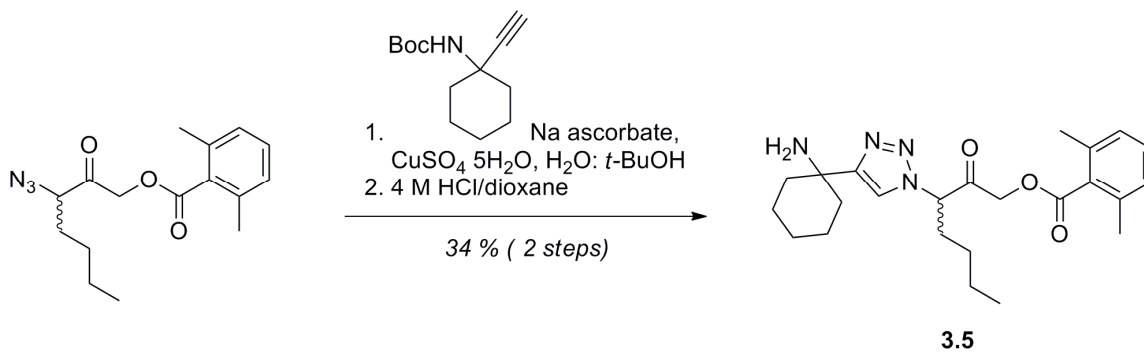
3.2



3.3

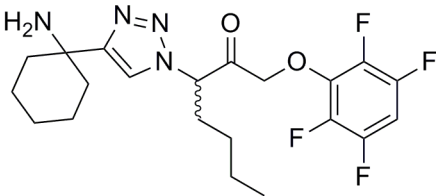
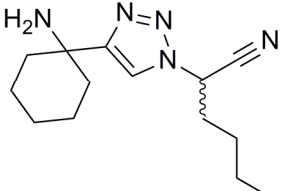
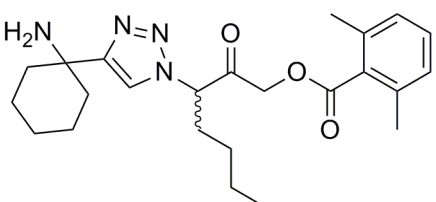
3.4

Scheme 3.2. Synthesis of irreversible aryloxymethyl ketone inhibitor (**3.5**)



3.5

Table 3.1. Potency of inhibitors incorporating various pharmacophores against DPAP1

Inhibitor	k_i ($M^{-1}s^{-1}$)	IC ₅₀ DPAP1 (nM)	EC ₅₀ Pot (nM)
	630 (30)	560 (40)	70 (30)
	1.7 (0.2)	>100,000	>100,000
	34 (2)	11,000 (1000)	6000 (3000)

To guide the synthesis of nonpeptidic inhibitors incorporating the optimal 2,3,5,6-tetrafluorophenoxymethyl ketone, we built a homology model of DPAP1 based on human cathepsin C (hCat C).²⁶ Inhibitor **3.1** was built into the DPAP1 active site and the model displayed a deep S2 pocket that was not adequately filled by the cyclohexane ring of inhibitor **3.1** (Figure 3.2). To maximize the binding interaction between the inhibitor and the S2 pocket, we synthesized mono- and di-substituted α -amine analogs as cyclohexane ring replacements. For the synthesis of the mono- and di-branched amine analogs, α -azido 2,3,5,6-tetrafluorophenoxymethyl ketone was reacted with various *tert*-butylsulfinyl-protected amines via a 1,4 dipolar cycloaddition followed by acidic cleavage of the sulfinyl group (Scheme 3.3). Evaluation of the inhibitory activity of the analogs resulted in useful structure activity relationships (Table 3.2). Substitution with the smaller methyl (**3.6**) and di-methyl (**3.7**) groups were slightly less active than **3.1**. Incorporating methyl-propyl (**3.8**) and di-ethyl (**3.9**) groups modestly increased the k_i value to 810 and 910, respectively. However, a substitution of two propyl (**3.10**) groups resulted in 2-fold decrease in k_i compared to **3.7**. Inhibitor **3.11**, which incorporated methyl and cyclopentyl groups, improved potency by more than 4-fold compared to benchmark inhibitor **3.1**. Adding benzyl groups in the α position (**3.12** -**3.13**)

dramatically decreased activity by >128-fold, due to possible steric clash between the large benzyl group and active site pocket. Chiral preference was observed by comparing the (*S*)-configured methyl-cyclohexyl inhibitor and the (*R*)-derivative. The (*S*)-derivative (**3.14**) resulted in a modest decrease in activity compared to the benchmark cyclohexyl inhibitor **3.1**. Notably, the (*R*)-analog (**3.15**) was >25-fold less active than (*S*)-analog **3.14**.

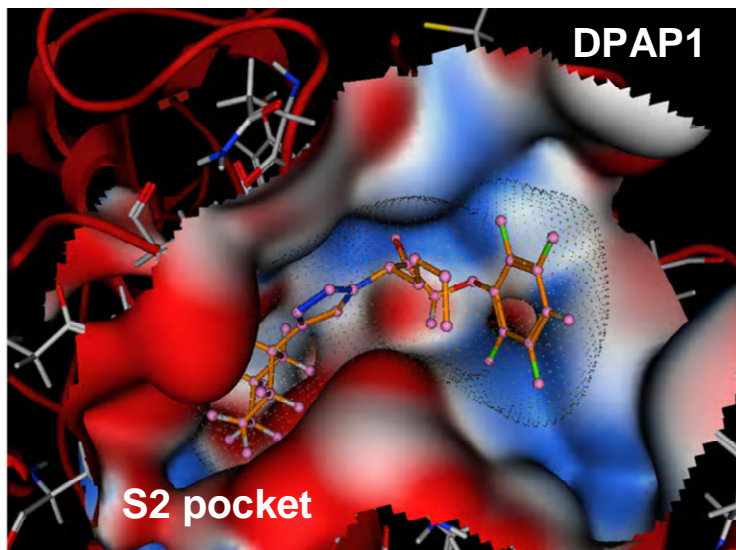


Figure 3.2. Docked **3.1** in homology model of DPAP1.

Scheme 3.3. Synthesis of mono- and di-branched amine inhibitor analogs

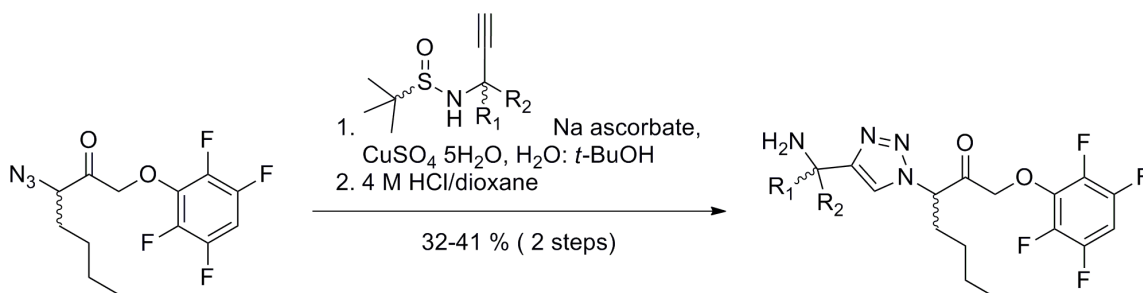
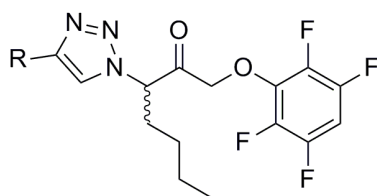


Table 3.2. Potency of mono- and di-branched amine inhibitors against DPAP1.



Inhibitor	R	k_i ($M^{-1}s^{-1}$)	IC_{50} DPAP1 (nM)	EC_{50} Pot (nM)
3.6		520 (30)	700 (40)	3000 (1300)
3.7		310 (30)	1100 (100)	1000 (500)
3.8		810 (50)	410 (30)	35,000 (30,000)
3.9		910 (50)	410 (10)	20 (10)
3.10		510 (40)	700 (50)	140 (60)
3.11		2070 (30)	186 (2)	19 (2)
3.12		4.9 (0.5)	74,000 (9000)	3000 (2000)
3.13		1.6 (0.2)	>100,000	35,000 (30,000)
3.14		500 (20)	700 (40)	60 (30)
3.15		<20	>20,000	3800 (3000)

Our next step involved synthesizing inhibitors that maximized binding interactions of the deep S2 pocket. First, we synthesized inhibitors that replaced the cyclohexane ring of **3.1** with a piperidine ring to further functionalize the distal nitrogen using similar reaction conditions previously described in Scheme 3.2. Unfortunately, the free piperidine (**3.16**), acetylated piperidine (**3.17**), and urea derivative (**3.18**) dramatically reduced activity and weakened potency against DPAP1 (Table 3.3). The final inhibitor (**3.19**) synthesized in this set, is a modified version of our most potent inhibitor (**3.11**) from Table 3.2. In place of a free amine, a secondary amine is incorporated within a pyrrolidine ring and derivatized with a methyl group at the α -position. Inhibitor **3.19** is ~1.4-fold more active than benchmark inhibitor **3.1** but 2.25-fold less active than the most potent inhibitor **3.11**.

Table 3.3. Potency of cyclic-branched amine inhibitors against DPAP1

Inhibitor	R	k_i ($M^{-1}s^{-1}$)	IC ₅₀ DPAP1 (nM)	EC ₅₀ Pot (nM)
3.16		<20	>20,000	220 (160)
3.17		<20	>20,000	>100,000
3.18		<20	>20,000	45,000 (26,000)
3.19		920 (70)	420 (30)	930 (130)

Our most potent and promising inhibitor **3.11** was previously synthesized and screened as a racemic mixture. Based on the structures of the (*R*)- and (*S*)-diastereomers built into the the DPAP1 active site and the difference in activity between **3.14** and **3.15**, we expected a more active (*S*)-diastereomer. Figure 3.3 shows the cyclopentyl ring of the (*S*)-configured isomer buried deep in the S2 pocket while the (*R*)-configured derivative has the ring exposed to solvent. To validate this hypothesis, both diastereomers were synthesized and their specificity, potency, and toxicity were measured. As expected, inhibitor **3.21** displayed improvement in k_i value by ~8-fold compared to **3.11** and a ~590-fold difference to the weakly active R-isomer **3.20** (Table 3.4).

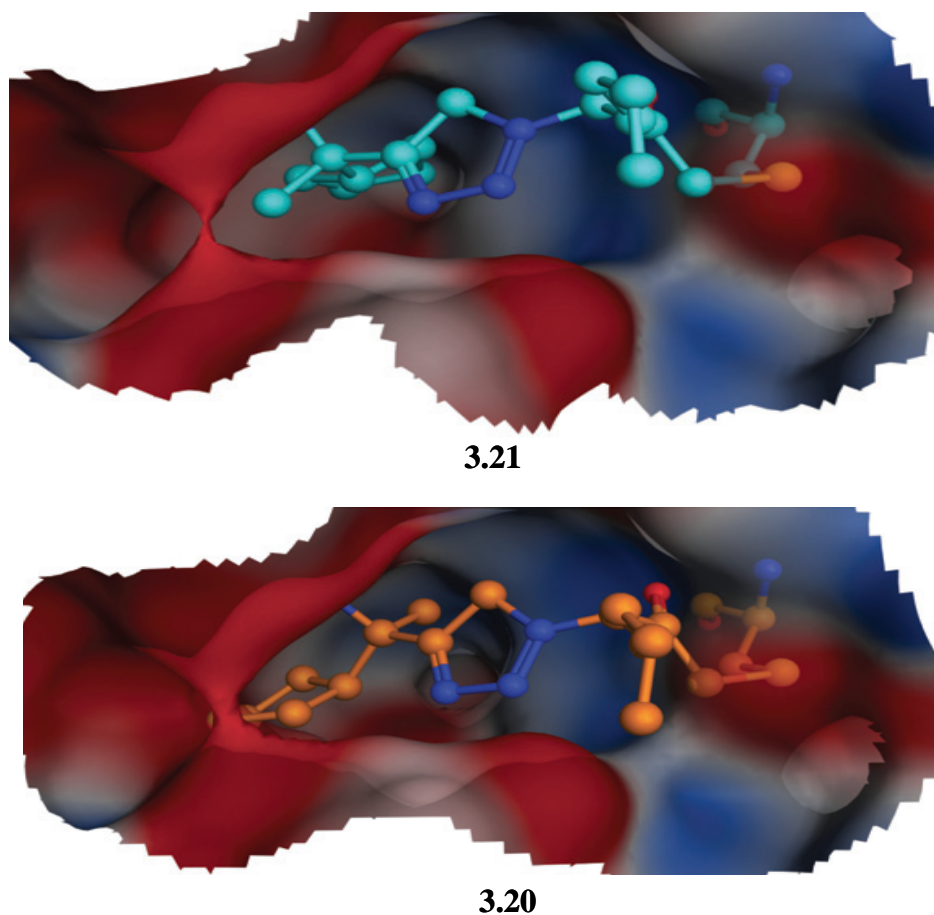
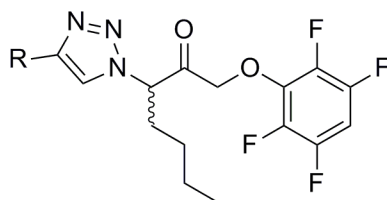


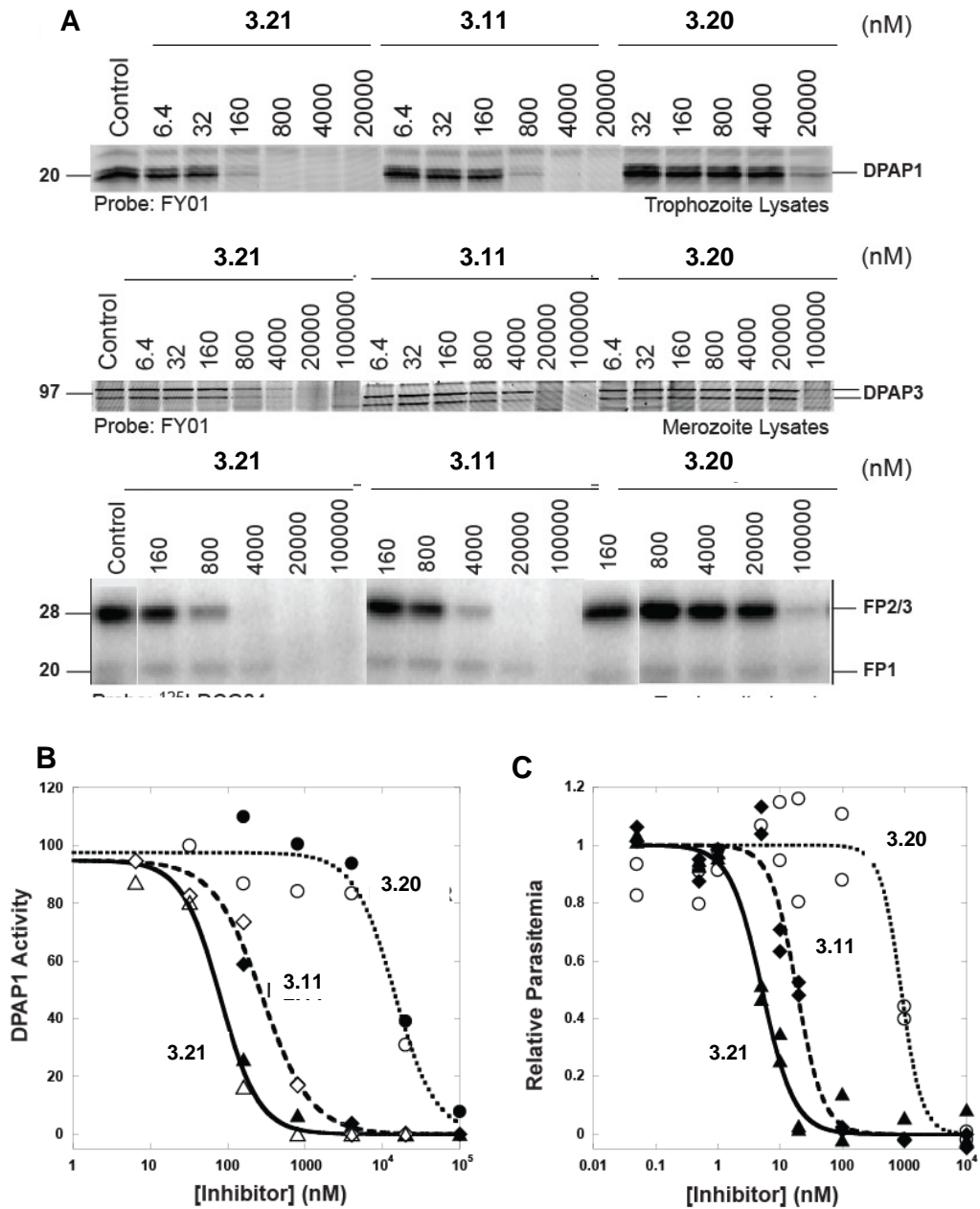
Figure 3.3. Docked methyl-cyclopentyl diastereomers in DPAP1 homology model.

Table 3.4. DPAP1 potency and toxicity of methyl-cyclopentyl branched inhibitors

Inhibitor	R	k_i ($M^{-1}s^{-1}$)	IC ₅₀ DPAP1 (nM)	EC ₅₀ Pot (nM)	EC ₅₀ Tox (nM)
3.11		2070 (30)	186 (2) ^a	19 (2)	9300 (600)
3.20		28 (3)	14,000 (1500) ^a	890 (520)	7000 (2000)
3.21		16,500 (1200)	19 (1)	5.2 (0.5)	8500 (1500)

A specificity screen against different *P. falciparum* cysteine proteases, showed **3.21** to be significantly more potent than **3.20**, while **3.11** showed intermediate potency (Figure 3.4 A and B). Notably, **3.21** was also active against DPAP3 and FP2/3 (although with reduced potency compared with DPAP1), indicating that it is a more broad spectrum inhibitor (Figure 3.4 A and D). To correlate target inhibition with potency against the parasite, inhibition studies were performed in intact parasites. These methyl-cyclopentyl inhibitors are cell permeable as they show the same trend of DPAP1 inhibition in intact parasites and in lysates (Figure 3.3 B). Additionally, the same pattern in potency observed in the competition studies in lysates was observed in the replication assay (Figure 3.4 C). To further correlate parasite death with DPAP1 inhibition, we compared the IC₅₀ values against DPAP1, DPAP3, and FP2/3 with potency in a 1 h replication assay since the IC₅₀ values were obtained after 0.5 h incubation of parasite lysates with compound prior to probe labeling for 1 h (Figure 3.4 D). For both **3.11** and **3.21**, we observed a direct correlation between specificity and parasite death, with only the IC₅₀

values for DPAP1 inhibition matching the EC_{50} Pot (1 h values in the replication assay). Although **3.20** is much less potent against DPAP1, its EC_{50} Pot (after 1 h) may reflect some off-target effects since this compound is also toxic to human foreskin fibroblast (HFF) cells at high concentrations (Figure 3.4 D). Importantly, the fact that **3.21** is >500-fold more potent than **3.20** at killing parasites, yet both have similar general toxicity level in HFF cells ($EC_{50Tox} \sim 10 \mu M$), suggests that potency in parasite killing is due to target inhibition rather than nonspecific toxic effects.



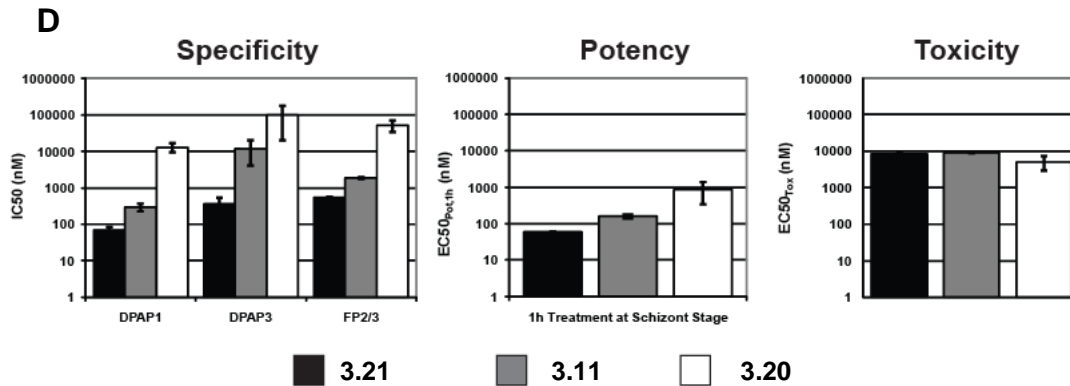


Figure 3.4. Specificity, potency, and toxicity of methyl-cyclohexyl inhibitors. (A) Specificity towards DPAPs and falcipains (FPs). (B) DPAP1 inhibition of intact parasites versus lysates. (C) Potency of killing parasites. (D) Specificity versus potency versus toxicity.

To determine the stability of our most potent nonpeptidic inhibitor, we measured the potency of **3.21** toward DPAP1 before and after overnight incubation in mouse serum at 37 °C (Figure 3.5 A). (*S*)-configured inhibitor **3.21** shows only minimal loss of potency after serum treatment and subsequently sustained DPAP1 inhibition in intact parasites (Figure 3.5 B). Interestingly, the kinetic inhibition studies in intact parasites suggest that 1 nM of **3.21** is sufficient to induce a prolonged inhibition of 70% of DPAP1 activity without killing parasites (i.e., virtually no effect at 1 nM on overall parasite replication; Figure 3.4 C). These results suggest that DPAP1 inhibition of at least 95% for ~2 h is required to efficiently kill parasites.

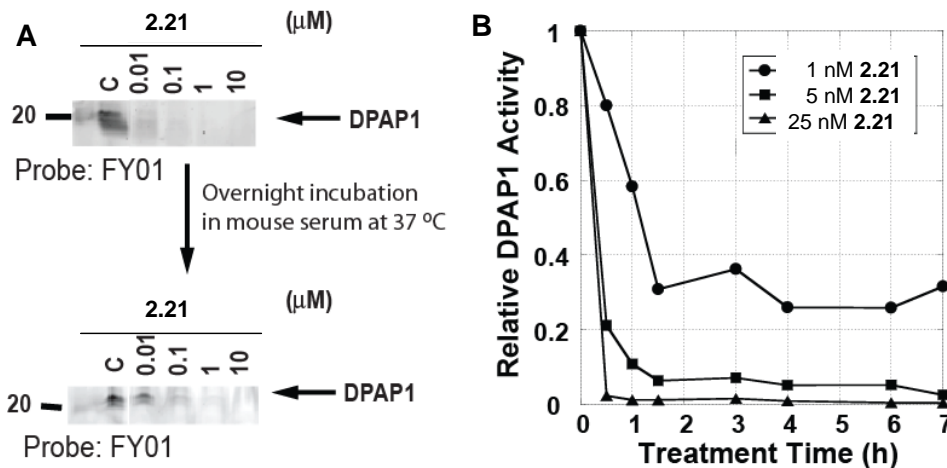
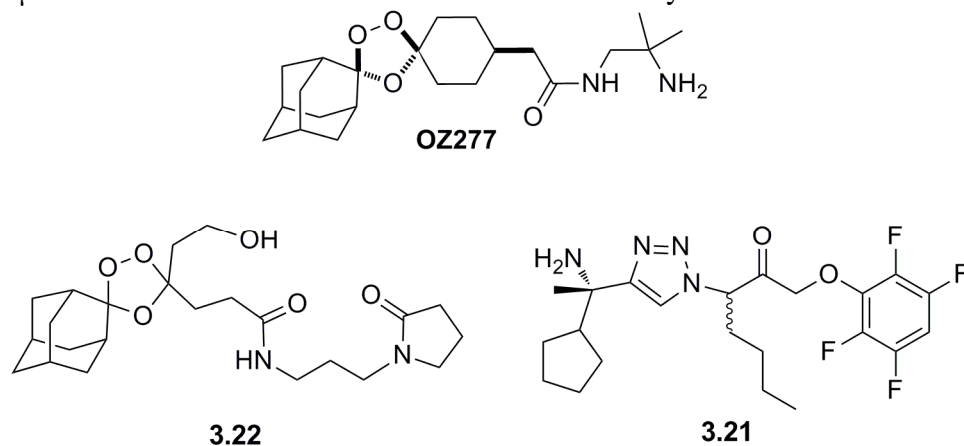


Figure 3.5. Potent inhibitor (**3.21**) is stable in mouse serum and maintains DPAP1 inhibition. (A) Serum stability of **3.21**. (B) Kinetics of DPAP1 inhibition by **3.21** in intact parasites.

Design and Synthesis of a Fragmenting Hybrid Approach

Artemisinin combination therapy (ACT) is considered the front-line treatment for *P. falciparum* induced malaria due to the importance of diminishing drug-resistance and overcoming the problem of reoccurrence of the disease associated with artemisinin monotherapy.⁵⁻⁷ Coartem was the first ACT to meet the World Health Organization's (WHO) criteria for treating uncomplicated malaria. The combination of artemether, an artemisinin derivative, and anti-malarial lumefantrine has resulted in one of the most efficient malaria treatment to date.²⁷ As an alternative approach to combination therapy, we set out to explore a strategy in which a hybrid molecule, consisting of two compounds, would undergo a parasite-targeted fragmentation to release optimal anti-malarial effects of both compounds.

To achieve parasite-specific fragmentation, an iron(II)-reactive 1,2,4-trioxolane ring system was used as the parasite-targeting moiety and a masked retro-Michael linker was incorporated to provoke hybrid fragmentation via a β -elimination. The parasite food vacuole contains free ferrous iron and heme that mediates the opening of the trioxolane ring to unmask the carbonyl group of the retro-Michael linker and enable hybrid fragmentation. The anti-malarial properties of 1,2,4-trioxolanes have been explored and a member of this class, OZ277/arterolane, is currently being investigated in late-stage human clinical trials as combination therapy with the anti-malarial piperazine.²⁷⁻³⁰ Therefore, we set out to design a hybrid containing a similar trioxolane **3.22** as a parasite-specific delivery moiety and our potent DPAP1 inhibitor **3.21** (Figure 3.7). Fragmenting hybrid **3.23** was synthesized from the carbamate linkage of free amine **3.21** and the free alcohol group of trioxolane **3.22** (for synthesis, see experimental section). Notably, the conjugation of amines and alcohols provides opportunity to use existing anti-malarial agents that possess amine and/or hydroxyl groups as fragmenting hybrid approach candidates. As a control, an amide-linked hybrid **3.24** was synthesized to prevent β -elimination and release of **3.21** after activation by ferrous iron.



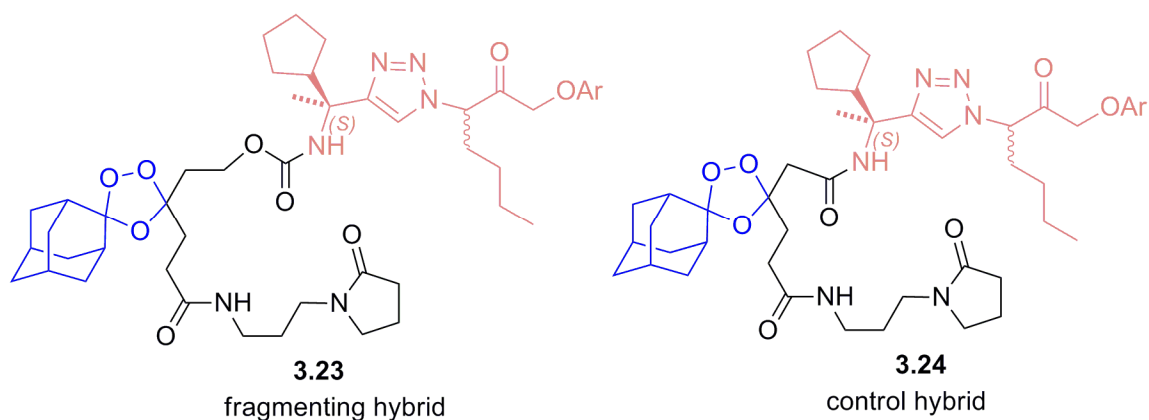
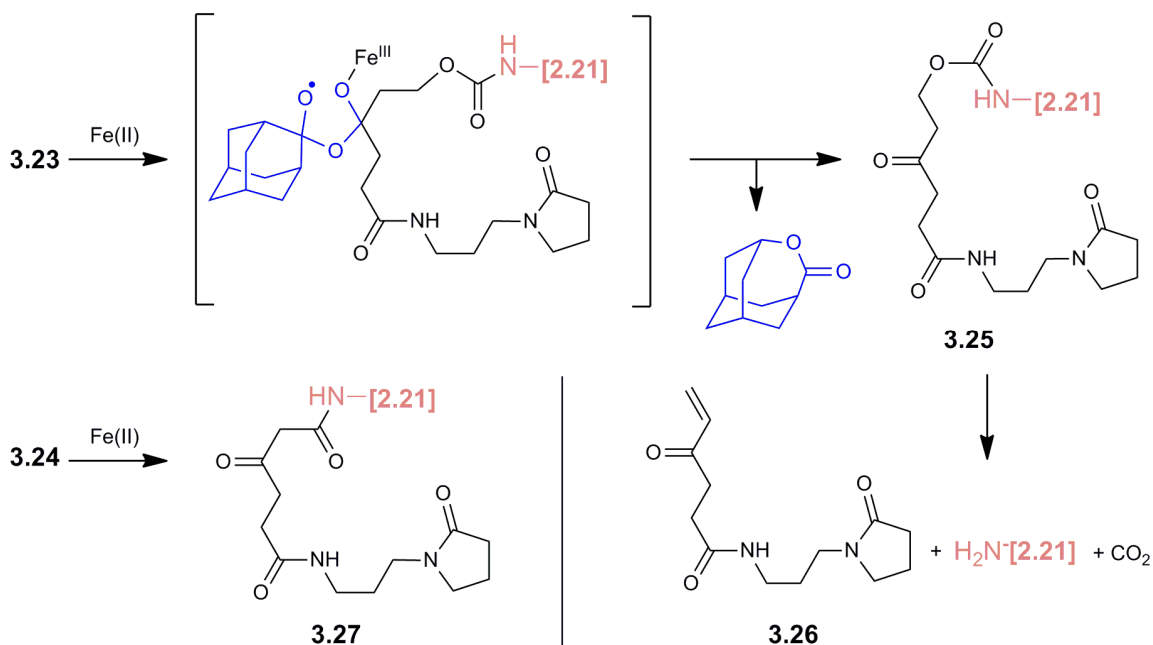


Figure 3.7. Structures of drug OZ277, new trioxolane **3.22**, and DPAP1 inhibitor **3.21**. fragmenting hybrid **3.23** and control hybrid **3.24**.

The proposed sequence for *in vitro* decomposition of fragmenting hybrid **3.23** was rationalized by previous work showing that iron(II)-promoted ring opening of 1,2,4-trioxalanes yield carbonyl agents *in vitro* (Scheme 3.4).³¹⁻³³ Ferrous iron salts are expected to promote the decomposition of hybrid **3.23** to afford a retro-Michael compound (**3.25**) and a well-established adamantane-derived side product via adamantyl radical recombination. Intermediate **3.25** undergoes β -elimination to release DPAP1 inhibitor **3.21**, linker side product **3.26**, and carbon dioxide. Notably, control hybrid **3.24** can undergo a iron(II) ring opening to afford **3.27**, but cannot release DPAP1 inhibitor **3.21** via β -elimination (Scheme 3.4).

Scheme 3.4. *In vitro* iron(II)-promoted decomposition of hybrid molecules



Evaluation of Fragmenting Hybrids *In Vitro* and *In Vivo*

To validate the hypothesized sequence, the ferrous iron-promoted decomposition of **3.23** was studied *in vitro* using LCMS. Treatment of hybrid **3.23** with excess (100 equivalents) of iron(II)bromide resulted in rapid (within minutes) decomposition of the trioxolane ring and clean formation of the adamantane derivative and retro-Michael product **3.25**. The β -elimination of **3.25** to afford linker side-product **3.26** and DPAP1 inhibitor **3.21** was monitored by LC/MS yielding a half-life ($t_{1/2}$) of ~9 h at 37 °C (Table 3.5).

Table 3.5. DPAP1 inhibition, anti-malarial activities, and rates of hybrid fragmentation *in vitro* and *in vivo*

Compound	DPAP IC ₅₀ (nM) ^a	<i>P. falciparum</i>		
		EC _{50 Pot} (nM) ^b	$t_{1/2}$ <i>in vitro</i> (h) ^c	$t_{1/2}$ <i>in vivo</i> (h) ^d
3.22	>10000	29 (13)	n.a.	n.a.
3.21	70 (3)	5.2 (0.4)	n.a.	n.a.
3.24	>10000	52 (7)	n.a.	n.a.
3.23	10000 (2000)	4.0 (0.2)	9	1.5 (0.25)

^a Half maximal inhibition of DPAP1 in parasite lysates after 30 min treatment with inhibitor. DPAP1 activity was measured using FY01 probe. ^b Antimalarial potency measured by treating a culture of *P. falciparum* at ring stage with increasing concentrations of compound. ^c Half-life for the release of **3.21** from hybrid species **3.23** as measured *in vitro* by LC/MS. ^d Half-life for the release of **3.21** from hybrid **3.23** in living parasites. n.a = non applicable. The standard deviation is shown in parantheses.

The inhibitory effects were measured *in vitro* by treating parasite lysates for 30 min with increasing concentrations of hybrid **3.23**, amide-linked control **3.24**, trioxolane **3.22**, and irreversible inhibitor **3.21**, followed by labeling with FY01 (Figure 3.6 A). After subsequent labeling of residual DPAP1 activity, both trioxolane **3.22** and amide-linked control hybrid **3.24** failed to block DPAP1 activity. As expected, both trioxolane **3.22** and control hybrid **3.24** exhibited trioxolane-based activity but did not inhibit DPAP1. Hybrid **3.23** was 100-fold less potent (IC₅₀ = 10 μ M) at inhibiting DPAP1 than free amine **3.21** (Table 3.5). Next, the potency of the agents was evaluated against intra-erythrocytic *P. falciparum* ring-stage parasites (Figure 3.6 B and Table 3.5). Compounds **3.22** and **3.23** exhibited half maximal parasite growth (EC_{50 Pot}) at concentrations in the

mid-nanomolar range, suggesting that they can cross erythrocyte and parasite membranes and become activated in the parasite food vacuole. Significantly, both **3.21** and hybrid **3.23** displayed potency at single digit nanomolar concentrations and were 10-fold more potent as anti-malarial agents than trioxolane **3.22** or control hybrid **3.24**. The enhanced anti-malarial activity of **3.23** relative to **3.24** implies that active DPAP1 inhibitor **3.21** is released from hybrid **3.23** inside parasites.

DPAP1 inhibition kinetics were measured to further evaluate the release of **3.21** from hybrid **3.23** *in vivo* (Figure 3.6 C). Inhibition of DPAP1 was not observed with trioxolane **3.22**, which indicates that the toxic effects of the trioxolane ring do not alter the levels of DPAP1 activity for at least 6 h. As expected, hybrid control **3.24** does not inhibit DPAP1 even after 6 h, while **3.21** inhibited all DPAP activity including at the shortest time point of 30 min. However, hybrid **3.23** inhibited DPAP1 in a time-dependent manner, with complete inhibition observed at 3 h. These inhibition kinetics are consistent with a slow release of inhibitor **3.21** from fragmenting hybrid **3.23**. Based on the second order rate constant for inhibition of DPAP1 by **3.21** *in vitro* ($k_i = 10200 \text{ M}^{-1} \text{ s}^{-1}$), the half-life for the release of inhibitor **3.21** from hybrid **3.23** *in vivo* was estimated to be $\sim 1.5 \text{ h}$ (Table 3.5), which is sufficiently short to be useful in anti-malarial therapy.

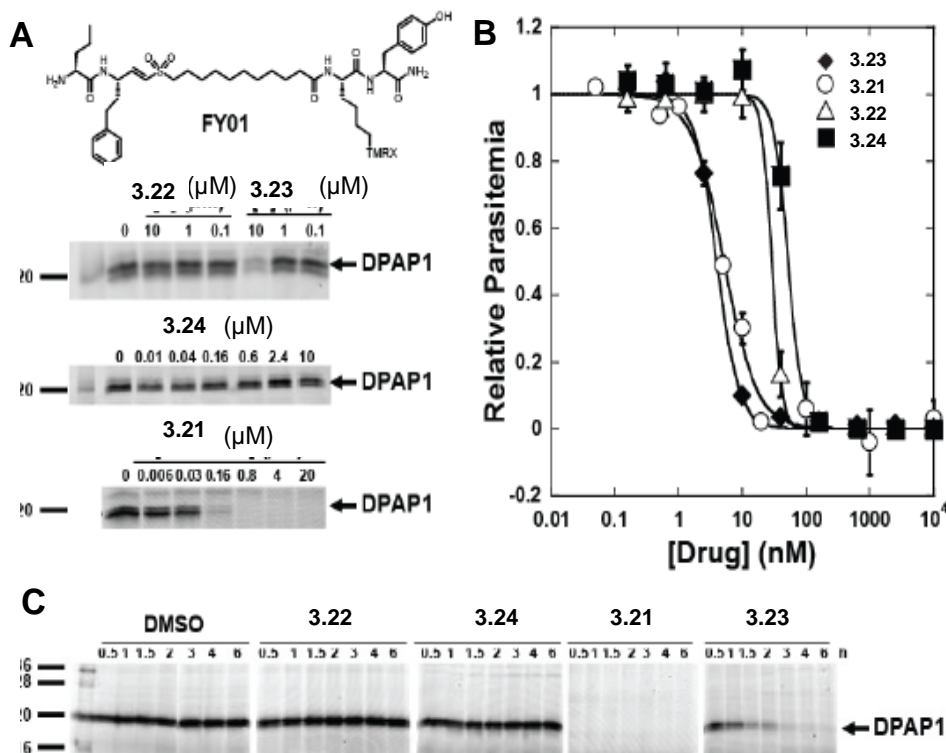


Figure 3.6. Validation of fragmenting hybrid strategy in live parasites. (A) DPAP1 activity of labeled by FY01 tag. (B) Parasitemia in *P. falciparum* ring stage parasites. $EC_{50_{Pot}}$ values are reported in Table 3.5. (C) Kinetics of DPAP1 inhibition *in vivo*.

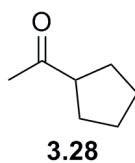
Conclusions

Homology modeling of DPAP1 with cathepsin C and computational docking were used to design non-peptidic irreversible inhibitors of DPAP1. These computational methods resulted in the optimization and improvement of initial hit **3.1**. Numerous non-peptidic inhibitors were active against *P. falciparum* at low nanomolar concentrations. Our data shows a correlation between DPAP1 inhibition and parasite death, suggesting that these inhibitors are not killing parasites by nonspecific toxic effects. We identified a lead inhibitor that is cell permeable, stable in mouse serum, and displays low toxicity in HFF cells. Additionally, our results validate DPAP1 as a viable anti-malarial target.

To sustain inhibition *in vivo*, a novel fragmenting hybrid approach was developed to deliver artemisinin-like activity with our lead DPAP1 inhibitor **3.21**. An iron(II)-reactive 1,2,4-trioxolane ring system was employed as the parasite-targeting moiety and a masked retro-Michael linker to result in hybrid fragmentation via β -elimination. This strategy is able to slowly release inhibitor ($t_{1/2} = 1.5$ h) and sustain DPAP1 inhibition in *P. falciparum* parasites. The slow release of the second anti-malarial agent (**3.21**) is similar to front-line ACT drugs that combine a slow acting drug with artemisinin. Optimistically, malarial targets that require inhibition for hours to efficiently block parasite development can be efficiently impaired with the slow release of a secondary anti-malarial agent via a fragmenting hybrid approach.

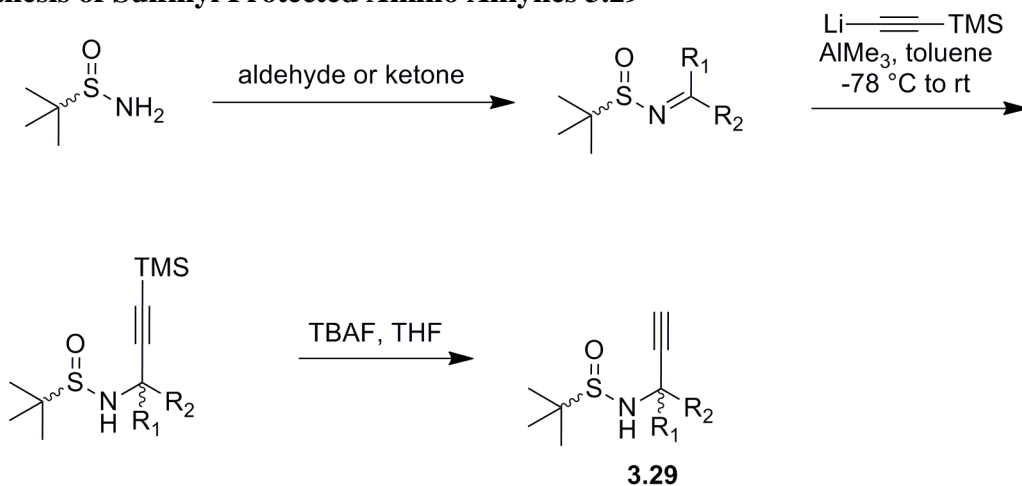
Experimental

General methods for synthesizing inhibitors and intermediates. Unless otherwise noted, all chemicals were obtained from commercial suppliers and used without further purification. (*R*)-*tert*-Butanesulfinamide and (*S*)-*tert*-Butanesulfinamide were provided by AllyChem Co. Ltd (Dalian, China). Anhydrous THF, CH₂Cl₂, Et₂O, and toluene were obtained from Seca Solvent Systems by GlassContour and were dried over alumina under a nitrogen atmosphere, and *i*-Pr₂EtN was distilled under N₂ from CaH₂ immediately prior to use. Reaction progress was monitored using thin-layer chromatography on Merck 60 F₂₅₄ 0.25 μ m silica plates. High-performance liquid chromatography (HPLC) analysis was performed with a C18 reverse phase column (4.6 x 100 mm) with UV detection at 220, 254, and 280 nm. Reaction progress was monitored using thin-layer chromatography on Merck 60 F₂₅₄ 0.25 μ m silica plates. Liquid chromatography-mass spectrometry (LC/MS) data were obtained using a Hewlett Packard 1100 series liquid chromatography instrument and mass selective detector. ¹H and ¹³C NMR spectra were measured with Bruker AVB-400 and AVQ-400 instruments. NMR chemical shifts are reported in ppm downfield relative to the internal solvent peak, and coupling constants are reported in Hz. High-resolution mass spectra (HRMS) were performed by the University of California at Berkeley Mass Spectrometry Facility.



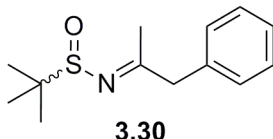
Synthesis of 1-cyclopentylethanone (3.28). 1-Cyclopentylethanol was oxidized to the corresponding ketone under Swern conditions. Oxalyl chloride (3.74 mL, 39.3 mmol) was dissolved in 98.0 mL of CH₂Cl₂, and the solution was cooled in a -78 °C bath. DMSO (4.60 mL, 65.5 mmol) was added, and the solution was stirred for 15 min. 1-Cyclopentylethanol (2.50 g, 13.1 mmol) was added dropwise as a solution in 262 mL CH₂Cl₂, and the solution was stirred for 30 min at -78 °C. NEt₃ (10.0 mL, 72.1 mmol) was added, and the solution was stirred for an additional 20 min at -78 °C. The solution was allowed to warm to rt over 10 min, and H₂O was added (180 mL). The organic layer was removed, and the aqueous layer was extracted with CH₂Cl₂ (3 x 200 mL). The combined organic layers were washed with 1.0 M HCl (2 x 400 mL) and brine (400 mL), dried with magnesium sulfate, filtered, and concentrated. Purification by silica gel chromatography (9:1 pentane:Et₂O) provided the desired product in quantitative yield. ¹H NMR corresponds to previously reported data.³⁴ ¹H NMR (400 MHz, CDCl₃): δ 1.53-1.80 (m, 8H), 2.10 (s, 3H), 2.77- 2.85 (m, 1H). ¹³C NMR (100 MHz, CDCl₃): δ 26.1, 28.8, 28.9, 52.3, 211.4.

Synthesis of Sulfinyl Protected Amino Alkynes 3.29

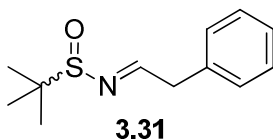


General Procedure A: Synthesis of *tert*-butanesulfinyl imines 3.29. A general procedure for the synthesis of *N-tert*-butanesulfinyl imines previously reported in the literature was followed for many of the intermediates.³⁵ A 0.50 M THF solution of aldehyde or ketone (1.10 – 2.00 equiv), *tert*-butanesulfinamide (1.00 equiv), and Ti(OEt)₄ (4.00 equiv) was added to a round-bottom flask fitted with a stir bar. The solution was stirred with heating to refluxing temperatures until the reaction was complete as

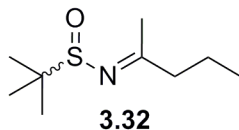
monitored by thin-layer chromatography (1:1 hexanes:EtOAc). The mixture was cooled immediately to rt upon completion. The mixture was poured into an equal volume of saturated aqueous sodium bicarbonate with rapid stirring. The resulting suspension was filtered through a plug of celite, and the filter cake was washed with EtOAc. The filtrate was transferred to a separatory funnel, and the organic layer was washed with brine. The brine layer was extracted once with EtOAc, and the combined organic portions were dried with sodium sulfate, filtered, and concentrated.



Synthesis of sulfinyl imine 3.30. General procedure A was followed with 1-phenylpropan-2-one (2.20 mL, 16.5 mmol), racemic *tert*-butanesulfinamide (2.0 g, 16.5 mmol), Ti(OEt)₄ (13.9 mL, 66.1 mmol) and 135 mL of THF. Purification via silica gel chromatography (7:3 hexane:EtOAc) afforded the *N*-sulfinyl ketimine in 64% yield as a ~4:1 mixture of rotamers by ¹H NMR. ¹H NMR (400 MHz, CDCl₃): δ Major rotamer: 1.12 (s, 9H), 2.17 (s, 3H), 3.66-3.76 (m, 2H), 7.26-7.34 (m, 5H).

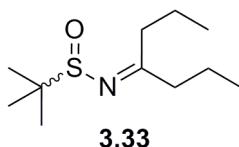


Synthesis of sulfinyl imine 3.31. A general procedure that was previously reported in the literature was followed.³⁶ To a solution of racemic *tert*-butanesulfinamide (0.200 g, 1.67 mmol) in 2.8 mL CH₂Cl₂ was added pyridinium *para*-toluenesulfonate (0.02 g, 0.08 mmol), magnesium sulfate (1.0 g, 8.35 mmol), and phenylacetaldehyde (0.60 mL, 5.0 mmol). The resulting mixture was stirred for 24 h. The mixture was filtered through a pad of celite and washed with 75 mL of CH₂Cl₂. The solution was dried with sodium sulfate, filtered, and concentrated. Purification via silica gel chromatography (8:2 hexane:EtOAc) afforded the *N*-sulfinyl aldimine in 65% yield. ¹H NMR (400 MHz, CDCl₃): δ 1.19 (s, 9H), 3.79-3.89 (m, 2H), 7.14-7.38 (m, 5H), 8.12-8.16 (t, 1H, *J* = 5.6 Hz); ¹³C NMR (100 MHz, CDCl₃): δ 22.4, 42.6, 56.9, 127.1, 128.8, 129.2, 134.7, 167.4.



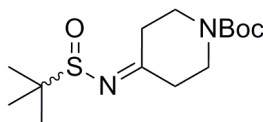
Synthesis of sulfinyl imine 3.32. General procedure A was followed with pentan-2-one (0.88 mL, 8.3 mmol), racemic *tert*-butanesulfinamide (1.00 g, 8.3 mmol), Ti(OEt)₄ (6.92 mL, 33.0 mmol) and 65 mL of THF. Purification via silica gel chromatography (7:3 hexane:EtOAc) afforded the *N*-sulfinyl ketimine in 77% yield. ¹H NMR (400 MHz, CDCl₃): δ 0.84-0.88 (t, 3H, *J* = 7.2), 1.18 (s, 9H), 1.52-1.60 (m, 2H),

2.23 (s, 3H), 2.28-2.38 (m, 2H); ^{13}C NMR (100 MHz, CDCl_3): δ 13.7, 19.0, 22.1, 23.0, 45.5, 56.2, 185.5.



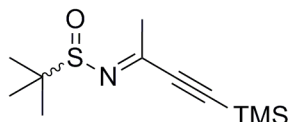
3.33

Synthesis of sulfinyl imine 3.33. General procedure A was followed with heptan-4-one (0.67 mL, 8.3 mmol), racemic *tert*-butanesulfinamide (1.00 g, 8.3 mmol), $\text{Ti}(\text{OEt})_4$ (6.92 mL, 33.0 mmol) and 65 mL of THF. Purification via silica gel chromatography (7:3 hexane:EtOAc) afforded the *N*-sulfinyl ketimine as a pale yellow oil in 58% yield. ^1H NMR (400 MHz, CDCl_3): δ 0.84-0.89 (m, 6H), 1.28 (s, 9H), 1.55-1.62 (m, 4H), 2.29-2.39 (m, 2H), 2.53-2.68 (m, 2H); ^{13}C NMR (100 MHz, CDCl_3): δ 13.9, 14.4, 19.1, 21.1, 22.4, 38.6, 43.0, 56.3, 188.8.



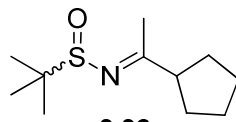
3.34

Synthesis of sulfinyl imine 3.34. General procedure A was followed with the commercially available 1-Boc-4-piperidone (Sigma-Aldrich, St. Louis, MO) (1.8 g, 9.1 mmol), racemic *tert*-butanesulfinamide (1.00 g, 8.3 mmol), $\text{Ti}(\text{OEt})_4$ (3.5 mL, 13.5 mmol) and 33 mL of THF. Purification via silica gel chromatography (7:3 hexane:EtOAc) afforded the *N*-sulfinyl ketimine in 41% yield. ^1H NMR (400 MHz, CDCl_3): δ 1.21 (s, 9H), 1.41 (s, 9H), 2.47-2.49 (m, 2H), 2.78-2.81 (m, 1H), 3.02-3.09 (m, 1H), 3.50-3.70 (m, 4H).



3.35

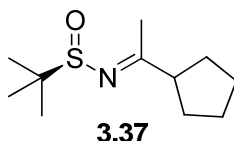
Synthesis of sulfinyl imine 3.35. General procedure A was followed with 4-(trimethylsilyl)but-3-yn-2-one (2.90 g, 20.6 mmol), racemic *tert*-butanesulfinamide (2.50 g, 20.6 mmol), $\text{Ti}(\text{OEt})_4$ (15.1 mL, 72.2 mmol) and 144 mL of THF. Purification via silica gel chromatography (7:3 hexane:EtOAc) afforded the *N*-sulfinyl ketimine as a pale yellow oil in 35% yield. ^1H NMR (400 MHz, CDCl_3): δ 0.13 (s, 9H), 1.20 (s, 9H), 2.31 (s, 3H). ^{13}C NMR (100 MHz, CDCl_3): δ -0.4, 22.2, 29.3, 57.2, 98.1, 110.1, 162.4.



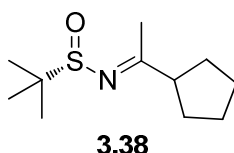
3.36

Synthesis of sulfinyl imine 3.36. General procedure A was followed with 1-cyclopentylethanone (1.02 g, 9.10 mmol), racemic *tert*-butanesulfinamide (1.0 g, 8.3 mmol), $\text{Ti}(\text{OEt})_4$ (6.90 mL, 33.0 mmol) and 65 mL of THF. Purification via silica gel chromatography (7:3 hexane:EtOAc) afforded the *N*-sulfinyl ketimine in 75% yield. ^1H

NMR (400 MHz, CDCl₃): δ 1.22 (s, 9H), 1.56-1.84 (m, 8H), 2.29 (s, 3H), 2.70-2.77 (m, 1H).

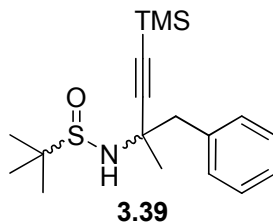


Synthesis of sulfinyl imine 3.37. General procedure A was followed with 1-cyclopentylethanone (1.00 g, 9.1 mmol), (*R*)-*tert*-butanesulfinamide (1.00 g, 8.3 mmol), Ti(OEt)₄ (6.90 mL, 33.0 mmol) and 65 mL of THF. Purification via silica gel chromatography (7:3 hexane:EtOAc) afforded the *N*-sulfinyl ketimine in 78% yield. ¹H NMR (400 MHz, CDCl₃): δ 1.19 (s, 9H), 1.51-1.78, (m, 8H), 2.26 (s, 3H), 2.71-2.76 (m, 1H).

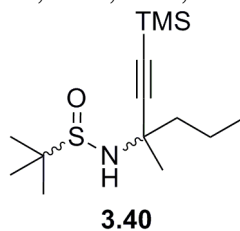


Synthesis of sulfinyl imine 3.38. General procedure A was followed with 1-cyclopentylethanone (1.00 g, 9.1 mmol), (*S*)-*tert*-butanesulfinamide (1.00 g, 8.3 mmol), Ti(OEt)₄ (6.90 mL, 33.0 mmol) and 65 mL of THF. Purification via silica gel chromatography (7:3 hexane:EtOAc) afforded the *N*-sulfinyl ketimine in 71% yield. ¹H NMR (400 MHz, CDCl₃): δ 1.19 (s, 9H), 1.51-1.71 (m, 8H), 2.26 (s, 3H), 2.68-2.76 (m, 1H); ¹³C NMR (100 MHz, CDCl₃): δ 22.3, 25.7, 30.0, 30.2, 52.4, 56.4, 188.1.

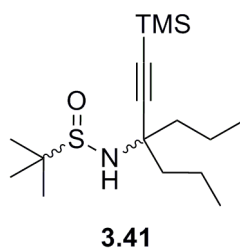
General Procedure B: Synthesis of trimethylsilyl protected alkynes. To a 0.86 M toluene solution of (trimethylsilyl)ethyne (3.5 equiv) at -78 °C in a 250 mL flask fitted with a stir bar was added butyllithium (2.2 equiv, as a 2.5 M solution in hexanes). The resulting solution was stirred for 15 min at -78 °C. In a separate 100 mL round-bottom flask, a 0.35 M toluene solution of *N*-sulfinyl imine (1.0 equiv) was cooled to -78 °C. A freshly prepared 1.0 M toluene solution of Me₃Al (1.2 equiv) was slowly added to the imine solution via cannula and the solution was stirred for 10 minutes at -78 °C (for addition to racemic imines, Me₃Al was not used, and the imine was instead simply dissolved in toluene). The resulting solution was then slowly added to the alkynyllithium solution via cannula, and stirring was continued at -78 °C for 2 h. The solution was then allowed to warm to rt over 12 h. The mixture was cooled in an ice-water bath. Saturated aqueous sodium sulfate was added dropwise until gas was no longer evolved upon addition. The resulting mixture was transferred to a separatory funnel and the organic layer was removed. The aqueous layer was extracted with EtOAc (3 x 50 mL). The combined organic layers were dried with sodium sulfate, filtered, and concentrated. To hydrolyze the unreacted *N*-sulfinyl imine, the crude material was dissolved in CH₃OH and a 1 M aqueous solution of CH₃CO₂H (2:1 ratio) was added followed by stirring at room temperature for 8 h. The mixture was then concentrated to remove the CH₃OH, and brine was added. The resulting aqueous mixture was then extracted with EtOAc (3 x 50 mL), dried with sodium sulfate, filtered, and concentrated.



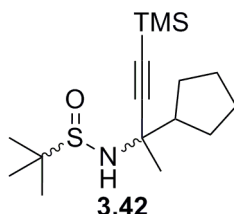
Synthesis of sulfinamide 3.39. General Procedure B was followed using (trimethylsilyl)ethyne (11.40 mL, 36.3 mmol), butyllithium (9.50 mL, 22.8 mmol, 2.5 M in hexanes), and ketimine **3.30** (2.46 g, 10.4 mmol) in 64.8 mL total volume of toluene. Purification by silica gel chromatography (5:1 hexane:EtOAc) afforded the pure propargyl sulfinamide in 35% yield. ^1H NMR (400 MHz, CDCl_3): δ 0.17 (s, 9H), 1.26 (s, 9H), 1.46 (s, 3H), 2.99-3.09 (m, 2H), 3.34 (s, 1H), 7.28-7.35 (m, 5H); ^{13}C NMR (100 MHz, CDCl_3): δ -0.0, 22.7, 28.8, 49.8, 54.1, 56.2, 90.1, 108.1, 127.3, 128.2, 131.3, 135.7.



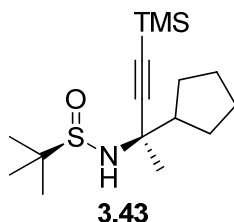
Synthesis of sulfinamide 3.40. General Procedure B was followed using (trimethylsilyl)ethyne (6.30 mL, 20.3 mmol), butyllithium (5.10 mL, 12.8 mmol, 2.5 M in hexanes), and ketimine **3.32** (1.10 g, 5.8 mmol) in 36 mL total volume of toluene. Purification by silica gel chromatography (5:1 hexane:EtOAc) afforded the pure propargyl sulfinamide in 80% yield. ^1H NMR (400 MHz, CDCl_3): δ 0.11 (s, 9H), 0.88-0.92 (t, 3H, $J = 7.2$), 1.22 (s, 9H), 1.55 (s, 3H), 1.59-1.69 (m, 2H), 1.71-1.87 (m, 2H), 4.19 (s, 1H); ^{13}C NMR (100 MHz, CDCl_3): δ 0.1, 14.3, 18.1, 22.7, 29.8, 45.5, 54.3, 56.3, 88.4, 108.7.



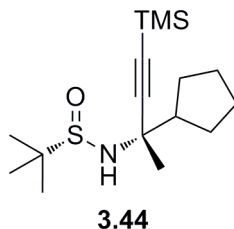
Synthesis of sulfinamide 3.41. General Procedure B was followed using (trimethylsilyl)ethyne (4.80 mL, 15.4 mmol), butyllithium (3.90 mL, 9.7 mmol, 2.5 M in hexanes), and ketimine **3.33** (0.95 g, 4.4 mmol) in 27 mL total volume of toluene. Purification by silica gel chromatography (5:1 hexane:EtOAc) afforded the pure propargyl sulfinamide as a white solid in 80% yield. ^1H NMR (400 MHz, CDCl_3): δ 0.11 (s, 9H), 0.89-0.93 (t, 6H, $J = 7.2$), 1.22 (s, 9H), 1.34-1.47 (m, 4H), 1.55-1.69 (m, 2H), 1.70-1.79 (m, 2H), 3.82 (s, 1H); ^{13}C NMR (100 MHz, CDCl_3): δ 0.1, 14.4, 17.7, 17.7, 21.2, 22.8, 43.3, 43.8, 56.5, 58.7, 89.9, 107.3.



Synthesis of sulfonamide 3.42. General Procedure B was followed using (trimethylsilyl)ethyne (6.70 mL, 21.2 mmol), butyllithium (5.70 mL, 14.3 mmol, 2.5 M in hexanes), and ketimine **3.36** (1.30 g, 6.1 mmol), in 38 mL total volume of toluene. Purification by silica gel chromatography (5:1 hexane:EtOAc) afforded the diastereomerically pure propargyl sulfonamide as a white solid in 64% yield. ^1H NMR (400 MHz, CDCl_3): δ 0.13 (s, 9H), 1.22 (s, 9H), 1.47 (s, 3H), 1.50-1.89 (m, 8H), 2.20-2.24 (m, 1H), 3.79 (s, 1H); ^{13}C NMR (100 MHz, CDCl_3): δ 0.1, 22.6, 26.1, 26.5, 28.2, 28.3, 28.6, 50.5, 56.5, 57.8, 88.8, 107.5.

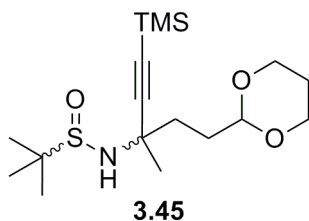


Synthesis of sulfonamide 3.43. General Procedure B was followed using (trimethylsilyl)ethyne (3.20 mL, 23.5 mmol), butyllithium (5.90 mL, 14.7 mmol, 2.5 M in hexanes), ketimine **3.37** (1.45 g, 6.7 mmol), and Me_3Al (1.60 mL, 8.2 mmol) in 54 mL total volume of toluene. Purification by silica gel chromatography (5:1 hexane:EtOAc) afforded the diastereomerically pure propargyl sulfonamide as a white solid in 73% yield. ^1H NMR (400 MHz, CDCl_3): δ 0.13 (s, 9H), 1.22 (s, 9H), 1.45 (s, 3H), 1.50-1.87 (m, 8H), 2.16-2.20 (m, 1H), 3.78 (s, 1H).

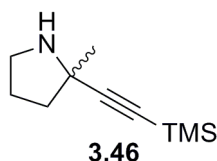


Synthesis of sulfonamide 3.44 General Procedure B was followed using (trimethylsilyl)ethyne (3.20 mL, 23.5 mmol), butyllithium (5.90 mL, 14.7 mmol, 2.5 M in hexanes), ketimine **3.38** (1.45 g, 6.7 mmol), and Me_3Al (1.60 mL, 8.2 mmol) in 54 mL total volume of toluene. Purification by silica gel chromatography (5:1 hexane:EtOAc) afforded the diastereomerically pure propargyl sulfonamide as a white solid in 70% yield. ^1H NMR (400 MHz, CDCl_3): δ 0.13 (s, 9H), 1.21 (s, 9H), 1.47 (s, 3H), 1.49-1.87 (m,

8H), 2.18-2.21 (m, 1H), 3.78 (s, 1H); ^{13}C NMR (100 MHz, CDCl_3): δ 0.1, 22.8, 26.1, 26.3, 28.2, 28.3, 28.7, 50.5, 56.4, 57.8, 88.8, 107.8.

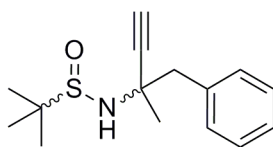


Synthesis of sulfinamide 3.45. A previously reported literature procedure was followed.³⁷ In a 3-neck reaction flask equipped with a reflux condenser, magnesium turnings (2.70g, 110 mmol) were flame dried with catalytic amounts of I_2 , and then 27 mL of Et_2O was added. A solution of 2-(2-bromoethyl)-1,3-dioxane (5.0 mL, 36.9 mmol) in 12 mL of Et_2O was added dropwise to the magnesium mixture via canula. To prevent refluxing, the reaction mixture was periodically cooled in a rt water bath. After the addition was complete, the reaction mixture was stirred for 1 h at rt. The solution was then transferred via canula filtration to a separate flask to remove the excess magnesium and the solution was cooled to $-48\text{ }^\circ\text{C}$. A solution of ketimine **3.35** (1.0 g, 4.1 mmol) in 4 mL of THF was added dropwise to the Grignard solution via canula. The solution was stirred for 10 h at $-48\text{ }^\circ\text{C}$ and then was slowly warmed to rt. The reaction was quenched with saturated aqueous NH_4Cl , and the resulting mixture was extracted with Et_2O (3 x 50 mL). The combined organic extracts were dried with sodium sulfate, filtered, and concentrated. The crude product was purified by silica gel chromatography (2:1 hexanes: EtOAc to 100% EtOAc) to yield the pure product in 33% yield. ^1H NMR (400 MHz, CDCl_3): δ 1.14 (s, 9H), 1.17 (s, 9H), 1.28-1.32, (m, 2H), 1.45 (s, 3H), 1.75-1.89 (m, 4H), 3.39 (s, 1H), 3.69-3.71 (m, 2H), 4.04-4.41 (m, 2H), 4.53-4.55 (m, 1H); ^{13}C NMR (100 MHz, CDCl_3): δ 0.1, 14.4, 22.7, 25.9, 29.5, 30.6, 37.3, 53.9, 56.1, 67.0, 88.8, 102.0, 108.2.



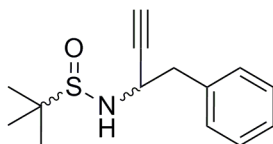
Synthesis of pyrrolidine 3.46. A general procedure that was previously reported in the literature was followed.³ Sulfinamide **3.45** (0.50g, 1.4 mmol) dissolved in 14 mL of 95:5 TFA: H_2O . After stirring for 30 min, Et_3SiH (2.20 mL, 14.0 mmol) was added to the reaction mixture and then stirred vigorously for 24 h. The reaction mixture was concentrated and purified by silica gel chromatography 20:1:0.1 CH_2Cl_2 : CH_3OH : NH_4OH to afford pure product in 96% yield. ^1H NMR (400 MHz, CDCl_3): δ 0.13 (s, 9H), 1.66 (s, 3H), 1.98-2.13 (m, 2H), 2.19-2.28 (m, 2H), 3.33-3.42 (m, 2H); ^{13}C NMR (100 MHz, CDCl_3): δ -0.1, 22.8, 24.5, 39.3, 44.1, 60.8, 92.3, 102.0.

General Procedure C: Trimethylsilyl deprotection. A 0.1 M THF solution of trimethylsilyl protected alkyne (1.0 equiv) was cooled in an ice-water bath, and then tetrabutylammonium fluoride (3.0 equiv) was added. The solution was stirred for 3 h at rt and then poured into saturated aqueous NH_4Cl solution with rapid stirring. The resulting mixture was extracted with Et_2O (3 x 100). The combined organic extracts were dried with sodium sulfate, filtered, and concentrated.



3.47

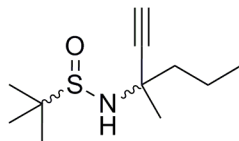
Synthesis of sulfinamide 3.47. General Procedure C was followed using **3.39** (0.92 g, 2.70 mmol) and tetrabutylammonium fluoride (2.75 g, 8.1 mmol). Purification by silica gel chromatography (1:1 hexanes:EtOAc) gave the pure product as a white solid in 98% yield. ^1H NMR (400 MHz, CDCl_3): δ 1.20 (s, 9H), 1.37 (s, 3H), 2.58 (s, 1H), 3.03 (d, 1H, $J=13.2$), 3.14 (d, 1H, $J=13.2$), 7.30-7.39 (m, 5H).



3.48

Synthesis of 3.48. General Procedure B was followed using (trimethylsilyl)ethyne (1.2 mL, 3.9 mmol), butyllithium (0.96 mL, 2.40 mmol, 2.5 M in hexanes), and *N*-sulfinyl imine **3.31** (0.24 g, 1.1 mmol) in 6.9 mL total volume of toluene. Purification by silica gel chromatography (5:1 hexane:EtOAc) afforded the propargyl sulfinamide in 76% yield.

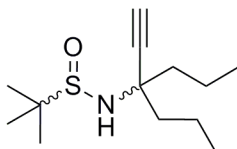
Following procedure C, the resulting sulfinamide (~0.30 g, 0.80 mmol) was directly treated with tetrabutylammonium fluoride (0.80 g, 2.50 mmol). Purification by silica gel chromatography (1:1 hexanes:EtOAc) gave the pure product in 97% yield. ^1H NMR (400 MHz, CDCl_3): δ 1.14 (s, 9H), 2.46 (s, 1H), 3.03-3.05 (apparent d, 2H, $J=6.8$ Hz), 3.37 (m, 1.0 H), 4.24-4.30 (m, 1H), 7.22-7.30 (m, 5H); ^{13}C NMR (100 MHz, CDCl_3): δ 22.6, 43.3, 49.0, 56.5, 74.3, 83.3, 127.2, 128.5, 130.0, 136.4.



3.49

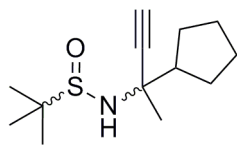
Synthesis of sulfinamide 3.49. General Procedure C was followed using **3.40** (0.58 g, 2.0 mmol) and tetrabutylammonium fluoride (1.89 g, 6.0 mmol). Purification by silica gel chromatography (1:1 hexanes:EtOAc) gave the pure product as a mixture of

diastereomers as a white solid in 87% yield. ^1H NMR (400 MHz, CDCl_3): δ 0.90-0.97 (m, 3H), 1.20 (s, 9H), 1.51 (s, 3H), 1.64-1.72 (m, 4H), 2.43 (s, 1H), 3.55 (s, 1H).



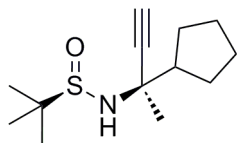
3.50

Synthesis of sulfinamide 3.50. General Procedure C was followed using **3.41** (1.00 g, 3.1 mmol) and tetrabutylammonium fluoride (2.90 g, 9.2 mmol). Purification by silica gel chromatography (1:1 hexanes:EtOAc) gave the pure product as a white solid in 78% yield. ^1H NMR (400 MHz, CDCl_3): δ 0.87-0.89 (m, 6H), 1.33 (s, 9H), 1.41-1.50 (m, 4H), 1.60-1.75 (m, 4H), 2.41 (s, 1H), 3.20 (s, 1H); ^{13}C NMR (100 MHz, CDCl_3): δ 14.3, 17.6, 22.7, 43.5, 56.3, 57.8, 73.6, 85.7.



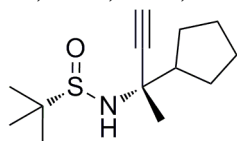
3.51

Synthesis of sulfinamide 3.51. General Procedure C was followed using alkyne **3.42** (0.65 g, 1.90 mmol) and tetrabutylammonium fluoride (1.81 g, 5.8 mmol). Purification by silica gel chromatography (1:1 hexanes:EtOAc) gave the pure product as a white solid in 80% yield. ^1H NMR (400 MHz, CDCl_3): δ 1.17 (s, 9H), 1.45 (s, 3H), 1.50-1.72 (m, 8H), 2.11-2.24 (m, 1H), 2.46 (s, 1H), 3.27 (s, 1H).



3.52

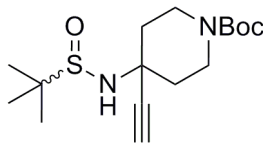
Synthesis of sulfinamide 3.52. General Procedure C was followed using **3.43** (1.47 g, 4.70 mmol) and tetrabutylammonium fluoride (4.45 g, 14.1 mmol). Purification by silica gel chromatography (1:1 hexanes:EtOAc) gave the pure product as a white solid in 89% yield. ^1H NMR (400 MHz, CDCl_3): δ 1.18 (s, 9H), 1.46 (s, 3H), 1.50-1.72 (m, 8H), 2.07-2.23 (m, 1H), 2.44 (s, 1H), 3.27 (s, 1H); ^{13}C NMR (100 MHz, CDCl_3): δ 22.8, 25.8, 26.1, 27.9, 28.2, 28.5, 50.5, 56.1, 56.8, 72.8, 85.6.



3.53

Synthesis of sulfinamide 3.53. General Procedure C was followed using **3.44** (1.47 g, 4.70 mmol) and tetrabutylammonium fluoride (4.45 g, 14.1 mmol). Purification by silica gel chromatography (1:1 hexanes:EtOAc) gave the pure product as a white solid

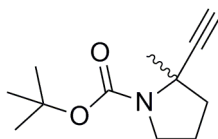
in 96% yield. ^1H NMR (400 MHz, CDCl_3): δ 1.17 (s, 9H), 1.47 (s, 3H), 1.51-1.72 (m, 8H), 2.07-2.23 (m, 1H), 2.46 (s, 1H), 3.27 (s, 1H); ^{13}C NMR (100 MHz, CDCl_3): δ 22.5, 25.8, 25.9, 27.8, 28.0, 28.3, 50.3, 55.9, 56.6, 72.7, 85.7.



3.54

Synthesis of sulfinamide 3.54 General Procedure B was followed using (trimethylsilyl)ethyne (3.30 mL, 10.5 mmol), butyllithium (2.6 mL, 6.6 mmol, 2.5 M in hexanes), and ketimine **3.34** (1.0 g, 3.4 mmol) in 21 mL total volume of toluene. Purification by silica gel chromatography (5:1 hexane:EtOAc) afforded the pure propargyl sulfinamide in 59% yield.

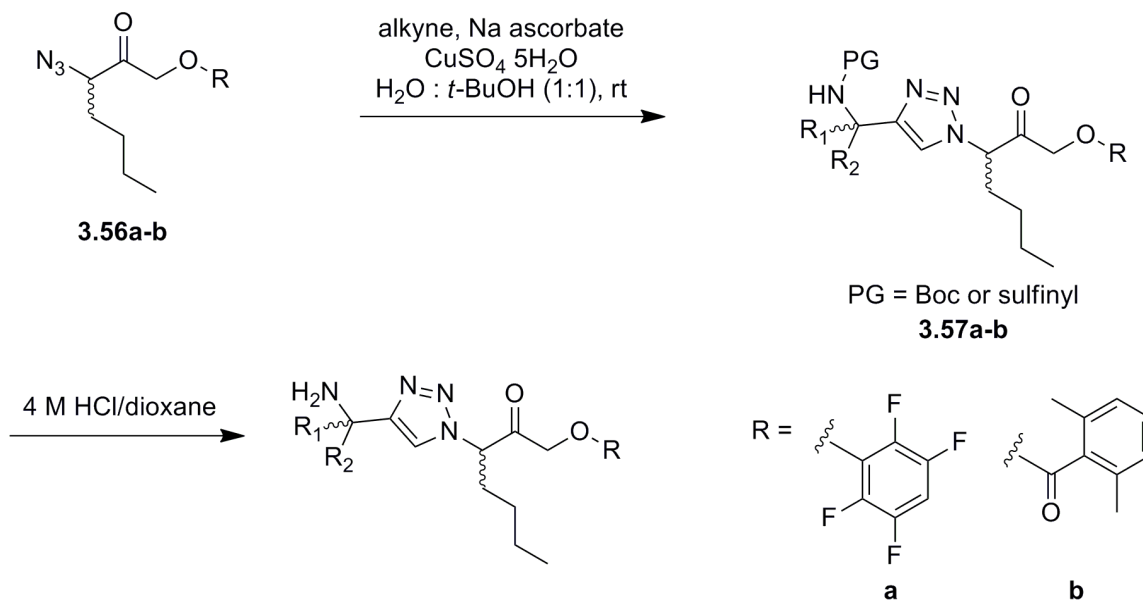
Following procedure C, the resulting sulfinamide (0.8 g, 1.9 mmol) was directly treated with tetrabutylammonium fluoride (1.8 g, 5.7 mmol). Purification by silica gel chromatography (1:1 hexanes:EtOAc) gave the pure product in 94% yield. ^1H NMR (400 MHz, CDCl_3): δ 1.18 (s, 9H), 1.46 (s, 9H), 1.50-1.72 (m, 2H), 1.70-1.96 (m, 2H), 2.44 (s, 1H), 3.05-3.15 (m, 2H), 3.30 (bs, 1H), 3.95 (bs, 2H).



3.55

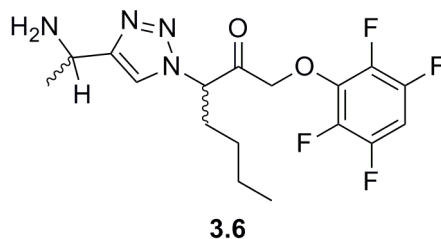
Synthesis of alkyne 3.55. Alkyne **3.46** was Boc-protected according to a standard procedure.³⁸ General Procedure C was followed using Boc protected-**3.46** (0.12 g, 0.44 mmol) and tetrabutylammonium fluoride (0.41 g, 1.31 mmol). Purification by silica gel chromatography (1:1 hexanes:EtOAc) gave the pure product in 98% yield. ^1H NMR (400 MHz, CDCl_3): δ 1.49 (s, 9H), 1.60 (s, 3H), 1.77-2.05 (m, 2H), 2.10-2.27 (m, 2H), 3.38 (m, 2H).

Synthesis of Aryloxy and Acyloxy Methyl Inhibitors



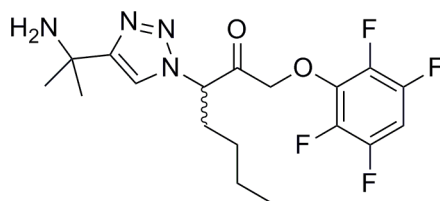
General Procedure D: Synthesis of amines via deprotection. To a 0.15 M CH₃OH solution of alkyne (1.0 equiv), was added HCl as a 4.0 M 1,4-dioxane solution (3-10 equiv). The solution was stirred at rt for 2 h and was then concentrated to afford product.

General Procedure E: Copper(I)-catalyzed 1,2,3-triazole formation. The procedure for the synthesis of ketones **3.57a-b** from the racemic α -azido ketones **3.56a-b** was adapted from a previous literature report, and ketones **3.56a-b** were synthesized according to the published method.²⁵ To a 0.25 M 1:1 H₂O/*t*-BuOH solution of azido-aryloxy methyl ketone **3.56a-b** (1.0 equiv) and protected amino alkyne (1.0 equiv), was added a freshly prepared 1.0 M aqueous solution of sodium ascorbate (1.0 equiv). A freshly prepared 0.3 M aqueous solution of copper(II) sulfate pentahydrate (0.1 equiv) was added to the reaction mixture, which was vigorously stirred overnight. The reaction mixture was diluted with 10 mL of water and then was extracted with CH₂Cl₂ (3 x 10 mL). The organic layer was washed with brine (15 mL), dried over sodium sulfate, filtered, and concentrated under reduced pressure. The crude product was purified by flash chromatography (7:3 hexanes:EtOAc) to afford the desired product as a ~ 1:1 mixture of epimers at the stereocenter alpha to the ketone.



Synthesis of inhibitor 3.6. The commercially available but-3-yn-2-amide (J&W PharmLab, Levittown, PA) was Boc-protected according to standard procedures,⁴ and General Procedure E was followed using azido-aryloxy methyl ketone **3.56a** (0.070 g, 0.36 mmol), *tert*-butyl but-3-yn-2-ylcarbamate (0.06 g, 0.36 mmol) in 1.44 mL of 1:1 H₂O/*t*-BuOH, 1.0 M aqueous solution of sodium ascorbate (0.36 mL, 0.36 mmol), and 0.3 M aqueous solution of copper(II) sulfate pentahydrate (0.12 mL, 0.036 mmol). Purification by flash chromatography afforded the desired product in 49% yield.

The Boc-protected triazole product (0.045 g, 0.09 mmol) was directly treated with HCl as a 4.0 M solution in 1,4-dioxane (0.21 mL, 0.90 mmol). The solution was stirred at rt for 2 h and was then concentrated to afford the crude product, which was purified by HPLC [preparatory reverse phase C₁₈ column (24.1 x 250 mm), CH₃CN/H₂O 0.1% TFA, 5:95 to 95:5 over 55 min; 10 mL/min, 254 nm detection]. Fractions were combined and the CH₃CN was evaporated. The resulting aqueous solution was extracted with CH₂Cl₂, dried with Na₂SO₄, filtered, and concentrated to yield the CF₃CO₂H salt of inhibitor **2.6** in 74% yield. ¹H NMR (400 MHz, CDCl₃): δ 0.83-0.94 (m, 3H), 1.14-1.36 (m, 4H), 1.71 (m, 3H), 1.98-2.03 (m, 1H), 2.25-2.29 (m, 1H), 4.70-4.73 (m, 1H), 4.91-5.01 (m, 2H), 5.71-5.75 (m, 1H), 6.78-6.86 (m, 1H), 8.01 (s, 1H). LRMS calculated for MH⁺ C₁₇H₂₀F₄N₄O₂, 389.2, found 389.0 and MH⁺ C₁₇H₂₁F₄N₄O₄ (hydrate), 406.2, found 407.0.

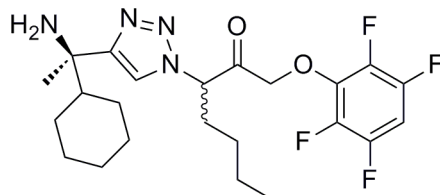


3.7

Synthesis of inhibitor 3.7. The commercially available 2-methylbut-3-yn-2-amine (Aldrich, St. Louis, MO) was Boc-protected according to standard procedures,⁴ and General Procedure E was followed using azido-aryloxy methyl ketone **3.56a** (0.08 g, 0.40 mmol), *tert*-butyl (2-methylbut-3-yn-2-yl)carbamate (0.07 g, 0.40 mmol) in 1.58 mL of 1:1 H₂O/*t*-BuOH, 1.0 M aqueous solution of sodium ascorbate (0.40 mL, 0.40 mmol), and 0.3 M aqueous solution of copper(II) sulfate pentahydrate (0.13 mL, 0.04 mmol). Purification by flash chromatography afforded the desired product in 52% yield.

The Boc-protected triazole product (0.044 g, 0.08 mmol) was directly treated with HCl as a 4.0 M solution in 1,4-dioxane (0.20 mL, 0.80 mmol). The solution was stirred at rt for 2 h and was then concentrated to afford the crude product, which was purified by HPLC [preparatory reverse phase C₁₈ column (24.1 x 250 mm), CH₃CN/H₂O 0.1% TFA, 5:95 to 95:5 over 55 min; 10 mL/min, 254 nm detection]. Fractions were combined and the CH₃CN was evaporated. The resulting aqueous solution was extracted with CH₂Cl₂, dried with Na₂SO₄, filtered, and concentrated to yield the CF₃CO₂H salt of inhibitor **3.7** in 78% yield. ¹H NMR (400 MHz, CD₃OD): δ 0.84-0.89 (m, 3H), 1.10-1.35 (m, 4H), 1.74 (s, 3H), 1.76 (s, 3H), 5.18 (s, 2H), 5.80-5.83 (m, 1H), 7.11-7.19 (m, 1H), 8.27 (s, 1H). Diastereomeric CD₃OD hemiacetal adducts equilibrate with the ketone product. The extent of hemiacetal formation depends on the amount of TFA and the time of incubation

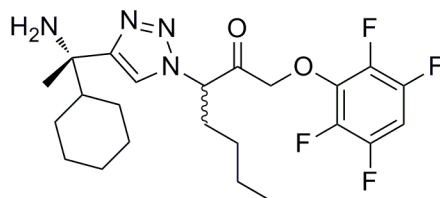
in CD₃OD (see ¹H NMR spectrum). Peaks corresponding to the ketone but not the hemiacetal are listed here. LRMS calculated for MH⁺ C₁₈H₂₂F₄N₄O₂, 402.2, found 402.1 and MH⁺ C₁₈H₂₄F₄N₄O₃ (hydrate), 420.2, found 420.1.



3.14

Synthesis of inhibitor 3.14. (*S*)-2-cyclohexylbut-3-yn-2-amine was prepared according to a previous literature procedure,³⁵ and was subsequently Boc-protected according to a standard procedure.⁴ General Procedure E was followed using azido-aryloxy methyl ketone **3.56a** (0.08 g, 0.42 mmol), (*S*)-*tert*-butyl (2-cyclohexylbut-3-yn-2-yl)carbamate (0.10 g, 0.42 mmol) in 1.65 mL of 1:1 H₂O/*t*-BuOH, 1.0 M aqueous solution of sodium ascorbate (0.42 mL, 0.42 mmol, and 0.3 M aqueous solution of copper(II) sulfate pentahydrate (0.14 mL, 0.04 mmol). Purification by flash chromatography afforded the desired Boc triazole product in 54% yield.

The Boc-protected triazole product (0.056 g, 0.10 mmol) was directly treated with HCl as a 4.0 M solution in 1,4-dioxane (0.25 mL, 1.0 mmol). The solution was stirred at rt for 2 h and was then concentrated to afford the crude product, which was purified by HPLC [preparatory reverse phase C₁₈ column (24.1 x 250 mm), CH₃CN/H₂O 0.1% TFA, 5:95 to 95:5 over 55 min; 10 mL/min, 254 nm detection]. Fractions were combined and the CH₃CN was evaporated. The resulting aqueous solution was extracted with CH₂Cl₂, dried with Na₂SO₄, filtered, and concentrated to yield the CF₃CO₂H salt of inhibitor **3.14** in 80% yield. ¹H NMR (400 MHz, CD₃OD): δ 0.85-0.89 (m, 3H), 0.91-1.12 (m, 4H), 1.25-1.42 (m, 5H), 1.49-1.52 (m, 1H), 1.68 (s, 3H), 1.69-1.84 (m, 4H), 1.92-1.95 (m, 1H), 2.12-2.21 (m, 1H), 2.32-2.38 (m, 1H), 5.17-5.19 (m, 2H), 5.80-5.83 (m, 1H), 6.92-6.97 (m, 1H), 8.26 (s, 1H). Diastereomeric CD₃OD hemiacetal adducts equilibrate with the ketone product. The extent of hemiacetal formation depends on the amount of TFA and the time of incubation in CD₃OD (see ¹H NMR spectrum). Peaks corresponding to the ketone but not the hemiacetal are listed here. LRMS calculated for MH⁺ C₂₃H₃₀F₄N₄O₂, 471.2, found 471.1.

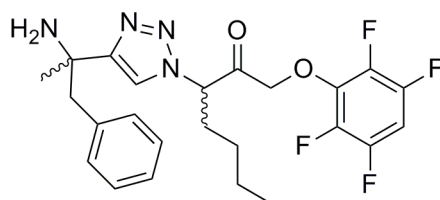


3.15

Synthesis of inhibitor 3.15. (*R*)-2-cyclohexylbut-3-yn-2-amine was prepared according to a previous literature procedure⁶ and was subsequently Boc-protected

according to a standard procedure.⁴ General Procedure E was followed using azido-aryloxy methyl ketone **3.56a** (0.08 g, 0.42 mmol), (*R*)-*tert*-butyl (2-cyclohexylbut-3-yn-2-yl)carbamate (0.10 g, 0.42 mmol) in 1.65 mL of 1:1 H₂O/*t*-BuOH, 1.0 M aqueous solution of sodium ascorbate (0.42 mL, 0.42 mmol), and 0.3 M aqueous solution of copper(II) sulfate pentahydrate (0.14 mL, 0.04 mmol). Purification by flash chromatography afforded the desired product in 52% yield.

The Boc-protected triazole product (0.051 g, 0.09 mmol) was directly treated with HCl as a 4.0 M solution in 1,4-dioxane (0.22 mL, 0.90 mmol). The solution was stirred at rt for 2 h and was then concentrated to afford the crude product, which was purified by HPLC [preparatory reverse phase C₁₈ column (24.1 x 250 mm), CH₃CN/H₂O 0.1% TFA, 5:95 to 95:5 over 55 min; 10 mL/min, 254 nm detection]. Fractions were combined and the CH₃CN was evaporated. The resulting aqueous solution was extracted with CH₂Cl₂, dried with Na₂SO₄, filtered, and concentrated to yield the CF₃CO₂H salt of inhibitor **3.15** in 70% yield. ¹H NMR (400 MHz, CD₃OD): δ 0.83-0.87 (m, 3H), 1.00-1.14 (m, 4H), 1.30-1.39 (m, 5H), 1.48-1.52 (m, 1H), 1.63 (s, 3H), 1.68-1.77 (m, 4H), 1.80-1.86 (m, 1H), 2.00-2.08 (m, 1H), 2.19-2.25 (m, 1H), 5.00-5.09 (m, 2H), 5.66-5.70 (m, 1H), 6.99-7.08 (m, 1H), 8.14 (s, 1H). Diastereomeric CD₃OD hemiacetal adducts equilibrate with the ketone product. The extent of hemiacetal formation depends on the amount of TFA and the time of incubation in CD₃OD (see ¹H NMR spectrum). Peaks corresponding to the ketone but not the hemiacetal are listed here. LRMS calculated for MH⁺ C₂₃H₃₀F₄N₄O₂, 471.2, found 471.1.



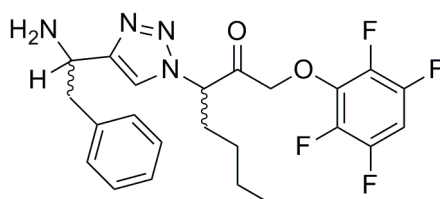
3.13

Synthesis of 3.13. General Procedure D was followed using alkyne **3.47** (0.70 g, 2.66 mmol) and HCl as a 4.0 M 1,4-dioxane solution (2.0 mL, 7.98 mmol) to afford the hydrochloride salt of 2-methyl-1-phenylbut-3-yn-2-amine in quantitative yield. The resulting amine was Boc protected by adding NEt₃ (0.18 mL, 1.30 mmol) and di-*tert*-butyl dicarbonate (0.26 g, 1.20 mmol) to amine salt (0.16 g, 0.80 mmol) in 1.20 mL of CH₂Cl₂ with stirring at rt for 12 h. The reaction mixture was concentrated and purified by silica gel chromatography with 6:4 hexanes:EtOAc as the eluent to yield product in 96% yield over the two steps.

The Boc-protected propargyl amine product (0.20 g, 0.77 mmol) was directly used in General Procedure E with azido-aryloxy methyl ketone **3.56a** (0.24 g, 0.77 mmol) in 3.08 mL of 1:1 H₂O/*t*-BuOH, 1.0 M aqueous solution of sodium ascorbate (0.77 mL, 0.77 mmol), and 0.3 M aqueous solution of copper(II) sulfate pentahydrate (0.26 mL, 0.08 mmol). Purification by flash chromatography afforded the desired product in 46% yield.

The Boc-protected triazole product (0.042 g, 0.07 mmol) was directly treated with HCl as a 4.0 M solution in 1,4-dioxane (0.18 mL, 0.70 mmol). The solution was stirred at

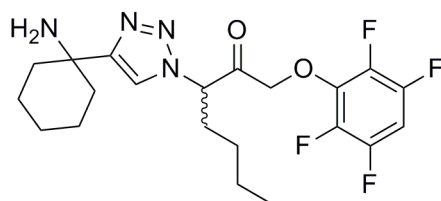
rt for 2 h and was then concentrated to afford the crude product, which was purified by HPLC [preparatory reverse phase C₁₈ column (24.1 x 250 mm), CH₃CN/H₂O 0.1% TFA, 5:95 to 95:5 over 55 min; 10 mL/min, 254 nm detection]. Fractions were combined and the CH₃CN was evaporated. The resulting aqueous solution was extracted with CH₂Cl₂, dried with Na₂SO₄, filtered, and concentrated to yield the CF₃CO₂H salt of inhibitor **3.13** in 70% yield. ¹H NMR (400 MHz, CD₃OD): δ 0.82-0.86 (m, 3H), 1.12-1.28 (m, 2H), 1.34-1.57 (m, 2H), 1.64 (m, 3H), 2.12-2.22 (m, 2H), 3.13-3.31 (m, 1 H), 3.44-3.57 (m, 1 H), 5.02-5.10 (m, 2H), 5.60-5.63 (m, 1H), 6.90-7.01 (m, 1H), 7.09-7.20 (m, 5H), 7.84 (m, 1H). Diastereomeric CD₃OD hemiacetal adducts equilibrate with the ketone product. The extent of hemiacetal formation depends on the amount of TFA and the time of incubation in CD₃OD (see ¹H NMR spectrum). Peaks corresponding to the ketone but not the hemiacetal are listed here. LRMS calculated for MH⁺ C₂₄H₂₆F₄N₄O₂, 479.1, found 479.1 and MH⁺ C₂₄H₂₈F₄N₄O₃ (hydrate), 497.1, found 497.1.



3.12

Synthesis of 3.12. General Procedure E was followed using azido-aryloxymethyl ketone **3.56a** (0.060 g, 0.19 mmol), 2-methyl-*N*-(1-phenylbut-3-yn-2-yl)propane-2-sulfonamide **3.48** (0.050 g, 0.19 mmol) in 0.77 mL of 1:1 H₂O/*t*-BuOH, 1.0 M aqueous solution of sodium ascorbate (0.19 mL, 0.19 mmol), and 0.3 M aqueous solution of copper(II) sulfate pentahydrate (0.06 mL, 0.02 mmol). Purification by flash chromatography afforded the desired product in 51% yield.

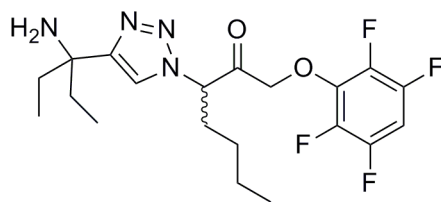
The sulfinyl-protected triazole product (0.06 g, 0.10 mmol) was directly treated with HCl as a 4.0 M solution in 1,4-dioxane (0.26 mL, 1.0 mmol). The solution was stirred at rt for 2 h and was then concentrated to afford the crude product, which was purified by HPLC [preparatory reverse phase C₁₈ column (24.1 x 250 mm), CH₃CN/H₂O 0.1% TFA, 5:95 to 95:5 over 55 min; 10 mL/min, 254 nm detection]. Fractions were combined and the CH₃CN was evaporated. The resulting aqueous solution was extracted with CH₂Cl₂, dried with Na₂SO₄, filtered, and concentrated to yield the CF₃CO₂H salt of inhibitor **3.12** in 71% yield. ¹H NMR (400 MHz, CDCl₃): δ 0.79-0.85 (m, 3H), 0.91-1.02 (m, 1H), 1.13-1.20 (m, 1H), 1.21-1.32 (m, 3H), 1.82-1.96 (m, 1H), 2.18-2.22 (m, 1H), 3.23-3.29 (m, 1 H), 3.49-3.55 (m, 1 H), 4.79-4.84 (m, 2H), 5.63-5.69 (m, 1H), 6.77-6.86 (m, 1H), 6.90-7.05 (m, 2H), 7.17-7.20 (m, 3H), 7.54 (m, 0.6H), 7.61 (s, 0.4H). LRMS calculated for MH⁺ C₂₃H₂₅F₄N₄O₂, 465.2, found 465.2 and MH⁺ C₂₄H₂₇F₄N₄O₃ (hydrate), 483.1, found 483.1.



3.1

Synthesis of 3.1. The commercially available 1-ethynylcyclohexanamine (Sigma-Aldrich, St. Louis, MO) was Boc-protected according to a standard procedure.⁴ General Procedure E was followed using azido-aryloxy methyl ketone **3.56a** (0.15 g, 0.50 mmol), *tert*-butyl (1-ethynylcyclohexyl)carbamate (0.11 g, 0.50 mmol) in 2.0 mL of 1:1 H₂O/*t*-BuOH, 1.0 M aqueous solution of sodium ascorbate (0.50 mL, 0.50 mmol, and 0.3 M aqueous solution of copper(II) sulfate pentahydrate (0.17 mL, 0.05 mmol). Purification by flash chromatography afforded the desired product in 58% yield.

The Boc-protected triazole product (0.074 g, 0.13 mmol) was directly treated with HCl as a 4.0 M solution in 1,4-dioxane (0.32 mL, 1.3 mmol). The solution was stirred at rt for 2 h and was then concentrated to afford the crude product, which was purified by HPLC [preparatory reverse phase C₁₈ column (24.1 x 250 mm), CH₃CN/H₂O 0.1% TFA, 5:95 to 95:5 over 55 min; 10 mL/min, 254 nm detection]. Fractions were combined and the CH₃CN was evaporated. The resulting aqueous solution was extracted with CH₂Cl₂, dried with Na₂SO₄, filtered, and concentrated to yield the CF₃CO₂H salt of inhibitor **2.1** in 78% yield. ¹H NMR (400 MHz, CDCl₃): δ 0.88-0.96 (m, 3H), 1.24-1.34 (m, 8H), 1.39-1.54 (m, 2H), 1.70-1.77 (m, 2H), 2.05-2.18 (m, 2H), 2.30-2.46 (m, 2H), 4.96 (d, 1H, *J*= 17.2), 4.98 (d, 1H, *J*= 17.2), -5.68 (m, 1H), 6.78-6.85 (m, 1H), 7.95 (s, 1H), 8.6 (br s, 2H). ¹⁹F NMR (376 MHz, CDCl₃): δ -156.3- -156.2 (m, 2F), -139.0- -138.2 (m, 2F).

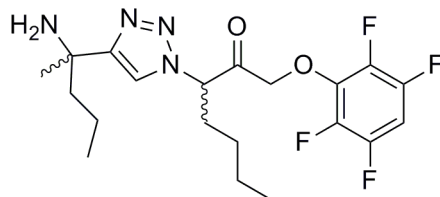


3.8

Synthesis of inhibitor 3.8. The commercially available 3-ethylpent-1-yn-3-amine (Acros Organics, Morris Plains, NJ) was Boc-protected according to a standard procedure.⁴ General Procedure E was followed using azido-aryloxy methyl ketone **3.56a** (0.10 g, 0.31 mmol), *tert*-butyl (3-ethylpent-1-yn-3-yl)carbamate (0.07 g, 0.31 mmol) in 1.25 mL of 1:1 H₂O/*t*-BuOH, 1.0 M aqueous solution of sodium ascorbate (0.31 mL, 0.31 mmol, and 0.3 M aqueous solution of copper(II) sulfate pentahydrate (0.10 mL, 0.03 mmol). Purification by flash chromatography afforded the desired product in 60% yield.

The Boc-protected triazole product (0.04 g, 0.08 mmol) was directly treated with HCl as a 4.0 M solution in 1,4-dioxane (0.19 mL, 0.75 mmol). The solution was stirred at rt for 2 h and was then concentrated to afford the crude product, which was purified by

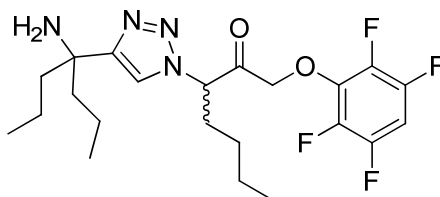
HPLC [preparatory reverse phase C₁₈ column (24.1 x 250 mm), CH₃CN/H₂O 0.1% TFA, 5:95 to 95:5 over 55 min; 10 mL/min, 254 nm detection]. Fractions were combined and the CH₃CN was evaporated. The resulting aqueous solution was extracted with CH₂Cl₂, dried with Na₂SO₄, filtered, and concentrated to yield the CF₃CO₂H salt of inhibitor **3.8** in 61% yield. ¹H NMR (400 MHz, CDCl₃): δ 0.80-0.83 (m, 3H), 0.88-0.89 (m, 6H), 1.02-1.20 (m, 1H), 1.23-1.34 (m, 3H), 2.06-2.11 (m, 5H), 2.23-2.28 (m, 1H), 4.86-4.90 (d, 1H, *J* = 17.6), 4.94-4.98 (d, 1H, *J* = 17.6), 5.63-5.66 (m, 1H), 6.74-6.82 (m, 1H), 7.24 (s, 1H), 8.49 (br s, 1H). LRMS calculated for MH⁺ C₂₀H₂₆F₄N₄O₂, 431.2, found 431.2 and MH⁺ C₂₀H₂₈F₄N₄O₃ (hydrate), 448.2, found 448.1.



3.9

Synthesis of inhibitor 3.9. General Procedure E was followed using azido-aryloxy methyl ketone **3.56a** (0.10 g, 0.30 mmol), sulfinamide **3.49** (0.07 g, 0.30 mmol) in 1.25 mL of 1:1 H₂O/*t*-BuOH, 1.0 M aqueous solution of sodium ascorbate (0.30 mL, 0.31 mmol), and 0.3 M aqueous solution of copper(II) sulfate pentahydrate (0.10 mL, 0.03 mmol). Purification by flash chromatography afforded the desired product in 55% yield.

The sulfinyl-protected triazole product (0.06 g, 0.10 mmol) was directly treated with HCl as a 4.0 M solution in 1,4-dioxane (0.26 mL, 1.0 mmol). The solution was stirred at rt for 2 h and was then concentrated to afford the crude product, which was purified by HPLC [preparatory reverse phase C₁₈ column (24.1 x 250 mm), CH₃CN/H₂O 0.1% TFA, 5:95 to 95:5 over 55 min; 10 mL/min, 254 nm detection]. Fractions were combined and the CH₃CN was evaporated. The resulting aqueous solution was extracted with CH₂Cl₂, dried with Na₂SO₄, filtered, and concentrated to yield the CF₃CO₂H salt of inhibitor **3.9** in 66% yield. ¹H NMR (400 MHz, CD₃OD): δ 0.83-0.95 (m, 6H), 1.11-1.21 (m, 2H), 1.24-1.38 (m, 4H), 1.73 (s, 3H), 1.92-2.03 (m, 2H), 2.06-2.16 (m, 2H), 5.06-5.17 (m, 2H), 5.79-5.83 (m, 1H), 6.9-7.19 (m, 1H), 8.23 (s, 1H). Diastereomeric CD₃OD hemiacetal adducts equilibrate with the ketone product. The extent of hemiacetal formation depends on the amount of TFA and the time of incubation in CD₃OD (see ¹H NMR spectrum). Peaks corresponding to the ketone but not the hemiacetal are listed here. LRMS calculated for MH⁺ C₂₀H₂₆F₄N₄O₂, 431.2, found 431.2 and MH⁺ C₂₀H₂₈F₄N₄O₃ (hydrate), 448.2, found 448.2.

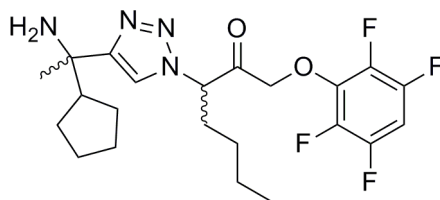


3.10

Synthesis of inhibitor 3.10. General Procedure E was followed using azido-aryloxy methyl ketone **3.56a** (0.10 g, 0.30 mmol), sulfinamide **3.50** (0.08 g, 0.30 mmol)

in 1.25 mL of 1:1 H₂O/*t*-BuOH, 1.0 M aqueous solution of sodium ascorbate (0.30 mL, 0.31 mmol, and 0.3 M aqueous solution of copper(II) sulfate pentahydrate (0.10 mL, 0.03 mmol). Purification by flash chromatography afforded the desired product in 48% yield.

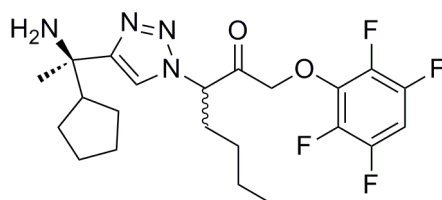
The sulfinyl-protected triazole product (0.07 g, 0.13 mmol) was directly treated with HCl as a 4.0 M solution in 1,4-dioxane (0.31 mL, 1.3 mmol). The solution was stirred at rt for 2 h and was then concentrated to afford the crude product, which was purified by HPLC [preparatory reverse phase C₁₈ column (24.1 x 250 mm), CH₃CN/H₂O 0.1% TFA, 5:95 to 95:5 over 55 min; 10 mL/min, 254 nm detection]. Fractions were combined and the CH₃CN was evaporated. The resulting aqueous solution was extracted with CH₂Cl₂, dried with Na₂SO₄, filtered, and concentrated to yield the CF₃CO₂H salt of inhibitor **3.10** in 65% yield. ¹H NMR (400 MHz, CD₃OD): δ 0.73-0.87 (m, 9H), 0.98-1.17 (m, 2H), 1.20-1.31 (m, 6H), 1.85-1.90 (m, 4H), 4.99-5.00 (m, 2H), 5.66-5.70 (m, 1H), 7.01-7.08 (m, 1H), 8.11 (s, 1H). Diastereomeric CD₃OD hemiacetal adducts equilibrate with the ketone product. The extent of hemiacetal formation depends on the amount of TFA and the time of incubation in CD₃OD (see ¹H NMR spectrum). Peaks corresponding to the ketone but not the hemiacetal are listed here. LRMS calculated for MH⁺ C₂₂H₃₀F₄N₄O₂, 458.2, found 458.2 and MH⁺ C₂₂H₃₂F₄N₄O₃ (hydrate), 482.2, found 448.3.



3.11

Synthesis of 3.11. General Procedure E was followed using azido-aryloxy methyl ketone **3.56a** (0.10 g, 0.31 mmol), sulfinamide **3.51** (0.08 g, 0.30 mmol) in 1.25 mL of 1:1 H₂O/*t*-BuOH, 1.0 M aqueous solution of sodium ascorbate (0.30 mL, 0.30 mmol, and 0.3 M aqueous solution of copper(II) sulfate pentahydrate (0.10 mL, 0.03 mmol). Purification by flash chromatography afforded the desired product in 56% yield.

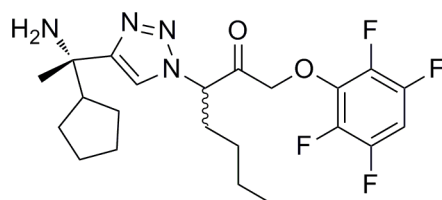
The sulfinyl-protected triazole product (0.05 g, 0.09 mmol) was directly treated with HCl as a 4.0 M solution in 1,4-dioxane (0.23 mL, 0.9 mmol). The solution was stirred at rt for 2 h and was then concentrated to afford the crude product, which was purified by HPLC [preparatory reverse phase C₁₈ column (24.1 x 250 mm), CH₃CN/H₂O 0.1% TFA, 5:95 to 95:5 over 55 min; 10 mL/min, 254 nm detection]. Fractions were combined and the CH₃CN was evaporated. The resulting aqueous solution was extracted with CH₂Cl₂, dried with Na₂SO₄, filtered, and concentrated to yield the CF₃CO₂H salt of inhibitor **3.11** in 73% yield. ¹H NMR (400 MHz, CD₃OD): δ 0.76-0.79 (m, 3H), 0.95-0.96 (m, 1H), 1.11-1.44 (m, 10H), 1.57 (s, 3H), 1.65-1.66 (m, 1H), 1.99-2.19 (m, 2H), 2.35-2.339 (m, 1H), 4.99-5.09 (m, 2H), 5.66-5.69 (m, 1H), 7.00-7.05 (m, 1H), 8.16 (s, 1H). Diastereomeric CD₃OD hemiacetal adducts equilibrate with the ketone product. The extent of hemiacetal formation depends on the amount of TFA and the time of incubation in CD₃OD (see ¹H NMR spectrum). Peaks corresponding to the ketone but not the hemiacetal are listed here. LRMS calculated for MH⁺ C₂₂H₂₈F₄N₄O₂, 457.2, found 457.2.



3.20

Synthesis of inhibitor 3.20. General Procedure E was followed using azido-aryloxy methyl ketone **3.56a** (0.10 g, 0.31 mmol), (*R*)-sulfonamide **3.52** (0.08 g, 0.30 mmol) in 1.25 mL of 1:1 H₂O/*t*-BuOH, 1.0 M aqueous solution of sodium ascorbate (0.30 mL, 0.30 mmol), and 0.3 M aqueous solution of copper(II) sulfate pentahydrate (0.10 mL, 0.03 mmol). Purification by flash chromatography afforded the desired product in 54% yield.

The sulfinyl-protected product (0.073 g, 0.30 mmol) was directly treated with HCl as a 4.0 M solution in 1,4-dioxane (0.23 mL, 3.0 mmol). The solution was stirred at rt for 2 h and was then concentrated to afford the crude product, which was purified by HPLC [preparatory reverse phase C₁₈ column (24.1 x 250 mm), CH₃CN/H₂O 0.1% TFA, 5:95 to 95:5 over 55 min; 10 mL/min, 254 nm detection]. Fractions were combined and the CH₃CN was evaporated. The resulting aqueous solution was extracted with CH₂Cl₂, dried with Na₂SO₄, filtered, and concentrated to yield the CF₃CO₂H salt of inhibitor **3.20** in 72% yield. ¹H NMR (400 MHz, CDCl₃): δ 0.83-0.89 (m, 3H), 1.21-1.51 (m, 11H), 1.66-1.77 (m, 1H), 1.78 (s, 1.5H), 1.79 (s, 1.5H), 2.01-2.08 (m, 1H), 2.24-2.33 (m, 1H), 2.49-2.53 (m, 1H), 4.93-4.96 (m, 2H), 5.62-5.72 (m, 1H), 6.78-6.84 (m, 1H), 7.96 (s, 0.5H), 7.99 (s, 0.5H), 8.65 (br s, 2H). LRMS calculated for MH⁺ C₂₂H₂₈F₄N₄O₂, 457.2, found 457.1.

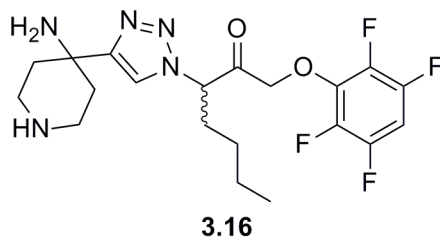


3.21

Synthesis of inhibitor 3.21. General Procedure E was followed using azido-aryloxy methyl ketone **3.56a** (0.07 g, 0.20 mmol), (*S*)-sulfonamide **3.53** (0.12 g, 0.20 mmol) in 0.88 mL of 1:1 H₂O/*t*-BuOH, 1.0 M aqueous solution of sodium ascorbate (0.20 mL, 0.20 mmol), and 0.3 M aqueous solution of copper(II) sulfate pentahydrate (0.07 mL, 0.02 mmol). Purification by flash chromatography afforded the desired product in 62% yield.

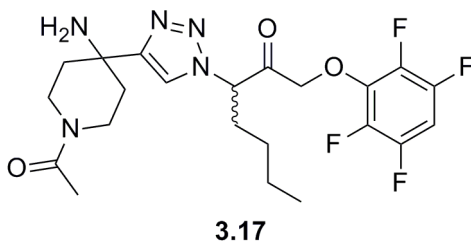
The sulfinyl-protected triazole product (0.073 g, 0.130 mmol) was directly treated with HCl as a 4.0 M solution in 1,4-dioxane (0.32 mL, 1.3 mmol). The solution was stirred at rt for 2 h and was then concentrated to afford the crude product, which was purified by HPLC [preparatory reverse phase C₁₈ column (24.1 x 250 mm), CH₃CN/H₂O 0.1% TFA, 5:95 to 95:5 over 55 min; 10 mL/min, 254 nm detection]. Fractions were

combined and the CH₃CN was evaporated. The resulting aqueous solution was extracted with CH₂Cl₂, dried with Na₂SO₄, filtered, and concentrated to yield the CF₃CO₂H salt of inhibitor **3.21** in 80% yield. ¹H NMR (400 MHz, CDCl₃): δ 0.81 (t, 1.5H), 0.82 (t, 1.5H), 1.07-1.47 (m, 11H), 1.61-1.64 (m, 1H), 1.75 (s, 1.5H), 1.77 (s, 1.5H), 2.02-2.07 (m, 1H), 2.21-2.29 (m, 1H), 2.47-2.51 (m, 1H), 4.85-4.87 (m, 2H), 5.56 (dd, 0.5H, *J* = 4.4, 10.4), 5.68 (dd, 0.5H, *J* = 4.4, 10.4), 6.73-6.83 (m, 1H), 7.94 (s, 0.5H), 7.99 (s, 0.5H), 8.4 (br s, 2H). ¹⁹F NMR (376 MHz, CDCl₃): δ -156.4- -156.2 (m, 2F), -138.4- -138.1 (m, 2F). LRMS calculated for MH⁺ C₂₂H₂₈F₄N₄O₂, 457.2, found 457.2.



Synthesis of inhibitor 3.16. General Procedure E was followed using azido-aryloxymethyl ketone **3.56a** (0.070 g, 0.22 mmol), *tert*-butyl 4-(1,1-dimethylethylsulfonamido)-4-ethynylpiperidine-1-carboxylate **3.54** (0.060 g, 0.22 mmol) in 0.90 mL of 1:1 H₂O/*t*-BuOH, 1.0 M aqueous solution of sodium ascorbate (0.22 mL, 0.22 mmol), and 0.3 M aqueous solution of copper(II) sulfate pentahydrate (0.07 mL, 0.02 mmol). Purification by flash chromatography afforded the desired product in 47% yield.

The sulfinyl-protected triazole product (0.070 g, 0.10 mmol) was directly treated with HCl as a 4.0 M solution in 1,4-dioxane (0.26 mL, 1.0 mmol). The solution was stirred at rt for 2 h and then was concentrated to afford the crude product, which was purified by HPLC [preparatory reverse phase C₁₈ column (24.1 x 250 mm), CH₃CN/H₂O 0.1% TFA, 5:95 to 95:5 over 55 min; 10 mL/min, 254 nm detection]. Fractions were combined and the CH₃CN was evaporated. The resulting aqueous solution was extracted with CH₂Cl₂, dried with Na₂SO₄, filtered, and concentrated to yield the CF₃CO₂H salt of inhibitor **3.16** in 70% yield. ¹H NMR (400 MHz, (CD₃)₂SO): δ 0.84-0.86 (t, *J* = 6.8 Hz, 3H), 0.90-0.95 (m, 1H), 1.12-1.29 (m, 3H), 2.03-2.08 (m, 1H), 2.15-2.21 (m, 3H), 2.59-2.62 (m, 2H), 2.69-2.74 (m, 2H), 3.36-3.39 (m, 2H), 5.29 (d, *J* = 18 Hz, 1H), 5.37 (d, *J* = 18 Hz, 1H), 5.80 (dd, *J* = 4.0, 15.2 Hz, 1H), 7.54-7.63 (m, 1H), 8.55 (s, 1H), 8.82 (br s, 2H). LRMS calculated for MH⁺ C₂₀H₂₆F₄N₅O₂, 444.1, found 444.1 and MH⁺ C₂₀H₂₈F₄N₅O₃ (hydrate), 462.1, found 462.1.

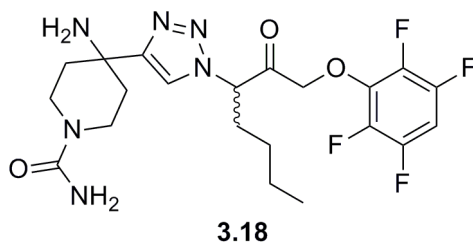


Synthesis of inhibitor 3.17. General Procedure E was followed using azido-aryloxy methyl ketone **3.56a** (0.09 g, 0.29 mmol), *tert*-butyl 4-(1,1-dimethylethylsulfonamido)-4-ethynylpiperidine-1-carboxylate **3.54** (0.10 g, 0.29 mmol) in 1.2 mL of 1:1 H₂O/*t*-BuOH, 1.0 M aqueous solution of sodium ascorbate (0.29 mL, 0.29 mmol), and 0.3 M aqueous solution of copper(II) sulfate pentahydrate (0.10 mL, 0.03 mmol). Purification by flash chromatography afforded the desired product in 45% yield.

The triazole product (0.080 g, 0.13 mmol) was subjected to selective Boc-deprotection conditions by directly treating with 1.2 mL of 5:1 CH₂Cl₂:TFA solution with stirring for 1 h. The mixture was added to 10 mL of saturated sodium bicarbonate solution and then was extracted with CH₂Cl₂ (3 x 10 mL). The combined organic layers were dried over sodium sulfate, filtered, and concentrated under reduced pressure to yield the product in 90% yield.

The resulting amine product (0.60 g, 0.11 mmol) was acetylated by treating with *i*-Pr₂EtN (0.05 mL, 0.28 mmol) and acetic anhydride (0.01 mL, 0.14 mmol) in 0.3 mL of DMF. The mixture was stirred at room temperature for 18 h. The mixture was then added to 10 mL of H₂O and extracted with EtOAc (3 x 10 mL). The combined organic layers were dried with sodium sulfate, filtered, and concentrated under reduced pressure. Purification by flash chromatography (6:4 hexane:EtOAc) afforded the desired product in 68% yield.

The acetylated product (0.05 g, 0.08 mmol) was directly treated with HCl as a 4.0 M solution in 1,4-dioxane (0.2 mL, 0.8 mmol). The solution was stirred at rt for 2 h and was then concentrated to afford the crude product, which was purified by HPLC [preparatory reverse phase C₁₈ column (24.1 x 250 mm), CH₃CN/H₂O 0.1% TFA, 5:95 to 95:5 over 55 min; 10 mL/min, 254 nm detection]. Fractions were combined and the CH₃CN was evaporated. The resulting aqueous solution was extracted with CH₂Cl₂, dried with Na₂SO₄, filtered, and concentrated to yield the CF₃CO₂H salt of inhibitor **3.17** in 73% yield. ¹H NMR (400 MHz, (CD₃)₂SO): δ 0.76-0.79 (t, *J* = 6.8 Hz, 3H), 0.90-0.96 (m, 1H), 1.13-1.26 (m, 3H), 1.78-1.90 (m, 2H), 1.93 (s, 3H), 1.99-2.05 (m, 2H), 2.19-2.20 (m, 1 H), 2.37-2.44 (m, 1H), 2.63-2.68 (m, 1H), 2.91-2.96 (m, 1H), 3.69-3.76 (m, 1H), 4.08-4.16 (m, 1 H), 5.27 (d, *J* = 18 Hz, 1H), 5.35 (d, *J* = 18 Hz, 1H), 5.76-5.80 (m, 1H), 7.54-7.63 (m, 1H), 8.47 (s, 1H), 8.53 (br s, 2H). LRMS calculated for MH⁺ C₂₂H₂₈F₄N₅O₃, 486.2, found 486.2 and MH⁺ C₂₂H₃₀F₄N₅O₄ (hydrate), 504.2, found 504.2.



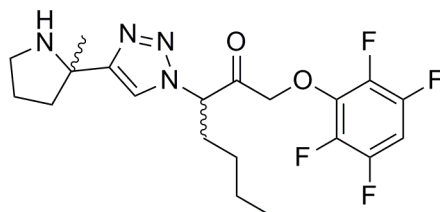
Synthesis of inhibitor 3.18. General Procedure E was followed using azido-aryloxymethyl ketone **3.56a** (0.09 g, 0.29 mmol), *tert*-butyl 4-(1,1-dimethylethylsulfonamido)-4-ethynylpiperidine-1-carboxylate **3.54** (0.10 g, 0.29 mmol) in 1.2 mL of 1:1 H₂O/*t*-BuOH, 1.0 M aqueous solution of sodium ascorbate (0.29 mL, 0.29

mmol, and 0.3 M aqueous solution of copper(II) sulfate pentahydrate (0.10 mL, 0.03 mmol). Purification by flash chromatography afforded the desired product in 47% yield.

The triazole product (0.08 g, 0.13 mmol) was subjected to selective Boc-deprotection conditions by directly treating with 1.2 mL of 5:1 CH₂Cl₂:TFA solution with stirring for 1 h. The mixture was added to 10 mL of saturated sodium bicarbonate solution and then was extracted with CH₂Cl₂ (3 x 10 mL). The combined organic layers were dried over sodium sulfate, filtered, and concentrated under reduced pressure to yield the product in 90% yield.

A general procedure previously reported in the literature³⁹ was used to transform the amine to a urea. The above amine product (0.070 g, 0.12 mmol) was directly treated with potassium cyanate (0.010 g, 0.18 mmol) and acetic acid (0.20 mL, 0.36 mmol) in 1.1 mL of 1:1 dioxane: H₂O. The mixture was stirred at room temperature for 24 h. The mixture was added to 10 mL of H₂O and extracted with EtOAc (3 x 10 mL). The combined organic layers were washed with brine and dried with sodium sulfate, filtered, and concentrated under reduced pressure. The crude product was purified by HPLC [preparatory reverse phase C₁₈ column (24.1 x 250 mm), CH₃CN/H₂O 0.1% TFA, 5:95 to 95:5 over 55 min; 10 mL/min, 254 nm detection]. Fractions were combined and the CH₃CN was evaporated. The resulting aqueous solution was extracted with CH₂Cl₂, dried with Na₂SO₄, filtered, and concentrated flash chromatography afforded the desired product in 51% yield.

The urea product (0.04 g, 0.06 mmol) was directly treated with HCl as a 4.0 M solution in 1,4-dioxane (0.2 mL, 0.6 mmol). The solution was stirred at rt for 2 h and was then concentrated to afford the crude product, which was purified by HPLC [preparatory reverse phase C₁₈ column (24.1 x 250 mm), CH₃CN/H₂O 0.1% TFA, 5:95 to 95:5 over 55 min; 10 mL/min, 254 nm detection]. Fractions were combined and the CH₃CN was evaporated. The resulting aqueous solution was extracted with CH₂Cl₂, dried with Na₂SO₄, filtered, and concentrated to yield the CF₃CO₂H salt of inhibitor **3.18** in 70% yield. ¹H NMR (400 MHz, (CD₃)₂SO): δ 0.77-0.80 (t, *J* = 6.8 Hz, 3H), 0.95-1.00 (m, 1H), 1.12-1.26 (m, 3H), 1.81-1.86 (m, 2H), 2.06-2.09 (m, 1H), 2.19-2.21 (m, 1H), 2.33-2.37 (m, 2H), 2.64-2.70 (m, 2H), 3.81-3.85 (m, 2H), 5.27 (d, *J* = 18 Hz, 1H), 5.35 (d, *J* = 18 Hz, 1H), 5.77 (dd, *J* = 4.0, 11.2 Hz, 1H), 6.08 (br s, 2H), 7.54-7.63 (m, 1H), 8.49 (br s, 2H), 8.53 (s, 1H). LRMS calculated for MH⁺ C₂₁H₂₇F₄N₆O₃, 487.2, found 487.2 and MH⁺ C₂₁H₂₉F₄N₆O₄ (hydrate), 505.2, found 505.2.

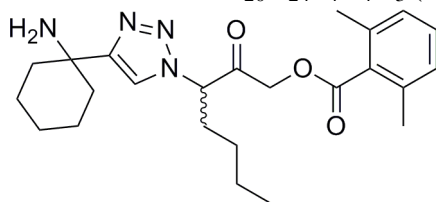


3.19

Synthesis of inhibitor 3.19. General Procedure E was followed using azido-aryloxy methyl ketone **3.56a** (0.11 g, 0.35 mmol), tert-butyl 2-ethynyl-2-methylpyrrolidine-1-carboxylate **3.55** (0.07 g, 0.40 mmol) in 1.4 mL of 1:1 H₂O/*t*-BuOH,

1.0 M aqueous solution of sodium ascorbate (0.35 mL, 0.40 mmol, and 0.3 M aqueous solution of copper(II) sulfate pentahydrate (0.12 mL, 0.04 mmol). Purification by flash chromatography afforded the desired product in 43% yield.

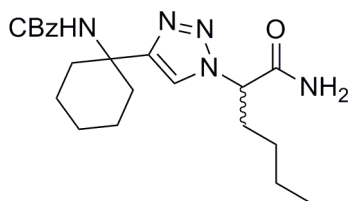
The Boc-protected triazole product (0.069 g, 0.13 mmol) was directly treated with HCl as a 4.0 M solution in 1,4-dioxane (0.32 mL, 1.3 mmol). The solution was stirred at rt for 2 h and was then concentrated to afford the crude product, which was purified by HPLC [preparatory reverse phase C₁₈ column (24.1 x 250 mm), CH₃CN/H₂O 0.1% TFA, 5:95 to 95:5 over 55 min; 10 mL/min, 254 nm detection]. Fractions were combined and the CH₃CN was evaporated. The resulting aqueous solution was extracted with CH₂Cl₂, dried with Na₂SO₄, filtered, and concentrated to yield the CF₃CO₂H salt of inhibitor **3.19** in 69% yield. ¹H NMR (400 MHz, CDCl₃): δ 0.81-0.87 (m, 3H), 1.2-1.35 (m, 6H), 1.95 (s, 3H), 2.11-2.29 (m, 6H), 2.78-2.82 (m, 1H), 4.99-5.04 (m, 2H), 5.64-5.71 (m, 1H), 6.77-6.85 (m, 1H), 8.35 (m, 1H), 9.723 (broad d, 1H). LRMS calculated for MH⁺ C₂₀H₂₄F₄N₄O₂, 429.2, found 429.1 and MH⁺ C₂₀H₂₄F₄N₄O₃ (hydrate), 447.2 found 447.1.



3.5

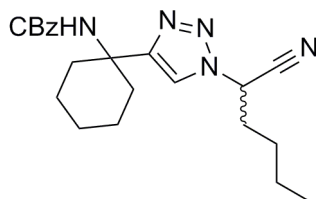
Synthesis of inhibitor 3.5. The commercially available 1-ethynylcyclohexanamine (Sigma-Aldrich, St. Louis, MO) was Boc-protected according to a standard procedure.⁵ General Procedure E was followed using azido-acyloxy methyl ketone **3.56b** (0.09 g, 0.30 mmol), *tert*-butyl (1-ethynylcyclohexyl)carbamate (0.07 g, 0.30 mmol) in 1.26 mL of 1:1 H₂O/*t*-BuOH, 1.0 M aqueous solution of sodium ascorbate (0.31 mL, 0.30 mmol, and 0.3 M aqueous solution of copper(II) sulfate pentahydrate (0.10 mL, 0.03 mmol). Purification by flash chromatography afforded the desired product in 45% yield.

The Boc-protected triazole product (0.048 g, 0.09 mmol) was directly treated with HCl as a 4.0 M solution in 1,4-dioxane (0.23 mL, 0.90 mmol). The solution was stirred at rt for 2 h and then was concentrated to afford the crude product, which was purified by HPLC [preparatory reverse phase C₁₈ column (24.1 x 250 mm), CH₃CN/H₂O 0.1% TFA, 5:95 to 95:5 over 55 min; 10 mL/min, 254 nm detection]. Fractions were combined and the CH₃CN was evaporated. The resulting aqueous solution was extracted with CH₂Cl₂, dried with Na₂SO₄, filtered, and concentrated to yield the CF₃CO₂H salt of inhibitor **3.5** in 75% yield. ¹H NMR (400 MHz, CD₃OD): δ 0.84-0.94 (m, 3H), 1.31-1.42 (m, 6H), 1.60-1.64 (m, 2H), 1.70-1.77 (m, 2H), 1.91-1.95 (m, 2H), 2.22 (s, 6H), 2.27-2.29 (m, 2H), 2.51-2.54 (m, 2H), 5.10 (d, 1H, *J* = 17.2), 5.22 (d, 1H, *J* = 17.2) (m, 2H), 5.75-5.78 (m, 1H), 7.05-7.08 (d, 2H, *J* = 7.6), 7.21-7.24 (t, 1H, *J* = 7.6), 8.37 (s, 1H).



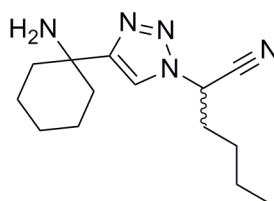
3.2

Synthesis of primary amide 3.2. The procedure for the synthesis of primary amide **3.2** from the racemic α -azido sieber amide resin **SA** was adapted from a previous literature report, and sieber amide resin **SA** was synthesized according to the published method.⁴⁰ To resin **SA** (0.7 mmol) that was preswollen in THF, was added a solution of benzyl (1-ethynylcyclohexyl)carbamate (0.27 g, 1.1 mmol) in 35 mL of THF along with *i*-Pr₂EtN (11.9 mL, 70.0 mmol) and CuI (0.41 g, 2.1 mmol). The mixture was shaken for 48 h. After removal of the solution, the resin was washed with (3 x 25 mL) each solvent of DMF, THF, CH₃OH, and THF. After removing solvent, the resin was swollen in 25 mL of CH₂Cl₂, then a solution of 9:1 CH₂Cl₂:(95% CF₃CO₂H, 2.5% H₂O, 2.5% triisopropylsilane) was added. The mixture was shaken for 2 h at rt. After removal of the solution, the resin was washed with CH₂Cl₂ (3 x 15 mL). The washes were combined and concentrated. The crude product was purified by silica gel chromatography 1:7 hexanes:EtOAc to yield pure product in 67% yield. ¹H NMR (400 MHz, CD₃OD): δ 0.85-0.89 (m, 3H), 1.14-1.23 (m, 4H), 1.35-1.54 (m, 6H), 1.96-1.99 (m, 2H), 2.00-2.02 (m, 2H), 2.26-2.30 (m, 2H), 4.99 (s, 2H), 5.22-5.26 (m, 1H), 7.28-7.32 (m, 5H), 7.90 (s, 1H).



3.3

Synthesis of Cbz-protected nitrile 3.3. A solution of primary amide **3.2** (0.14 g, 0.30 mmol) in 2.2 mL of DMF was cooled in an ice-water bath and 2,4,6-trichlorotriazine (0.60 g, 0.30 mmol) was added. The reaction mixture was stirred for 2 h at rt and then 25 mL of EtOAc was added. The reaction mixture was washed with H₂O (3 x 20 mL), dried with sodium sulfate, filtered, and concentrated. The crude product was purified by HPLC [preparatory reverse phase C₁₈ column (24.1 x 250 mm), CH₃CN/H₂O 0.1% TFA, 5:95 to 95:5 over 55 min; 10 mL/min, 254 nm detection]. Fractions were combined and the CH₃CN was evaporated. The resulting aqueous solution was extracted with CH₂Cl₂, dried with Na₂SO₄, filtered, and concentrated to yield the pure product in 69% yield. ¹H NMR (400 MHz, CDCl₃): δ 0.87-0.91 (m, 3H), 1.20-1.30 (m, 2H), 1.34-1.49 (m, 6H), 2.19-2.29 (m, 4H), 4.97 (s, 2H), 5.13 (s, 1H), 5.39-5.44 (m, 1H), 7.24-7.31 (m, 5H), 7.68 (s, 1H).



3.4

Synthesis of inhibitor 3.4. The Cbz group was cleaved by adding 0.4 mL of 45% HBr/AcOH to nitrile **3.3** (0.030g, 0.070 mmol). The solution was stirred for 50 min at rt. The crude product was purified by HPLC [preparatory reverse phase C₁₈ column (24.1 x 250 mm), CH₃CN/H₂O 0.1% TFA, 5:95 to 95:5 over 55 min; 10 mL/min, 254 nm detection]. Fractions were combined and the CH₃CN was evaporated. The product was obtained by removing H₂O from the resulting aqueous solution via lyophilization in 73% yield. ¹H NMR (400 MHz, CD₃OD): δ 0.89-0.93 (m, 3H), 1.31-1.41 (m, 6H), 1.58-1.62 (m, 2H), 1.72-1.76 (m, 2H), 1.89-1.92 (m, 2H), 2.18-2.21 (m, 2H), 2.49-2.50 (m, 2H), 5.38-5.42 (m, 1H), 8.37 (s, 1H). LRMS calculated for MH⁺ C₁₄H₂₃N₅, 262.2, found 262.1.

Protease Activity and Parasite Studies of Inhibitors

Parasite culture, harvesting and lysate preparation. 3D7 and D10 *P. falciparum* clones were cultured with media containing Albumax (Invitrogen) using standard procedures^{41,42}. D10 parasites were synchronized every 48 h at ring stage by treatment with 5 % sorbitol, which results in a synchrony window of ~ 6 h. To tightly synchronize parasites within a 1 h window, schizonts were harvested 6 h prior to rupture using a 70 % percol gradient⁴²⁻⁴⁴ and cultured until they were rupturing. Blood was then added to this culture of bursting schizonts, and merozoites were allowed to invade uninfected RBCs for 1 h. Newly formed rings (0-1 h old) were purified from the remaining schizonts with a sorbitol treatment. 3D7 parasites were grown asynchronously and were used when a mixedstage parasite culture was needed.

Parasite pellets at all intracellular stages were harvested by selectively lysing the RBC membrane with 0.15 % saponin (Calbiochem, San Diego, CA). Merozoites were purified by passing the supernatant of a culture of rupturing schizonts (obtained as described above) through a SuperMACSTM II separator (Miltenyi Biotec, Auburn, CA) as described in⁴⁵. All purified parasites were stored at -80 °C. Lysates were prepared by treating 1 volume of parasite pellet with 2 volumes of 1 % nonidet P40 in PBS for 1 h on ice. If needed, the soluble and insoluble fractions were separated by a 5 min microcentrifugation at 13000 rpms.

Labeling of cysteine protease activity with ABPs and competition of labeling by protease inhibitors. Two ABPs were used to label the activity of papain fold cysteine proteases in parasites. FY01, a cell permeable BODIPY-TMR fluorescently-tagged probe, labels DPAP1 and DPAP3 activities in intact parasites and lysates⁴⁴. Radiolabeled ¹²⁵I-DCG04 was used to label FPs activities in lysates⁴⁶. ABPs (1 μM FY01 or ¹²⁵I-

DCG04) were usually incubated for 1 h at room temperature in a 1:10 dilution of parasite lysates in acetate buffer (50 mM sodium acetate, 5 mM MgCl₂, and 5 mM DTT at pH 5.5) or intact schizonts in PBS. To measure the specificity of an inhibitor against any given cysteine protease, intact parasites or lysates were treated for 30 min with inhibitor prior to labeling. After probe treatment, samples were boiled in SDS-loading buffer and run on a SDS-PAGE gel. FY01 labeled bands were directly detected in a flatbed laser scanner. Gels run with ¹²⁵I-DCG04 treated samples were dried and analyzed by autoradiography. All gel images were taken with a 9410 Typhoon Scanner (Amersham Bioscience, GE Healthcare). Fully processed DPAP1 runs as a doublet at 20 kDa and is present at all intracellular life stages. DPAP3 activity is mainly detected in merozoites where three differentially processed forms of the enzyme are labeled (bands at 42, 95 and 120 kDa)⁴⁴. FP2, FP2' and FP3 have very similar molecular weights and cannot be easily differentiated by SDS-PAGE. Their combined activities are observed as a single band at 28 kDa. FP1 runs as a single band at 22 kDa, right above DPAP1. Note that in some instances, FY01 is also able to label FP1.

***ki* determination using a fluorogenic activity assay for DPAP1.** We recently proved that (Pro-Arg)2-Rho is a DPAP1 specific substrate in parasite lysates (brief communication). DPAP1 activity was measured at room temperature in acetate buffer containing 1 % of parasite lysates and 10 μM (Pro-Arg)2-Rho. Substrate turnover was measured for 5 min in a 96-well plate at 530 nm (using an excitation wavelength of 492 nm and an emission cutoff filter at 515 nm) in a Spectramax M5 plate-reader (Molecular Devices).

Accurate *ki* were obtained by treating a 1:10 dilution of parasite lysates in acetate buffer with increasing inhibitor concentrations for a given period of time (usually 30 min). Residual DPAP1 activity was measured with 10 μM substrate after diluting the treated samples 10-fold in assay buffer. The rates of substrate turnover relative to DMSO controls (v/v₀) were fitted to a simple irreversible inhibitor model $E + I \xrightarrow{k_i} E-I$ (equation 1).

$$(eq\ 1)\ v/v_0 = \exp(-k_i*[I]*t)$$

where [I] is the concentration of inhibitor, t is the treatment time of lysates with inhibitor, and *ki* is the second order rate constant of inhibition.

Kinetics of DPAP1 inhibition and activation in intact parasite. A mix-stage culture of 3D7 parasites at ~ 20 % parasitemia was cultured with different concentrations of inhibitor or DMSO. 200 μl aliquots of culture were taken after 0.5 to 7 h of treatment, and the RBCs were lysed in 100 μL of acetate buffer by three cycles of freezing in liquid nitrogen and thawing at 37 °C. DPAP1 activity was measured using the fluorogenic assay by adding 100 μL of 20 μM (Pro-Arg)2-Rho in acetate buffer.

***P. falciparum* replication assay.** 200 μL of synchronized cultures of D10 parasites (~ 2 % parasitemia and 0.5 % hematocrit) were treated at ring stage (~ 9 h post RBC infection) with increasing concentrations of compound and were left to grow in 96-

well plates for 1.5 life cycles, when the DMSO controls reach schizont stage (~ 75h). Cells were fixed in 0.05 % glutaraldehyde (Sigma) in PBS for at least 12 h at 4 °C, permeabilized for 5 min with 0.25 % Triton X in PBS, and stained with 0.05 mg/mL of propidium iodide (Sigma) in water. Infected and uninfected RBCs were quantified by FACS as the populations with positive and negative fluorescence in the propidium iodide channel, respectively⁴⁴. All FACS measurements were taken on a BD FACScan flow cytometer (Becton, Dickinson and Co.). All EC50Pot values for parasite death were obtained by fitting the percentage parasitemia to a dose response curve.

Susceptibility of the different life cycle stages to DPAP1 inhibition. Tightly synchronized parasites (obtained as described above) were treated with increasing concentrations of Ala-4(I)Phe-DMK or DMSO at early rings (1 h post invasion- 1 h p.i.), rings (10 h p.i.), late rings (18 h p.i.), trophozoites (30 h p.i.), schizonts (38 h p.i.), or late schizonts (46 h p.i.). After 1 h of treatment, cells were washed three times with media and cultured until the DMSO control parasites progressed through egress, and newly infected RBCs reached schizont stage (~ 80 h p.i.). Percentage parasitemia was quantified by FACS analysis as described above.

Cell toxicity. 200 μ L of an HFF cell culture were incubated in a 96-well plate format for 24 h with increasing concentrations of inhibitor or DMSO. Cell viability was measured as the amount of ATP production using the CellTiter-Glo[®] Assay (Promega) according to the manufacturer's instructions. EC50Tox values were obtained by fitting the data to a dose response curve.

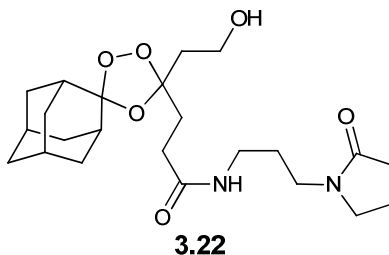
Homology modeling and docking. The homology model of DPAP1 was built based on the crystal structure of hCatC covalently bound to the Gly-Phe-diazomethane inhibitor (PDB 2DJF;⁴⁷) using the default parameters of the Molecular Operating Environment (MOE) software (Chemical Computing group). To dock HN3019 in the homology model of DPAP1, the inhibitor backbone was oriented according to the structure of human cathepsin S bound to a non-peptidic chloro-methyl ketone inhibitor (PDB 2H7J;⁴⁸) that has the same inhibitor backbone as HN3019 (both have a methyl-ketone warhead and a P1 and P2 side chain linked through a triazole ring). We decided to dock the structure of HN3019 such that it mimics an intermediate in the reaction between the warhead and the active site. The α -carbon of TFPAMK was covalently linked to the catalytic cysteines in order to account for the protein-ligand interactions of the warhead moiety.

Energy minimizations of the P2, P1, and warhead regions of **2.1** were performed sequentially followed by an energy minimization of the full molecule and the catalytic cysteine side chain. A final energy minimization including **2.1** and all side chains within 4.5 Å yielded our final model of DPAP1 bound to **2.1**. All energy minimizations were performed using the default parameters in MOE. To dock other non-peptidic inhibitors such as **2.21**, the P2 position of **2.1** bound to DPAP1 was modified to that of the new inhibitors, and the structure of the inhibitor-protein complex energy minimized as described above.

Determination of parasitemia in mouse blood. Parasitemia was quantied by FACS analysis when it reached more than 2 % (days 6-15). From day 2 through 5, the parasite load was too low to get accurate quantification by FACS (the population of propidium iodide positive cells was very similar to that of the background signal), and parasitemia was quantified from Geimsa-stained thin blood smears visualized in an Olympus CX31 microscope (Center Valley, PA) at 100X. The percentage parasitemia was estimated by counting all infected RBCs in 15-20 optical fields that contained between 200 and 1000 cells. For each field the total number of RBCs was roughly estimated. The final parasitemia for each mouse and day was determined from an estimate of more than 10,000 RBCs per slide. When using this method the origin of the slides-whether they came from treated or untreated mice- was hidden from the person estimating the parasitemia.

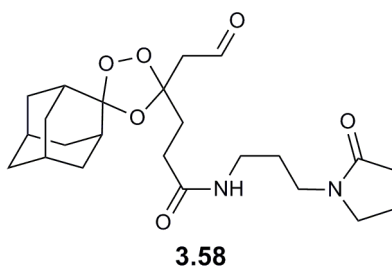
Synthesis of Fragmenting Hybrids and Intermediates

General methods for synthesizing fragmenting hybrids and intermediates. ^1H NMR spectra were recorded on a Varian INOVA-400 400 MHz spectrometer. Chemical shifts are reported in δ units (ppm) relative to TMS as an internal standard. Coupling constants (J) are reported in hertz (Hz). All reagents and solvents were purchased from Aldrich Chemical or Acros Organics and used as received unless otherwise indicated. Some synthetic intermediates were synthesized according to literature methods as indicated. Air and/or moisture sensitive reactions were carried out under an argon atmosphere in oven-dried glassware using anhydrous solvents from commercial suppliers. Air and/or moisture sensitive reagents were transferred via syringe or cannula and were introduced into reaction vessels through rubber septa. Solvent removal was accomplished with a rotary evaporator at ca 10-50 Torr. Column chromatography was carried out using a Biotage SP1 chromatography system and silica gel cartridges from Biotage. Analytical TLC plates from EM Science (Silica Gel 60 F254) were employed for TLC analyses. Mass analyses and compound purity were determined using Waters Micromass ZQTM, equipped with Waters 2795 Separation Module and Waters 2996 Photodiode Array Detector. Separations were carried out with an XTerra[®] MS C18, 5 μm , 4.6x50 mm column, at ambient temperature (unregulated) using a mobile phase of water-acetonitrile containing a constant 0.20 % formic acid.

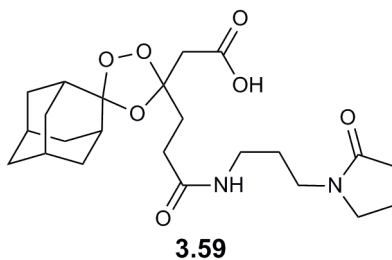


Synthesis of intermediate 3.22. A solution of adamantane-2-spiro-3'-9'-oxo-1',2',4',8'-tetraoxaspiro[4.6]undecane (160 mg, 0.55 mmol) prepared as described

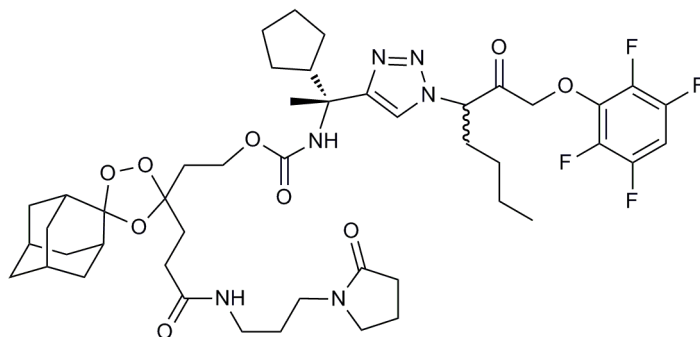
previously⁴⁹ was dissolved in the minimum amount of toluene. To this solution was added 1-(3-aminopropyl)-2-pyrrolidinone (0.15 ml, 1.11 mmol) and the reaction mixture was stirred at 50 °C for 5 hr. The solvent was evaporated and the residue was dissolved in CH₂Cl₂ (10 ml). The organic layer was washed with water, dried (Na₂SO₄), filtered, and evaporated to afford oil. The crude oil was purified using silica gel chromatography (0-10% MeOH-CH₂Cl₂) to afford alcohol **3.22** (153 mg, 0.35 mmol, 64% yield) as a colorless oil. ¹H NMR (400 MHz, CDCl₃) δ: 6.87 (t, *J* = 5.6 Hz, 1H), 3.76 (s, 2H), 3.36 (m, 2H), 3.30 (t, *J* = 6.4 Hz, 2H), 3.15 (m, 2H), 3.01 (s, 1H), 2.38-1.60 (m, 26 H); ¹³C NMR (100 MHz, CDCl₃) δ: 176.2, 172.6, 112.4, 110.92, 58.66, 47.56, 39.75, 37.92, 36.83, 36.45, 35.72, 35.16, 34.97, 31.84, 31.31, 31.13, 26.92, 26.54, 18.09. LRMS calculated for C₂₃H₃₆N₂O₆ MH⁺ 436.54 found 437.4.



Synthesis of intermediate 3.58. A solution of **3.22** (200 mg, 0.46 mmol) in CH₂Cl₂ (2 ml) was treated with the Dess-Martin periodinane (291 mg, 0.68 mmol) and stirred at room temperature for 30 min. The reaction was then quenched by addition of 10 ml of 1:1 mixture of saturated aqueous NaHCO₃ and saturated aqueous Na₂S₂O₃. The mixture was stirred until organic and aqueous phases became clear. The layers were separated and the aqueous phase was extracted twice with diethyl ether (10 ml). The combined organic layers were dried over Na₂SO₄, filtered and concentrated to afford aldehyde **3.58**, which was used in the next reaction without further purification. ¹H NMR (400MHz, CDCl₃) δ: 9.70 (s, 1H), 6.82 (br s, 1H), 3.36-3.29 (m, 4H), 3.13 (m, 2H), 2.76 (m, 2H), 2.36-1.63 (m, 24 H); ¹³C NMR (100 MHz, CDCl₃) δ: 199.19, 176.16, 171.86, 113.29, 108.39, 50.58, 47.54, 39.66, 36.48, 35.73, 31.08, 26.56, 18.11. LRMS calculated for C₂₃H₃₄N₂O₆ MH⁺ 434.53 found 435.23.



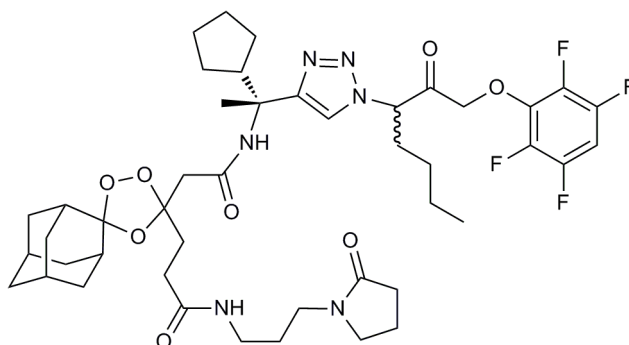
Synthesis of intermediate 3.59. The aldehyde **3.58** prepared above (150 mg, 0.34 mmol) was dissolved in a mixture of *tert*-butanol and water (5:1, 6 ml) and the reaction mixture cooled to 0 °C. Next, a 2.0 M solution isobutylene solution in THF (0.5 ml, excess) was added, followed by Na₂HPO₄ (139 mg, 1.00 mmol) and NaClO₂ (93 mg, 1.03 mmol). The reaction mixture was stirred for 3 hrs at 0 °C. The solvent was evaporated and the residue purified by silica gel chromatography (0-10% MeOH-EtOAc) to afford carboxylic acid **3.59** as a white powder (90 mg, 0.20 mmol, 59 % yield). ¹H NMR (400 MHz, CDCl₃) δ: 6.93 (br s, 1H), 3.39-3.31 (m, 4H), 3.20 (m, 2H), 2.80 (q, *J*_{AB} = 14.4, 2H), 2.44-1.66 (m, 24 H); ¹³C NMR (100 MHz, CDCl₃) δ: 176.62, 173.06, 171.31, 113.08, 108.29, 47.75, 42.95, 40.09, 36.86, 36.46, 35.42, 35.01, 34.42, 31.31, 30.84, 30.35, 27.13, 26.57, 18.22. LRMS calculated for C₂₃H₃₄N₂O₇ MH⁺ 450.53 found 451.6.



3.23

Synthesis of fragmenting hybrid 3.23. A solution of compound **3.22** (100 mg, 0.23 mmol) in 5 ml of anhydrous CH₂Cl₂ was treated with triethylamine (64 μl, 0.46 mmol), *p*-nitrophenyl chloroformate (93 mg, 0.46 mmol) and 4-dimethylaminopyridine (28 mg, 0.23 mmol). The reaction mixture was stirred under argon for 4 hrs and then diluted with CH₂Cl₂ (20 ml) and washed with saturated aqueous NaHCO₃ thrice (20 ml). The organic layer was then dried (Na₂SO₄), filtered and evaporated. The residue was passed through a short silica gel column (0-5% MeOH-CH₂Cl₂) and relevant fractions collected and concentrated to afford the 4-nitrophenyl carbonate intermediate as a yellow oil (90 mg, ~0.15 mmol). A portion of this intermediate (20 mg, 0.032 mmol) in anhydrous dimethylformamide (0.3 ml) was added **3.21** (10 mg, 0.021), diisopropylethylamine (8 μl, 0.042 mmol) and 4-dimethylaminopyridine (0.5 mg, 0.004 mmol). The reaction mixture was stirred overnight under argon and then diluted with EtOAc (10 ml) and washed with saturated NaHCO₃ (10 ml) and brine (10 ml). The organic layer was dried (Na₂SO₄), filtered, and evaporated. The residue obtained was purified using silica gel chromatography (0-5% MeOH-EtOAc) to afford hybrid **3.23** (8 mg, 0.008 mmol, 16 % overall). ¹H NMR (400 MHz, CDCl₃) δ: 7.62 (d, *J* = 2.4 Hz, 0.5 H), 7.61 (d, *J* = 2.4 Hz, 0.5 H), 6.83 (m, 1H), 6.80 (m, 1H), 5.75 (br s, 1H), 5.52 (br s, 1H), 4.84 (m, 2H), 4.08 (m, 2H), 3.37-3.30 (m, 4H), 3.16 (m, 2H), 2.35-2.45 (m, 2H), 2.25-2.30 (m, 2H), 2.25-1.25 (m, 40 H), 0.85 (m, 3H); ¹³C NMR (100 MHz, CDCl₃) δ: 199.74, 176.20, 172.60, 155.07, 152.66, 147.88, 121.77, 112.70, 109.84, 100.09, 65.87,

60.16, 56.37, 47.53; ^{19}F NMR, (CDCl_3) δ : -157.490 (m, 2F), -139.443 (m, 2F). LRMS calculated for $\text{C}_{46}\text{H}_{62}\text{F}_4\text{N}_6\text{O}_9\text{MH}^+$ 919.01 found 919.23.



3.24

Synthesis of hybrid control 3.24. To a solution of 2-(5,5-spiroadamantyl-3-(3-(2-oxopyrrolidin-1-yl-amino)-3-oxopropyl)-1,2,4-trioxolan-3-yl) acetic acid **3.59** (12 mg, 0.026 mmol) in anhydrous dimethylformamide (0.3 ml) was added $\text{H}_2\text{N-DPAP-i}$ (8 mg, 0.017 mmol), diisopropylethylamine (8.9 μl , 0.051 mmol) and 2-(7-aza-1H-benzotriazole-1-yl)-1,1,3,3-tetramethyluronium hexafluorophosphate (9 mg, 0.026 mmol). The reaction was stirred for 2 hr after which it was diluted with EtOAc (10 ml) and washed with saturated NaHCO_3 (10 ml) and brine (10 ml). The organic layer was then separated, dried (Na_2SO_4), filtered and evaporated. The residue obtained was purified using silica gel chromatography (0-5% MeOH-EtOAc) to afford **3.24** (6 mg, 0.007 mmol, 27 % yield). ^1H NMR (400 MHz, CDCl_3) δ : 7.78 (s, 0.5 H), 7.77 (s, 0.5 H), 6.87-6.68 (m, 3H), 5.53 (m, 1H), 4.88 (m, 2H), 3.37-3.30 (m, 4H), 3.20 (m, 2H), 2.50-2.25 (m, 6H), 2.20-1.14 (m, 38), 0.86 (m, 3H); ^{13}C NMR (100MHz, CDCl_3) δ : 199.85, 175.73, 172.85, 167.08, 151.97, 122.27, 113.19, 108.87, 99.97, 65.97, 56.85, 49.03, 47.32; ^{19}F NMR, (CDCl_3) δ : -157.40 (m, 2F), -139.78 (m, 2F). LRMS calculated for $\text{C}_{45}\text{H}_{60}\text{F}_4\text{N}_6\text{O}_8\text{MH}^+$ 888.99 found 889.7.

Studies of Fragmenting Hybrids and Controls in live Parasites and Parasite Lysates

Parasite culture, harvesting and lysate preparation. D10 *P. falciparum* clones were cultured with media containing Albumax (Invitrogen) using standard procedures^{41,42}. D10 parasites were synchronized every 48 h at ring stage by treatment with 5 % sorbitol. Parasite pellets were harvested at trophozoite stage by selectively lysing the RBC membranes with 0.15 % saponin (Calbiochem, San Diego, CA). Lysates were prepared by treating 1 volume of parasite pellet with 2 volumes of 1 % nonidet P40 in PBS for 1 h on ice. The soluble fraction was separated from the insoluble one by a 5 min microcentrifugation at 13000 rpms.

***P. falciparum* replication assay.** 200 μL of synchronized cultures of D10 parasites (~ 2 % parasitemia and 0.5 % hematocrit) were treated at ring stage with

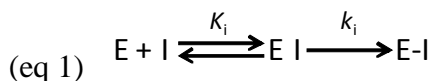
increasing concentrations of compound and were left to grow in 96-well plates for ~75 h. Cells were fixed in 0.05 % glutaraldehyde (Sigma) in PBS for at least 12 h at 4 °C, permeabilized for 5 min with 0.25 % Triton X in PBS, and stained with 0.05 mg/mL of propidium iodide (Sigma) in water. Infected and uninfected RBCs were quantified by FACS as the populations with positive and negative fluorescence in the propidium iodide channel, respectively ⁴⁴. All FACS measurements were taken on a BD FACScan flow cytometer (Becton, Dickinson and Co.). All EC50Pot values for parasite death were obtained by fitting the percentage parasitemia to a dose response curve.

Labeling of DPAP1 activity with FY01. FY01 is a cell permeable BODIPY-TMR fluorescently-tagged probe containing a vinyl sulfone reactive group that covalently modifies the catalytic cysteine of DPAP1 ⁴⁴. Parasite lysates were diluted 10-times in acetate buffer (50 mM sodium acetate, 5 mM MgCl₂, and 5 mM DTT at pH 5.5) and treated with 1 μM FY01 for 1 h at room temperature. To measure the specificity of an inhibitor against DPAP1, parasite lysates were treated with increasing concentrations of inhibitor for 30 min prior to labeling with FY01. Samples were then boiled in SDS-loading buffer and run on a SDS-PAGE gel. DPAP1 labeled bands run as a doublet around 20 kD and were directly detected in a 9410 Typhoon Scanner (Amersham Bioscience, GE Healthcare).

Kinetics of DPAP1 inhibition in living parasites. A synchronous culture of parasites (~ 20 % parasitemia) at trophozoite stage was cultured with 50 nM of compounds **3.21**, **3.22**, **3.23**, **3.24** or DMSO. 1mL aliquots of culture were taken after 0.5 to 6 h of treatment, and the RBC membranes were lysed with 0.15 % saponin. Parasites pellet were resuspended in acetate buffer containing 1 % nonidet P40, and DPAP1 activity was labeled with 1 μM FY01 at room temperature for 1 h.

Determination of 3.21 *k_i* using a fluorogenic activity assay for DPAP1. Trophozoite lysates in acetate buffer (1 to 10 dilution) were treated with increasing concentrations of **3.21** for 15 min to 1.5 h. Residual DPAP1 activity was measured as the turnover rate of (Pro-Arg)₂-Rho, a DPAP1 specific substrate in parasite lysates [DPAP1 assay paper], by diluting the treated samples 10-fold in acetate buffer containing 10 μM of substrate. Substrate turnover was measured for 5 min in a 96-well plate at 530 nm (using an excitation wavelength of 492 nm and an emission cutoff filter at 515 nm) in a Spectramax M5 plate-reader (Molecular Devices).

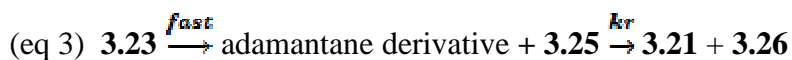
The rates of substrate turnover relative to DMSO controls (v/v0) were fitted to an irreversible inhibitor model (eq 1) with eq 2.



$$(eq\ 2) \quad \frac{v}{v_0} = \frac{\exp\left(-\frac{k_i[I] \cdot t}{K_i + [I]}\right)}{1 + [I]/K_i}$$

where E, I, E I, and E-I represent free enzyme, inhibitor, inhibitor bound to the enzyme, and the enzyme-inhibitor covalent complex, respectively. t is the treatment time of lysates with inhibitor, K_i the dissociation constant of the non-covalent enzyme:inhibitor complex, and k_i is the rate constant of covalent modification of the enzyme by the inhibitor.

Estimation of the rate of 3.21 release from hybrid 3.23 in living parasites. Three assumptions were taken to estimate the rate of the retro-Michael reaction for hybrid **3.23** *in vivo*: 1) The rate of DPAP1 inhibition by **3.21** inside the food vacuole is identical to that measured *in vitro* in acetate buffer. 2) The initial concentration of hybrid **3.23** inside the parasites is identical to the one in the media. 3) The kinetic of the β -elimination reaction can be approximated to a simple single exponential decay (eq 3).



where k_r is the average rate of release of **3.21** in the food vacuole, which is much slower than the reaction between iron(II) and the trioxolane group of compound **3.23**. The formation of H2N-DPAP-i can therefore be described by (eq 4).

$$(eq\ 4) \quad [\mathbf{3.21}] = [\mathbf{3.23}]_0 (1 - \exp(-k_r t))$$

where k_r is the average rate of release of **3.21** in the food vacuole, and $[\mathbf{3.23}]_0$ is the initial concentration of hybrid **3.23**, i.e. 50 nM. To obtain k_r , the residual DPAP1 activity values, measured during the treatment of a parasite culture with 50 nM of hybrid **3.23**, were fitted to eq 2 where $[I]$ was replaced by $[\mathbf{3.21}]$ as it is defined in eq 4, and the k_i and K_i values were fixed to those determined *in vitro* for **3.21**.

References

- (1) World Health Organization, World Malaria Report 2009: http://www.who.int/publications/2009/9789241563901--_eng.pdf
- (2) Chaijaroenkul, W.; Bangchang Kesara, N.; Mungthin, M.; Ward Stephen, A. *Malaria Journal* **2005**, *4*, 37.
- (3) Wilairatana, P.; Krudsood, S.; Treeprasertsuk, S.; Chalermrut, K.; Looareesuwan, S. *Archives of Medical Research* **2002**, *33*, 416.

- (4) Wongsrichanalai, C.; Pickard, A. L.; Wernsdorfer, W. H.; Meshnick, S. R. *Lancet Infectious Diseases* **2002**, *2*, 209.
- (5) Dondorp, A. M.; Nosten, F.; Yi, P.; Das, D.; Phyto, A. P.; Tarning, J.; Lwin, K. M.; Ariey, F.; Hanpithakpong, W.; Lee, S. J.; Ringwald, P.; Silamut, K.; Imwong, M.; Chotivanich, K.; Lim, P.; Herdman, T.; An, S. S.; Yeung, S.; Singhasivanon, P.; Day, N. P. J.; Lindegardh, N.; Socheat, D.; White, N. J. *New England Journal of Medicine* **2009**, *361*, 455.
- (6) Noedl, H.; Socheat, D.; Satimai, W. *New England Journal of Medicine* **2009**, *361*, 540.
- (7) Rogers, W.; Sem, R.; Tero, T.; Chim, P.; Lim, P.; Muth, S.; Socheat, D.; Ariey, F.; Wongsrichanalai, C. *Malaria Journal* **2009**, *8*, 10.
- (8) Gardner, M. J.; Hall, N.; Fung, E.; White, O.; Berriman, M.; Hyman, R. W.; Carlton, J. M.; Pain, A.; Nelson, K. E.; Bowman, S.; Paulsen, I. T.; James, K.; Eisen, J. A.; Rutherford, K.; Salzberg, S. L.; Craig, A.; Kyes, S.; Chan, M.-S.; Nene, V.; Shallom, S. J.; Suh, B.; Peterson, J.; Angiuoli, S.; Pertea, M.; Allen, J.; Selengut, J.; Haft, D.; Mather, M. W.; Vaidya, A. B.; Martin, D. M. A.; Fairlamb, A. H.; Fraunholz, M. J.; Roos, D. S.; Ralph, S. A.; McFadden, G. I.; Cummings, L. M.; Subramanian, G. M.; Mungall, C.; Venter, J. C.; Carucci, D. J.; Hoffman, S. L.; Newbold, C.; Davis, R. W.; Fraser, C. M.; Barrell, B. *Nature* **2002**, *419*, 498.
- (9) Goldberg, D. E. *Current topics in microbiology and immunology* **2005**, *295*, 275.
- (10) Binder, E. M.; Kim, K. *Traffic* **2004**, *5*, 914.
- (11) Blackman, M. J. *Cellular Microbiology* **2008**, *10*, 1925.
- (12) Roiko, M. S.; Carruthers, V. B. *Cellular Microbiology* **2009**, *11*, 1444.
- (13) Greenbaum, D. C.; Baruch, A.; Grainger, M.; Bozdech, Z.; Medzihradzsky, K. F.; Engel, J.; DeRisi, J.; Holder, A. A.; Bogyo, M. *Science* **2002**, *298*, 2002.
- (14) Rosenthal, P. J. *International Journal for Parasitology* **2004**, *34*, 1489.
- (15) Klemba, M.; Gluzman, I.; Goldberg, D. E. *Journal of Biological Chemistry* **2004**, *279*, 43000.
- (16) Olsen, J. G.; Kadziola, A.; Lauritzen, C.; Pedersen, J.; Larsen, S.; Dahl, S. W. *FEBS Letters* **2001**, *506*, 201.
- (17) Turk, D.; Janjic, V.; Stern, I.; Podobnik, M.; Lamba, D.; Dahl, S. W.; Lauritzen, C.; Pedersen, J.; Turk, V.; Turk, B. *EMBO Journal* **2001**, *20*, 6570.
- (18) Dalal, S.; Klemba, M. *Journal of Biological Chemistry* **2007**, *282*, 35978.
- (19) Klemba, M. *Proceedings of the National Academy of Sciences of the United States of America* **2009**, *106*, E55.
- (20) Ragheb, D.; Bompiani, K.; Dalal, S.; Klemba, M. *J. Biol. Chem.* **2009**, *284*, 24806.
- (21) Arastu-Kapur, S.; Ponder, E. L.; Fonovic, U. P.; Yeoh, S.; Yuan, F.; Fonovic, M.; Grainger, M.; Phillips, C. I.; Powers, J. C.; Bogyo, M. *Nature Chemical Biology* **2008**, *4*, 203.
- (22) Pham, C. T. N.; Ley, T. J. *Proceedings of the National Academy of Sciences of the United States of America* **1999**, *96*, 8627.

- (23) Adkison, A. M.; Raptis, S. Z.; Kelley, D. G.; Pham, C. T. N. *Journal of Clinical Investigation* **2002**, *109*, 363.
- (24) Methot, N.; Rubin, J.; Guay, D.; Beaulieu, C.; Ethier, D.; Reddy, T. J.; Riendeau, D.; Percival, M. D. *Journal of Biological Chemistry* **2007**, *282*, 20836.
- (25) Brak, K.; Doyle, P. S.; McKerrow, J. H.; Ellman, J. A. *Journal of the American Chemical Society* **2008**, *130*, 6404.
- (26) Molgaard, A.; Arnau, J.; Lauritzen, C.; Larsen, S.; Petersen, G.; Pedersen, J. *Biochemical Journal* **2007**, *401*, 645-650.
- (27) Olliaro, P.; Wells, T. N. C. *Clinical Pharmacology & Therapeutics* **2009**, *85*, 584.
- (28) Dong, Y.; Chollet, J.; Matile, H.; Charman, S. A.; Chiu, F. C. K.; Charman, W. N.; Scorneaux, B.; Urwyler, H.; Santo Tomas, J.; Scheurer, C.; Snyder, C.; Dorn, A.; Wang, X.; Karle, J. M.; Tang, Y.; Wittlin, S.; Brun, R.; Vennerstrom, J. L. *Journal of Medicinal Chemistry* **2005**, *48*, 4953.
- (29) Tang, Y.; Dong, Y.; Karle, J. M.; DiTusa, C. A.; Vennerstrom, J. L. *The Journal of Organic Chemistry* **2004**, *69*, 6470.
- (30) Vennerstrom, J. L.; Arbe-Barnes, S.; Brun, R.; Charman, S. A.; Chiu, F. C. K.; Chollet, J.; Dong, Y.; Dorn, A.; Hunziker, D.; Matile, H.; McIntosh, K.; Padmanilayam, M.; Santo Tomas, J.; Scheurer, C.; Scorneaux, B.; Tang, Y.; Urwyler, H.; Wittlin, S.; Charman, W. N. *Nature* **2004**, *430*, 900.
- (31) Creek, D. J.; Charman, W. N.; Chiu, F. C.; Prankerd, R. J.; McCullough, K. J.; Dong, Y.; Vennerstrom, J. L.; Charman, S. A. *Journal of Pharmaceutical Sciences* **2007**, *96*, 2945.
- (32) Creek, D. J.; Charman, W. N.; Chiu, F. C. K.; Prankerd, R. J.; Dong, Y.; Vennerstrom, J. L.; Charman, S. A. *Antimicrobial Agents and Chemotherapy* **2008**, *52*, 1291.
- (33) Tang, Y.; Dong, Y.; Wang, X.; Sriraghavan, K.; Wood, J. K.; Vennerstrom, J. L. *The Journal of Organic Chemistry* **2005**, *70*, 5103.
- (34) Clerici, F.; Di Mare, A.; Gelmi, M. L.; Pocar, D. *Synthesis* **1987**, 719.
- (35) Patterson Andrew, W.; Ellman Jonathan, A. *The Journal of Organic Chemistry* **2006**, *71*, 7110.
- (36) Liu, G.; Cogan, D. A.; Ellman, J. A. *Journal of the American Chemical Society* **1997**, *119*, 9913.
- (37) Brinner, K. M.; Ellman, J. A. *Organic & Biomolecular Chemistry* **2005**, *3*, 2109.
- (38) Bodanszky, M. *Principles of Peptide Synthesis*, 1984.
- (39) Alker, D.; Campbell, S. F.; Cross, P. E.; Burges, R. A.; Carter, A. J.; Gardiner, D. G. *Journal of Medicinal Chemistry* **1990**, *33*, 1805.
- (40) Patterson, A. W.; Wood, W. J. L.; Hornsby, M.; Lesley, S.; Spraggon, G.; Ellman, J. A. *Journal of Medicinal Chemistry* **2006**, *49*, 6298.
- (41) Trager, W.; Jensen, J. B. *Science* **1976**, *193*, 673.
- (42) Blackman, M. J. *Methods in Cell Biology* **1994**, *45*, 213.
- (43) Gabriel, J.; Berzins, K. *Clinical and Experimental Immunology* **1983**, *52*, 129.

- (44) Arastu-Kapur, S.; Ponder, E. L.; Fonovic, U. P.; Yeoh, S.; Yuan, F.; Fonovic, M.; Grainger, M.; Phillips, C. I.; Powers, J. C.; Bogyo, M. *Nature Chemical Biology* **2008**, *4*, 203.
- (45) Le Roch, K. G.; Zhou, Y.; Blair, P. L.; Grainger, M.; Moch, J. K.; Haynes, J. D.; De La Vega, P.; Holder, A. A.; Batalov, S.; Carucci, D. J.; Winzeler, E. A. *Science* **2003**, *301*, 1503.
- (46) Greenbaum, D. C.; Baruch, A.; Grainger, M.; Bozdech, Z.; Medzihradzky, K. F.; Engel, J.; DeRisi, J.; Holder, A. A.; Bogyo, M. *Science* **2002**, *298*, 2002.
- (47) Molgaard, A.; Arnau, J.; Lauritzen, C.; Larsen, S.; Petersen, G.; Pedersen, J. *Biochemical Journal* **2007**, *401*, 645.
- (48) Patterson, A. W.; Wood, W. J.; Hornsby, M.; Lesley, S.; Spraggon, G.; Ellman, J. A. *Journal of Medicinal Chemistry* **2006**, *49*, 6298.
- (49) Vennerstrom, J. L.; Dong, Y.; Chollet, J.; Matile, H.; Padmanilayam, M.; Tang, Y.; Charman, W. N.; (Medicines for Malaria Venture MMV, Switz.). Application: US, 2004, p 50 pp

Chapter 4. Future Directions.

This chapter will summarize the projects discussed in this dissertation as well as briefly propose future directions of the projects if they were to continue.

Identification and Evaluation of Novel Small Molecule Pan-Caspase Inhibitors in Huntington's Disease Models

Chapter 2 discusses the identification of potent, non-peptidic pan-caspase inhibitors and their application towards Huntington's disease (HD) models. We utilized a substrate-based fragment approach called Substrate Activity Screening (SAS)¹⁻⁵ to develop non-peptidic inhibitors of caspase-3 and caspase-6. In the SAS method, weak binding non-peptidic substrate fragments are identified, optimized, and then converted to potent inhibitors. By applying SAS, we identified three novel, nonpeptidic irreversible inhibitors that blocked proteolysis of Htt at caspase-3 and caspase-6 sites. In HD models, these irreversible inhibitors suppressed Hdh^{111Q/111Q}-mediated toxicity and rescued HttN90Q73-induced degeneration of rat striatal and cortical neurons.⁶ These results further implicate caspases as promising targets for HD therapeutic development.

Future work on this project would include *in vivo* studies involving treatment of transgenic mice models of HD with the pan-caspase inhibitors. A major challenge of effective treatment of brain disorders is the requirement of crossing the blood-brain barrier. In order to evaluate the therapeutic effect of the inhibitors, immunoblotting of the striatum and cerebral cortex of treated HD mice models would be conducted. Comparing *in vivo* with *ex vivo* results on the degree of neuronal cell death rescue would provide evidence on the ability of our pan-caspase inhibitors to cross the blood-brain barrier. This data would further validate caspases as viable therapeutic targets for HD.

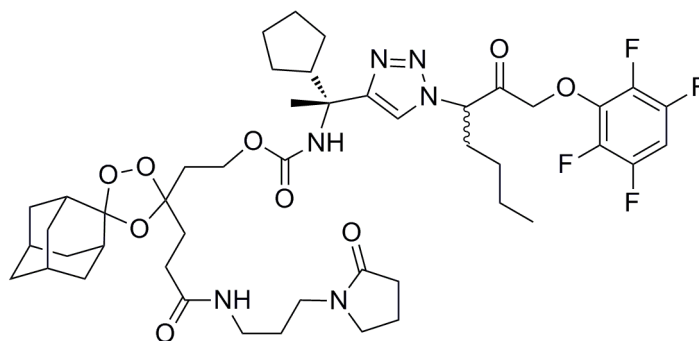
Design of *Plasmodium falciparum* Dipeptidyl Aminopeptidase I Inhibitors and Development of Fragmenting Hybrid Approach for Anti-malarial Delivery

Chapter 3 discusses the use of homology modeling and computational docking to design and synthesize nonpeptidic irreversible dipeptidyl aminopeptidase I (DPAP1) inhibitors. The most potent inhibitors killed *Plasmodium falciparum* in nanomolar concentrations in culture. Our lead inhibitor displayed cell permeability, low toxicity in HFF cells, and stability in mouse serum. Our data shows a correlation between DPAP1 inhibition and parasite death, suggesting that these inhibitors are not killing parasites by nonspecific toxic effects. These results validate DPAP 1 as a viable anti-malarial target.⁷

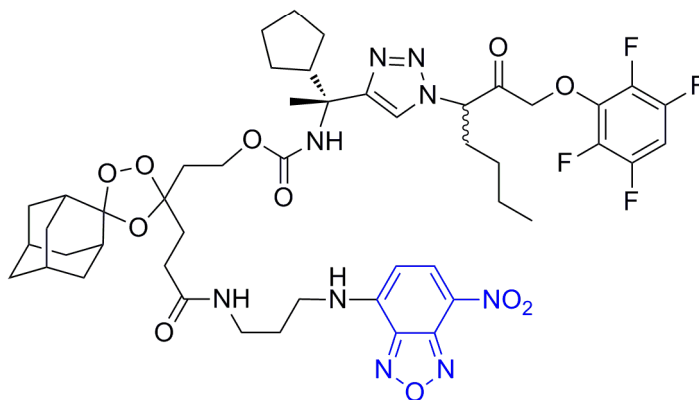
Additionally, the incorporation of our lead DPAP 1 inhibitor into a novel approach as an alternative to artemisinin combination therapy (ACT) was briefly discussed. A fragmenting hybrid (**4.1**) containing a trioxolane analog conjugated with our most potent DPAP 1 inhibitor was developed and achieved ACT-like activity. Notably, two anti-malarial agents were successfully released into parasite-infected erythrocytes.

Future work on this project would include the further evaluation of the fragmenting hybrid in erythrocytes using fluorescence microscopy. Specifically, fluoregenic hybrid models would be synthesized and studied for their localization and distribution in parasite-infected erythrocytes. The 4-nitrobenzo-2-oxa-1,3,-diazole (NBD) fluorophore has been recently studied in living malaria parasites through labeled anti-malarial endoperoxides.⁸ A fluorogenic model system (**4.2**) can be developed by

conjugating our fragmenting hybrid and a NBD fluorophore (Figure 4.1). Our fragmenting hybrid approach builds upon the known event of iron(II)-promoted trioxolane decomposition reaction sequence promoted by free ferrous iron or heme in the parasite food vacuole. Localizing our hybrid molecules in *Plasmodium falciparum* food vacuoles via fluorescent visualization, would further validate our novel approach.



4.1



4.2

Figure 4.1. Fragmenting hybrid (4.1) and fluorogenic fragmenting hybrid model (4.2).

Conclusions

Proteases play a vital role in many biological processes and are critical to the life cycle of many pathogens. Therefore, protease inhibitors have been strongly pursued to treat various diseases. While the most widely used approach rapidly identifies peptidic protease inhibitors, it has proven to be difficult to convert peptidic inhibitors into nonpeptidic, drug-like structures with favorable absorption, distribution, metabolism and elimination properties. The projects in this dissertation are all related by the importance of protease activity in relevant diseases. In Chapter 2, the SAS method was successfully applied to caspase-3 and -6 to identify potent, nonpeptidic inhibitors. These inhibitors have been used as tools to study proteases involvement of caspases and DPAP1 in Huntington's disease and the malaria-causing *Plasmodium falciparum* parasite,

respectively. The efficient inhibition of caspase-3 and -6 suppressed toxicity and rescued neurodegeneration in HD models, which validate the role of caspases in HD. Chapter 3 described the in silico design of nonpeptidic, DPAP1 inhibitors and their further development into fragmenting hybrids. Our results showed a correlation between DPAP1 inhibition and parasite death, which suggests that the recently discovered DPAP1 protease is a viable antimalarial target. While these projects contribute significantly to the field of protease inhibitor development, they also serve as notable starting points for further understanding the role of relevant proteases in pertinent diseases.

References

- (1) Brak, K.; Doyle, P. S.; McKerrow, J. H.; Ellman, J. A. *Journal of the American Chemical Society* **2008**, *130*, 6404.
- (2) Patterson, A. W.; Wood, W. J. L.; Hornsby, M.; Lesley, S.; Spraggon, G.; Ellman, J. A. *Journal of Medicinal Chemistry* **2006**, *49*, 6298.
- (3) Inagaki, H.; Tsuruoka, H.; Hornsby, M.; Lesley Scott, A.; Spraggon, G.; Ellman Jonathan, A. *Journal of Medicinal Chemistry* **2007**, *50*, 2693.
- (4) Soellner, M. B.; Rawls, K. A.; Grundner, C.; Alber, T.; Ellman, J. A. *Journal of the American Chemical Society* **2007**, *129*, 9613.
- (5) Wood, W. J. L.; Patterson, A. W.; Tsuruoka, H.; Jain, R. K.; Ellman, J. A. *Journal of the American Chemical Society* **2005**, *127*, 15521.
- (6) Leyva, M. J.; DeGiacomo, F.; Kaltenbach, L. S.; Holcomb, J.; Zhang, N.; Gafni, J.; Park, H.; Lo, D. C.; Salvesen, G. S.; Ellerby, L. M.; Ellman, J. A. *Chemistry & Biology* **2010**, *17*, 1189.
- (7) Deu, E.; Leyva, M. J.; Albrow, V. E.; Rice, M. J.; Ellman, J. A.; Bogoyo, M. *Chemistry & Biology* **2010**, *17*, 808.
- (8) Stocks, P. A.; Bray, P. G.; Barton, V. E.; Al-Helal, M.; Jones, M.; Araujo, N. C.; Gibbons, P.; Ward, S. A.; Hughes, R. H.; Biagini, G. A.; Davies, J.; Amewu, R.; Mercer, A. E.; Ellis, G.; O'Neill, P. M. *Angewandte Chemie International Edition* **2007**, *46*, 6278.